INAUGURAL – DISSERTATION

zur

Erlangung der Doktorwürde

der

Naturwissenschaftlich – Mathematischen

Gesamtfakultät

der

Ruprecht-Karls-Universität

Heidelberg

Vorgelegt von

Diplom-Mineralogin Carola Franzen

aus Delmenhorst

Tag der mündlichen Prüfung: 24.07.2013

Determination of Atmospheric Mercury and its Deposition in Remote Areas of the Northern and Southern Hemisphere

Gutachter: Prof. Dr. Heinz Friedrich Schöler
Prof. Dr. Harald Biester

The trouble with being punctual is that nobody's there to appreciate it.

- Franklin P. Jones

Abstract

Mercury (Hg) is a pollutant of global concern. Due to its high vapor pressure Hg is a very mobile element and therefore is evident in all environmental compartments and can be both, intra-hemispherically and interhemispherically dispersed.
In order to understand the global mercury cycle and the anthropogenic impact on it, a large number of research activities have been carried out in recent years. On the one hand mercury species in ambient air have been scope of various studies with the objective to characterize the contemporary mercury fate and behavior in the global atmosphere. On the other hand, historical records of mercury in a variety of archives have been used to estimate human impacts on the biogeochemical cycling of mercury.

The first objective of this study was to contribute information on the worldwide distribution and trend of atmospheric mercury. For this the atmospheric species Total Gaseous Mercury (TGM), Reactive Gaseous Mercury (RGM), Total Particulate Mercury (TPM) and mercury in precipitation have been analyzed in remote areas in both, the Northern and the Southern Hemisphere. In order to ensure the determination of reliable data, the establishment of compliant and reliable sampling and analytical set-ups capable for remote sampling areas was the first milestone for this part of the study.
One other intent of the study was to answer the question under which constraints mercury records in peat bogs and lacustrine sediments reflect atmospheric deposition rates and thus can be used to estimate human impacts on the biogeochemical cycling of mercury. With the atmospheric mercury data obtained, contemporary deposition rates were calculated and compared to existing historical mercury records in ombrothrophic peat bogs and lacustrine sediments to test the reliability of these geochemical archives.

The atmospheric data show that there is a significant diurnal and spatial variability of the different species, mainly controlled by meteorological conditions and biogeochemical processes in soils.
The new data contribute to the the existing small data set from remote areas, especially from the Southern Hemisphere, and are a helpful complementary approach to the few stationary sites established for long period observations. Particularly for the region of South America no baseline measurements in remote areas have been performed before. The results provide basic information about the worldwide distribution and trend in atmospheric mercury dynamics.
The calculated mercury wet deposition of 1.3 – 3.5 µg m^{-2} a^{-1} found for the different sampling sites in Patagonia show a much better correlation to the Hg accumulation rate found in the lacustrine sediment and evidence that the uncorrected accumulation rates in the upper part of peat bogs and thus the assumed contemporary atmospheric flux might be overestimated.

Zusammenfassung

Quecksilber (Hg) zählt zu den Umweltschadstoffen von globaler Bedeutung. Durch seinen hohen Dampfdruck ist Hg sehr mobil, dispergiert sowohl intra- als auch interhemisphärisch und ist daher in allen Umweltkompartimenten nachweisbar.
In den letzten Jahrzehnten wurden zahlreichen Studien durchgeführt, die dazu beitragen sollen, den globalen Hg-Kreislauf zu erklären und den anthropogenen Einfluss zu quantifizieren. Dies sind einerseits Messungen der verschiedenen atmosphärischen Hg-Spezies mit dem Ziel den Verbleib und das Verhalten des globalen Hg besser zu verstehen. Andererseits wurden verschiedene hochauflösende Umweltarchive auf ihre Hg-Konzentrationen ausgewertet, um den anthropogenen Einfluss auf den Hg-Kreislauf besser einschätzen zu können.

Veranlassung dieser Studie war daher einesteils einen Beitrag zur Aufklärung der globalen Verteilung und des Verhaltens von Quecksilber in der Atmosphäre zu leisten. Dafür wurden die atmosphärischen Quecksilberspezies TGM (Gesamtes Gasförmiges Hg), RGM (Reaktives Gasförmiges Hg), TPM (Gesamtes Partikuläres Hg) sowie Quecksilber im Niederschlag in anthropogen wenig beeinflussten Gebieten der Nord- und Südhemisphäre bestimmt.
Dazu war vor allem die Entwicklung eines zuverlässigen, transportablen Beprobungs- und Analysevorgehens für die Untersuchungen in den schwer zugänglichen Regionen notwendig.
Ein weiterer Schwerpunkt der Studie war die Frage unter welchen Umständen Quecksilberprofile in Torfen und Seesedimenten die atmosphärische Deposition von Quecksilber widerspiegeln und somit die Profile zur Abschätzung des anthropogenen Einflusses auf den Quecksilber-Kreislauf genutzt werden können. Auf der Grundlage der eigenen atmosphärischen Quecksilberdaten wurden aktuelle Depositionsraten berechnet. Diese wurden mit Quecksilberprofilen aus ombrothrophen Torfkernen und Seebohrkernen aus früheren Studien verglichen.

Die atmosphärischen Daten zeigen eine erhebliche tageszyklische und räumliche Variabilität der einzelnen Spezies, maßgeblich beeinflusst durch die meteorologischen Bedingungen und biogeochemische Prozesse in Böden.
Diese neuen Daten bauen die wenigen bisher vorliegenden Daten besonders von der Südhalbkugel aus. Sie sind ein wichtiger ergänzender Beitrag zu den Ergebnissen aus Langzeitstudien von den wenigen etablierten Forschungsstationen. Insbesondere für Südamerika stellen die Untersuchungen die ersten Grundlagenmessungen aus Reinluftgebieten dar. Die Ergebnisse liefern damit wichtige Informationen zur weltweiten Verbreitung und der Entwicklung von Quecksilber in der Atmosphäre.
Die für unterschiedliche Bereiche aus Patagonien ermittelten Depositionsraten von 1.3 – 3.5 $\mu g\ m^{-2}\ a^{-1}$ zeigen eine sehr gute Korrelation mit den Hg-Akkumulationsraten in Seesedimenten. Sie weisen zudem nach, dass teilweise bisher angenommene Akkumulationsraten aus den oberen Teilen von Torfbohrkernen und somit der daraus abgeleitete atmosphärische Fluss deutlich überschätzt wurden

Content

Acronyms and abbreviations

AAS	Atomic Absorption Spectrometry
AFS	Atomic Fluorescence Spectrometry
AMAP	Arctic Monitoring and Assessment Program
AMDE	Atmospheric Mercury Depletion Event
AMNet	Atmospheric Mercury Network
APD	Annual Precipitation Depth
ASGM	Artisanal Small scale Gold Mining
AvD	Averaged Daytime Peaks
AvN	Averaged Nighttime Concentrations
CAMNet	Canadian Atmospheric Mercury Network
CARIBIC	Civil Aircraft for Regular Investigation of the Atmosphere Based on an Instrumented Container
CGMMN	Coordinated Global Mercury Monitoring Network
CV-AAS	Cold Vapor Atomic Absorption Spectrometry
CV-AFS	Cold Vapor Atomic Fluorescence Spectrometry
DGM	Dissolved Gaseous Mercury
DGM	Divalent Gaseous Mercury
DM	Dry Mass
DOAS	Differential Optical Absorption Spectroscopy
EEA	European Environment Agency
EMEP	European Monitoring and Evaluation Programme
GAW	Global Atmosphere Watch
GC	Gran Campo (sampling site in Patagonia)
GEM	Gaseous Elemental Mercury
GMA	Global Mercury Assessment
GMP	Global Mercury Project
GOM	Gaseous Oxidized Mercury
GOME	Global Ozone Monitoring Experiment
Hg_P	Particulate Mercury
Hg_T	Total Mercury
ICMGP	International Congress on Mercury as a Global Pollutant
IQR	Interquartile Range
ITCZ	Inner Tropical Convergence Zone
LMP	Lago Muy Profundo (Sampling site in Patagonia)
MAMCS	Mediterranean Atmospheric Mercury Cycle System

MBL	Marine Boundary Layer
MERCYMS	Mercury Cycling in the Mediterranean Sea Basin
MDE	Mercury Depletion Event
MDN	Mercury Deposition Network
MOE	Mercury Species over Europe (Project)
NA	Not Determined / No data available
NADP	National Atmospheric Deposition Program
NADP-MDN	National Atmospheric Deposition Program- Mercury Deposition Network
ND	No data
NH	Northern Hemisphere
NL	Norm Liter
OM	Organic matter
OSPAR	Oslo and Paris Convention for the Protection of the Marine Environment of the North-East Atlantic
PBr	Peninsula Brunswick (sampling site in Patagonia)
PE	Polyethylene
PFA	Perfluoroalkoxy
PHg	Particulate Mercury
PM	Particulate Mercury
POP	Persistent Organic Pollutant
PP	Polypropylene
PPM	Particulate Phase Mercury
PTE	Periodic Table of Elements
PTFE	Polytetrafluoroethylene
PVF	Polyvinyl Fluoride
RGM	Reactive Gaseous Mercury
SH	Southern Hemisphere
Sky	Skyring (Sampling Site in Patagonia)
TGM	Total Gaseous Mercury
TPM	Total Particulate Mercury
UNEP	United Nations Environmental Programme
US EPA	United States Environmental Protection Agency
VWM	Volume-weighted mean
WMO	World Meteorological Organization
X	Halogen

1 INTRODUCTION

Mercury is a non-essential heavy metal. Particularly, because of its ability to form highly toxic metabolites, mercury has been subject of intensive scientific research since the middle of the 20th century. Today, mercury is classified to be a pollutant of global concern (e.g. Nriagu, 1989; Mason et al., 1994; Pleijel and Munthe, 1995; Pacyna and Keeler, 1995; Pirrone et al., 1996 a,b,c; Pirrone et al., 1998; Petersen et al., 1998; Pirrone et al., 2000; Wängberg et al., 2001; Munthe et al., 2001; Horvat, 2002; Pacyna et al., 2010).

Mercury has been noted for being toxic for a long time. Regardless, consequences in terms of health and environmental policy have only been advanced after the first great catastrophe of toxication in the 20th century; the so called Minamata Disease. In the 50's of the 20th century, a number of unknown diseases of the nervous system accumulated at the insulars of the island Kyushu, Japan. Nearly 100 deaths were registered at that time and considerable more insulars have been affected (Harada, 1995). It took until 1968 until the source for these diseases was officially notified. The Chisso Corporation's chemical factory, which used mercury compounds as catalysts for the production of acetaldehyde from 1932 until 1968 discharged the mercury containing waste in the sea water in Minamata Bay. In the sea water the mercury compounds were transformed to methylmercury by microorganisms. This highly toxic chemical bio-accumulated in fish in Minamata Bay and the Shiranui Sea, which when eaten by the local population resulted in mercury poisoning. As of March 2001, 2,265 victims had been officially recognized (1,784 had died) and over 10,000 had received financial compensation from Chisso. Lawsuits and claims for compensation continue to this day (Ministry of the Environment, Japan, 2002). A comparable severe tragedy occurred in 1971/1972 in Iraq. During the winter of 1971-1972, mercury poisoning occurred in rural areas of Iraq. Wheat seeds, intended for crop planting, which had been treated with methylmercury and phenylmercury acetate as fungicide, were distributed for free in rural areas. Some seeds were ground into flour, baked into bread and consumed. Of an estimated 50,000 people exposed to the contaminated bread, 459 died, and 6,530 were hospitalized (Cox et al., 1989; Cox et al., 1995).

Due to these tragedies, mercury became the subject of many environmental studies.
However, these two cases are examples for only local pollutions with direct contact to the mercury sources.

Since the 70's of the 20th century, a growing number of aquatic systems in Scandinavia and Northern America have been reported to bear high mercury burdens (Håkansson et al., 1988; McMurtry et al., 1989; Lindqvist, 1991; Meili, 1991a; Lathrop et al., 1991; Wren et al., 1991; Lucotte et al., 1995). In some cases, the presence of mercury may also be predominately a reflection of local anthropogenic sources (Iverfeldt, 1991a; Lathrop et al., 1991; Johansson et al., 1991; Nater and Grigal, 1992). However, for some remote areas, only more global scale processes with a uniform distribution of mercury over large continental areas can be the explanation (Steinnes and Andersson, 1991; Slemr and Langer, 1992; Swain et al., 1992).

These findings resulted in a number of studies concerning the global cycle of mercury. Following its release into the atmosphere, particulate Hg is deposited locally or regionally within a few weeks (Iverfeldt, 1991a; Slemr and Langer, 1992). In contrast, the residence time of gaseous Hg^0 is estimated to be about 1-2 years, and may therefore be transported over thousands of kilometers from its source before being deposited (Lindqvist and Rhode, 1985; Slemr et al., 1985; Glass et al., 1986; Slemr and Langer, 1992; Lindberg et al., 2007).

The subsequent deposition of mercury in remote areas was investigated by many researcher groups (e.g. Lindqvist and Rodhe, 1985; Bloom et al., 1991; Lindqvist et al., 1991; Sheppard et al., 1991; Lucotte et al., 1995; Fitzgerald and Mason, 1996; AMAP, 1998; Boutron et al., 1998; Hermanson, 1998; Biester et al., 2002; Ribeiro Guevara et al., 2010; Jiang et al., 2011). These investigations were based on the measurement of mercury in geochemical archives, such as sediments, soils, bogs, and ice. These historical records of mercury accumulation have often been used to estimate human impacts on the biogeochemical cycling of mercury. However, Biester et al. (Biester et al. 2002; Franzen et al., 2003; Biester et al., 2003; Biester et al., 2007) have shown that modern mercury accumulation rates derived from peat bogs tend to overestimate deposition.

Another approach to get a better understanding about the global mercury cycle and the anthropogenic impact to it is the direct measurement of atmospheric mercury species. The most commonly measured and monitored fractions are Gaseous Elemental Mercury (GEM), Total Gaseous Mercury (TGM), Reactive Gaseous Mercury (RGM), Total Particulate Mercury (TPM) and mercury in precipitation. Considering these species, TGM/ GEM is maybe the only component that is easily and accurately measured in the field,

nowadays. RGM and TPM are operationally defined and thus measurements from different sites may be quite complex to intercompare.
Mercury concentrations in air and wet deposition have been monitored since 1995 (Slemr et al., 2011) at an increasing number of sites in the Northern Hemisphere (e.g. Slemr et al., 2003; Temme et al., 2007; Prestbo and Gay, 2009; Cole and Steffen, 2010) but only at one non-polar site in the Southern Hemisphere (Slemr et al., 2008).

The aim of this work is to contribute information on the worldwide distribution and trend of atmospheric mercury and to contribute mercury baseline concentrations from remote areas. For this, the study provides short-term measurements of the species TGM, RGM, TPM and mercury in precipitation from different sampling sites from both the Northern and the Southern Hemisphere. The sampling sites were selected to be complementary to the various long-term monitoring sites and were therefore chosen in areas where no atmospheric mercury measurements had been performed before. In order to investigate natural processes influencing the mercury cycle and to obtain baseline concentrations, the sampling sites were chosen in remote areas with no mercury emission point source in the vicinity.
The study comprises an examination of the following aspects:

- Spatial variability of atmospheric Hg species from different climatic zones within one area in Patagonia, Chile.
- Spatial variability of atmospheric Hg species from the Northern- and Southern Hemisphere.
- Comparison of atmospheric Hg species from coastal sites with inland sites.
- Factors influencing the diurnal variation of atmospheric Hg species.
- Comparison between mercury wet deposition rates and mercury accumulation rates in peat bogs and sediments.
- Mercury transfer from snow to atmosphere.

2 MERCURY IN THE ENVIRONMENT

Mercury is a natural element with seven stable isotopes. The existing radio-isotopes are very short-lived and no stable isotope can be synthesized. Hence, more or less the same amount of mercury has existed on the planet since the Earth was formed. Its fraction of the upper Earth's crust is estimated to be approximately 5×10^{-5} %. According to the natural abundance of chemical elements, it is on 62nd position (Falbe and Regitz, 1995). Natural and anthropogenic activities can redistribute this element in the atmospheric, soil, and water ecosystems through a complex combination of transport and transformations. During the Industrial Age it has been employed in a wide array of applications and as a result the amount of mercury mobilized and released into the atmosphere has increased compared to pre-industrial levels.

Due to its high vapor pressure of about 1.2×10^{-3} Torr at 20 °C, Hg is a very mobile element and therefore is evident in all environmental compartments. Typical recent background concentrations are listed below (Tab. 2-1).

Tab. 2-1 Total mercury content in different environmental compartments (modified after Temme, 2003).

Environmental Compartment	Total Mercury Content	Source
Air		
Atlantic Ocean	1 – 3 ng m^{-3}	Slemr & Langer, 1992
Rural Areas of North America	1.6 – 1.9 ng m^{-3}	Burke et al., 1995
Europe-West Coast, Ireland	1.4 – 2.4 ng m^{-3}	Ebinghaus et al., 2002a
Water		
Open Ocean	0.5 – 3.0 ng L^{-1}	Schroeder, 1989
Groundwater	2.0 – 4.0 ng L^{-1}	Krabbenhoft & Barbiaz, 1992
Great Lakes, USA	0.9 – 3.9 ng L^{-1}	Driscoll et al., 1994
Soil		
Mean value of different soils, Canada	0.06 µg g^{-1} DM	McKeague & Wollynetz, 1980
Forest Soil, TN, USA	0.3 – 0.8 µg g^{-1} DM	Kim & Lindberg, 1995
Geogenically enriched Soil, Nevada, USA	0.1 – 15 µg g^{-1} DM	Gustin et al., 1999

Research on atmospheric emissions, transport and deposition mechanisms to terrestrial and aquatic receptors, chemical transformations of elemental mercury to more toxic species (i.e. methylmercury), studies on the bioaccumulation of mercury in the aquatic food chain as well as exposure and risk assessments has driven the scientific and political communities to consider this toxic element as a pollutant of global concern (i.e. Nriagu, 1989; Mason et al., 1994; Pleijel and Munthe, 1995; Pacyna and Keeler, 1995; Pirrone et al., 1996 a,b,c; Pirrone et al., 1998; Petersen et al., 1998; Pirrone et al., 2000; Wängberg et al., 2001; Munthe et al., 2001; Horvat, 2002; Pacyna et al., 2010).

Fig. 2-1 shows a conceptualization of the global mercury cycle after Stein et al. (1996). As indicated, mercury is emitted to the atmosphere from a variety of point and diffuse sources, is dispersed and transported in the air, deposited to the earth and stored in or redistributed between water, soil, and atmospheric compartments. Therefore, mercury cycling and mercury partitioning between different environmental compartments are complex phenomena that depend on numerous environmental parameters.

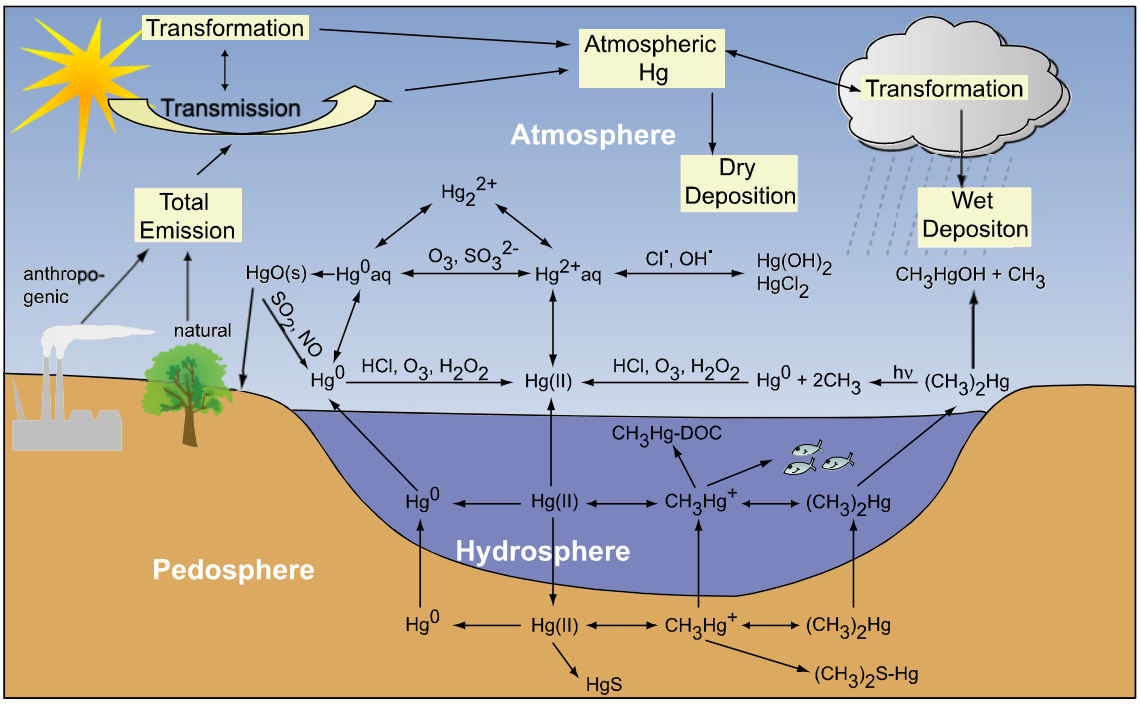

Fig. 2-1 Transformation and transport of mercury in the global mercury cycle (modified after Stein et al., 1996 and Temme, 2003).

For a better understanding of the global cycle several properties of mercury and key factors that affect the fate and transport of mercury in the environment have to be taken into account. Some of the most important aspects are described in the following chapters.

2.1 Physical and Chemical Properties

Mercury belongs to the group of heavy metals and is the only metal and besides bromine the only element being in liquid state at standard room temperature and pressure. Because of its high surface tension it does not wet the base but forms flat globules (cohesion). The liquid state of mercury is due to a unique electron configuration ($4f^{14}5d^{10}6s^2$), which does not permit a stable binding between different atoms (Norrby, 1991).

The atoms of the other metals are held together electrostatically by the so called electron gas. This electron gas consists of delocalized electrons of the outer atom shells, which jump from the valence band to the conduction band of the atoms and back. Due to this interaction, the atoms are held together and a metallic bond exists.

As an element of the 12^{th} group of the PSE, mercury has completely filled s and d orbitals, which is a highly stable conformation. The conduction band is empty. Zinc and cadmium that are in the same group as mercury are solid at room temperature. That is because the energetic difference between valence band and conduction band is very small, so that the electrons are able to jump. A metallic bond is formed. The specialty with mercury is the additional f-orbital. While zinc and cadmium have 12 electrons in the outer shell, mercury has 26 electrons. In cause of the lanthanide contraction and the relativistic effect a mass build-up and a better shield of the nuclear charge occurs. Occupied orbitals like the valence band will be pulled to the nucleus while the empty orbitals like the conduction band won't. As a result the energy difference between the valence band and the conduction band is so big that no electrons can build up the electron gas or the metallic bond. This also explains the high volatility and the poor conductivity of mercury.

A mercury atom forms a stronger bond with other metal atoms with the exception of some metals like e.g. Fe, Co, Mn than it does with mercury atoms. When mercury unites with any of several different metals, the metallic bonds created result in unique metal alloys called amalgams, which, depending upon their mercury contents can either be solid or liquid (Hollemann and Wiberg, 1985). Due to the electron configuration mercury can exist in three oxidation states – as Hg^0 (metallic), Hg(I) (Hg_2^{2+} - mercurous) and Hg(II) (Hg^{2+} - mercuric).

2.1.1 Elemental Mercury

The most important physical and chemical characteristics of elemental mercury are listed in Tab. 2-2.

Tab. 2-2 Physical and Chemical Properties of Elemental Mercury. Date marked with [1] are from Schroeder et al. 1991)

General	Name, Symbol, Number in PSE CAS-Number Chemical Series Group, period, block Appearance	Mercury, Hg, 80 7439-97-6 Transition metals 12 (IIB), 6, d Silvery white
Atomic properties	Atomic mass Electron configuration Electrons per shell 1. Ionization energy[1)] 2. Ionization energy[1)] 3. Ionization energy [1)]	200.59 g mol^{-1} $[Xe]4f^{14}5d^{10}6s^{2}$ 2, 8, 18, 32, 18, 2 241 kcal mol^{-1} 432 kcal mol^{-1} 789 kcal mol^{-1}
Physical properties	Phase Density[1)] Crystal Structure Melting point[1)] Boiling point[1)] Critical point Heat of fusion Heat of vaporization Vapor pressure[1)] Henry- constant	Liquid 13.5 g cm^{-3} Rhombohedral -38.8°C 356.7°C 1750 K, 172.00 MPa 2.29 kJ mol^{-1} 59.2 kJ mol^{-1} 1.2 * 10^{-3} Torr at 20°C 729 Pa m^3 mol^{-1}
Chemical properties	Oxidation states Standard potential Electronegativity Saturated Air Concentration[1)] Water solubility at 20°C[1)] Water solubility at 25°C[1)]	**2**, 1 0.851 V (Hg^{2+} + $2e^{-}$ -> Hg) 2.00 (Pauling scale) 13.18 µg L^{-1} 45.0 µg L^{-1} 63.9 µg L^{-1}
Miscellaneous	Magnetic ordering Electrical resistivity Thermal conductivity Thermal expansion Speed of sound	Diamagnetic (25°C) 961 nΩ m (300 K) 8.30 W m^{-1} K^{-1} (25°C) 60.4 µm m^{-1} K^{-1} (293.15 K) 1407 m s^{-1}

Under environmental conditions, the only reactions with elemental mercury are oxidation reactions. However, with most of the natural occurring oxidants, elemental mercury only reacts very slowly.

It behaves mostly inert against ambient oxygen, water, and diluted non-oxidizing acids. It also reacts only very slowly with water-dissolved oxygen. Comprehensive reviews of Hg speciation and transport in hydrothermal systems are provided by Varekamp and Buseck (1984), Krupp (1988) and Barnes and Seward (1997). According to them, mercury may be transported in hydrothermal fluids as elemental Hg species in aqueous solution or in the gas phase.

Elemental Hg is also soluble in hydrocarbons (Varekamp and Buseck, 1984; Bloom, 2000).
With other non-metals like sulphur, halogens, phosphor, or selenium Hg reacts already at room temperature. With nearly all metals (with exception of Fe, Co, Mn, Mo, and W) it forms solid or liquid solutions, called amalgams (Hollemann and Wiberg, 1985).
For mercury as a global pollutant, especially the poor water solubility and the high vapor pressure are of great importance.

2.1.2 Hg_2^{2+} (Hg(I)) Compounds

Hg^+ does not have a stable electron configuration and only exists as a dimer Hg_2^{2+} with a covalent bond. This dimer underlies the disproportionation according to the following equation:

$$Hg_2^{2+} \leftrightarrow Hg^{2+} + Hg^0 \qquad \text{(Eq. 2-1)}$$

Chemically, the equilibrium would be on the left side (Munthe and McElroy, 1992). In nature however, the equilibrium is far on the right side, because Hg^0 volatizes out of the system and the Hg^{2+} ion forms stable complexes.
Hg(I) compounds are with the exception of some hardly soluble compounds like e.g. halogenides only fairly stable. Hence, it is generally assumed, that in the environment only Hg^0 and Hg(II) exist (Kaiser and Tölg, 1980). Up to now, its evidence could only be provided for Hg(I) compounds in Hg-ores (Wallschläger, 1996).
In the laboratory, the existence of stable mercurous ions (Hg_2^{2+}) in addition to mercuric ions (Hg^{2+}) in the aqueous phase has been frequently demonstrated (Fujita et al., 1973; Wigfield and Perkins, 1985). Mercurous ions have been obtained by reduction of mercuric salts. Not many studies on stable Hg^+ species as the result of gas-phase reactions exist. One study (Raofie and Ariya, 2004) has provided the first experimental product study of BrO-initiated oxidation of elemental mercury. The authors identified, in the course of the BrO + Hg^0(g) reactions, stable Hg^+ in the form of HgBr under tropospheric conditions.

2.1.3 Hg^{2+} Hg(II) Compounds

Most divalent mercury compounds have a covalent character, like oxides, hydroxides, halogenides and the sulphur compounds. They dissolve in water as complex compounds or they are poorly soluble like HgS.

Compounds with strongly electronegative anions like fluoride, nitrate, or chlorate have a salt character. They disproportionate or hydrolyze in aqueous solution, if not stabilized by the addition of an acid.

The Hg^{2+} cation as well as the $MeHg^{+}$ cation shows a distinct tendency to form complexes. The Hg^{2+} cation normally forms twofold or fourfold coordinated complexes, which are linear or tetrahedral. Especially within the twofold coordinated complexes the bond between Hg and the ligand shows distinct covalent character (Cotton and Wilkinson, 1985). The complexes of Hg^{2+} with divalent ligands like S^{2-} or O^{2-} have a polymer structure and are comparatively fairly soluble and fairly volatile. The analogous complexes of the $MeHg^{+}$ with their already existing C-Hg bond are monomer and therefore better soluble.

2.2 Toxicology of Mercury

The impact of mercury on human health and the environment depends upon several mechanisms primarily depending on the toxicokinetics of its major chemical forms present in different environmental media including elemental mercury (Hg^0), inorganic mercury (i.e. $HgCl_2$), and organic mercury (i.e. CH_3Hg^{+}). These toxicokinetic mechanisms include absorption, distribution, metabolism and excretion (EU Position Paper, 2001). Therefore, depending on the chemical form of mercury the combination on these mechanisms will determine the risk associated to the exposure of humans to mercury and its compounds.

Since the catastrophes of Minamata, Japan in the 50ies and 60ies and of Iraq in 1972 it became obvious how tremendous the consequences of mercury contaminations are. Mercury compounds or elemental mercury emitted into the environment are accumulated in the pedosphere as well as in the biosphere. During the Minamata tragedy mercury contents in fish were around 10 to 30 mg kg^{-1}. For comparison: The admissible maximum value for Hg in fish, crustaceans, mollusks, and their products in Germany is 0.5 mg kg^{-1} (SHmV, 2006).

2.2.1 Elemental Mercury

Elemental Mercury in a liquid or vapor form is not well absorbed by the gastro-intestinal tract (possibly less than 0.01 %) (Bornmann et al., 1970) and is therefore only poorly toxic in the oral form.

However, vapor of elemental mercury is rapidly absorbed via the lungs. In humans 75-85 % of an inhaled dose is absorbed (Hursh et al., 1980; WHO, 1991). Elemental

mercury is lipid soluble and its diffusion into the lungs and dissolution in blood lipids is rapid (Berlin, 1986, WHO, 1991). It is distributed throughout the body, and readily crosses the placental barrier and the blood-brain barrier (Vimy et al., 1990; Drasch et al., 1994).

Signs and symptoms observed in mercury vapor poisoning differ depending on the level and duration of exposure. Acute poisoning possibly leads to gingivitis, pulmonary inflammation, tremor, or degeneration of the kidney (Marquardt, 1994). Chronic intoxication is remediable if the function of the kidneys has not been affected and if the person is no longer within the field of contamination. Mercury concentrations in blood decrease rapidly with an initial half-life of approximately two to four days, and a slower phase of a few weeks (Cherian et al., 1978; Bårregard et al., 1992; Sällsten et al., 1993). In urine the half-life is 40-90 days (Roels et al., 1991; Bårregard et al., 1992; Sällsten et al., 1994). These results therefore reflect the existence of compartments with elimination half-lives of about 2 months, presumably in the kidney.

2.2.2 Inorganic Mercury Compounds

The toxicity of inorganic mercury compounds increases with increasing solubility of the substance. However, all inorganic mercury compounds are less toxic than organic compounds, particularly less toxic than methylmercury. Mercury (I) compounds are principally less toxic than the according divalent compounds. The reason for the different behavior is the high affinity of divalent compounds to sulfhydryl groups or disulphide groups of proteins. On this way the active center of these proteins can be blocked and the structure can be modified (Magos, 1988).

The symptoms of inorganic mercury toxication are relatively easy diagnosable and can be treated with sulphur or selenium compounds (Hollemann and Wiberg, 1985). Both therapeutic agents prevent resorption of mercury on the proteins.

2.2.3 Organic Mercury Compounds

The (trans-) formations of organo-metallic compounds in nature are of great ecotoxicologic importance. Due to methylation of inorganic mercury compounds or elemental mercury different organic compounds can be created; for example methylmercury, dimethylmercury, or methylmercurychloride. These compounds are more lipophilic than inorganic mercury compounds. Hence, their up-take by biological cells is much higher. Methylmercury is formed in lake and sea sediments. Micro-organisms

reduce the mercury cation to elemental mercury or they transform it into methyl- or dimethylmercury (Hamdy and Noyes, 1975).
As a lipophilic substance methylmercury easily passes biological membranes. About 95 % of the methylmercury in fish ingested by humans was found to be absorbed from the gastrointestinal tract (Åberg et al., 1969; WHO, 1990). Although the oral exposure route is most important for humans, it should be noted that methylmercury is also readily absorbed through the skin and the lungs. Once absorbed into the blood stream, methylmercury enters the red blood cells bound to hemoglobin. A smaller fraction is found in the plasma (Åberg et al., 1969, Kershaw et al., 1980; WHO, 1990).

2.3 History, Occurrence, and Extraction of Mercury

Mercury was known to the ancient Chinese and Hindus and was found in Egyptian tombs that date from 1500 BC. In China, India, and Tibet, mercury use was thought to maintain generally good health and prolong life (Leicester, 1961). China's first emperor, Qin Shihuang Di, is said to have been buried in a tomb that contained rivers of flowing mercury, representative of the rivers of China. The ancient Greeks used mercury in ointments and the Romans used it in cosmetics. By 500 BC mercury was used to make amalgams with other metals. Alchemists often thought of mercury as the first matter from which all metals were formed. Different metals could be produced by varying the quality and quantity of sulphur contained within the mercury. An ability to transform mercury into any metal resulted from the essentially mercurial quality of all metals. The purest of these was gold, and mercury was required for the transmutation of base (or impure) metals into gold. This was a primary goal of alchemy. The Indian word for alchemy is *Rasavātam* which means 'the way of mercury' (NGDTJ, Internet; Science24, Internet).

In alchemical times the element was named after the Roman god Mercury, known for speed and mobility (Falbe and Regitz, 1995). It is associated with the planet Mercury. Mercury is the only metal for which the alchemical planetary name became the common name. The astrological symbol for the planet is also one of the alchemical symbols for the metal. Other symbols for mercury are shown in Fig. 2-2. The modern chemical symbol for mercury is Hg. It comes from hydrargyrum, a Latinized form of the Greek word `Υδραργυρος (hydragyros), which is a compound word meaning 'water' and 'silver' – since it is liquid, like water, and yet has a silvery metallic sheen.

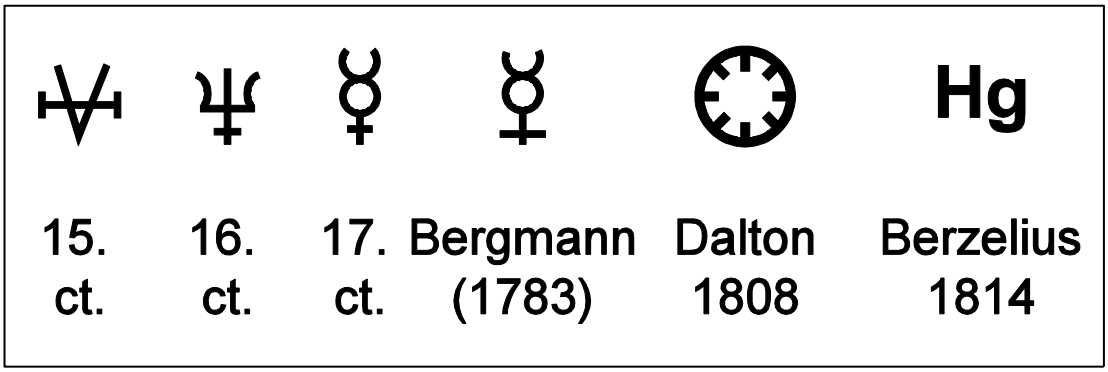

Fig. 2-2 Symbols for the element mercury at different times.

More than 20 mercury minerals are known, of which the most important ones are cinnabar (HgS) and Levingstonite ($Hg[Sb_4S_7]$). Occasionally, mercury also occurs native as small droplets, enclosed in rocks.
The most famous cinnabar deposit is in Almadén, Spain, which had been mined since Roman times. Other major cinnabar deposits are/were at Idria, Slovenia, and at Huancavelica, Peru. The ore of Almadén contained 3.5 % Hg in the upper layers and up to 14 % Hg in the deeper layers. In general, the mean content of Hg in ores lies between 0.2 and 1 % (Falbe and Regitz, 1995). However both Idria and Almadén have been shut down due to the fall of the price of mercury.

The process for extracting mercury from its ores has not changed much to the rules Aristotle first described over 2,300 years ago. Cinnabar ore is crushed and heated. The heated cinnabar (HgS) reacts with the oxygen (O_2) in the air to produce sulphur dioxide (SO_2), allowing the mercury to rise as a vapor (Eq. 2-2). This process is called roasting. The mercury vapor is then cooled, condensed, and collected. Almost 95 % of the mercury content of cinnabar ore can be recovered using this process.

$$HgS + O_2 \rightarrow Hg + SO_2 \qquad \text{(Eq. 2-2)}$$

Worldwide mercury mining annually produces around 1000 tons of the metal. In 2004 it was around 2000 tons. The top producers are China, Kyrgyzstan, and Algeria (British Geological Survey, 2010).

2.4 Anthropogenic and Natural Mercury Sources

Global mercury emissions have increased substantially at least during the past 100 to 150 years (Fig. 2-4) and they have accumulated in various ecosystems (Hudson et al., 1995; Fitzgerald et al., 1998). Evaluating the impact of anthropogenic emissions requires a precise knowledge about both natural and anthropogenic sources and emissions. In Fig. 2-3, a schematic description of the main source types is presented (modified after AMAP/UNEP, 2008). The primary anthropogenic sources are those where mercury of geological origin is mobilized. The two main source categories of this type are mining and extraction of fossil fuels. The secondary anthropogenic sources are those where emissions occur from the intentional use of mercury. Primary natural sources, are defined as those where mercury of geological origin is released via natural processes. In addition to these source types, the distribution of mercury is affected by its remobilization and re-emission pathways. In the latter case, mercury released can be of either natural or anthropogenic origin and it is currently not possible to experimentally distinguish between the two.

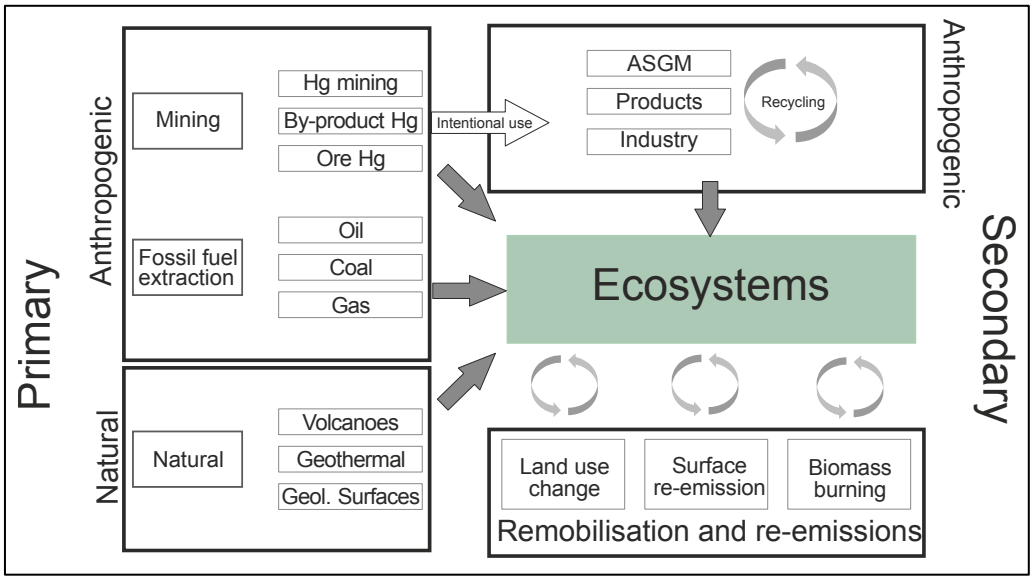

Fig. 2-3 Schematic description of emissions sources types and remobilization processes affecting mercury distribution in the environment. ASGM: Artisanal Gold Mining. Modified after AMAP/UNEP, 2008.

A current estimate of global mercury emissions suggests that the contribution from natural sources (primary emissions + re-emissions) is around 5207 t a^{-1}, and from primary and secondary anthropogenic sources is around 2320 t a^{-1}, resulting in an overall contribution of 7527 t a^{-1} (Pirrone et al., 2010).

2.4.1 Anthropogenic Mercury Sources

The anthropogenic use of Hg already began more than 2000 years ago with the onset of mercury mining in Spain (Hernández, 1999; Martínez-Cortizas, 1999; Higueras, 2006). A model of the historical anthropogenic Hg emission since 1500 A.D. is shown in Fig. 2-4.

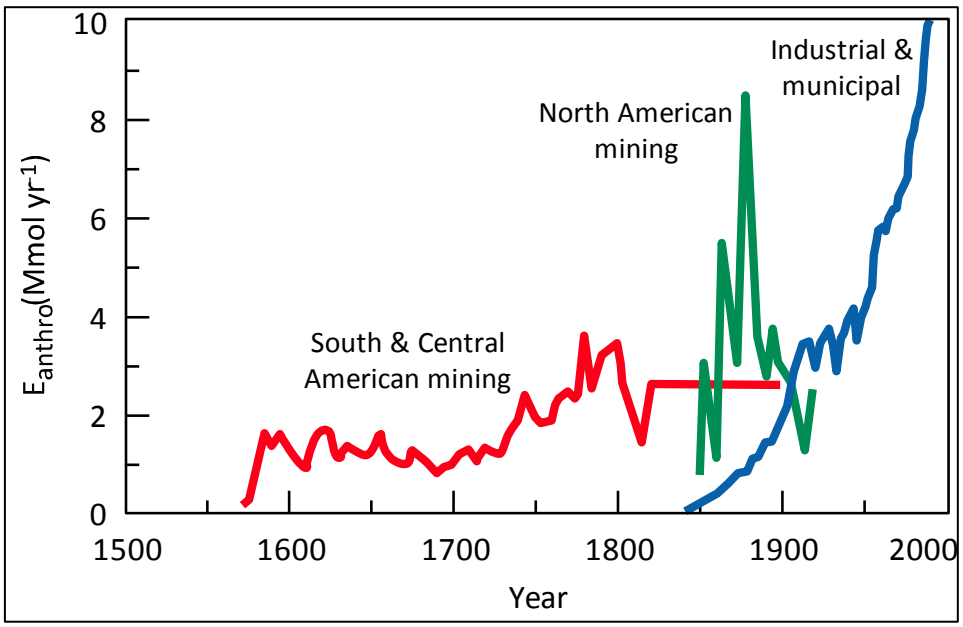

Fig. 2-4 Historical anthropogenic Hg emission since 1500 (after Hudson *et al.*, 1995).

Recent anthropogenic emissions were estimated to be around 1660 t a^{-1} for the year 1990 (Pacyna and Pacyna, 1996) and 2200 t a^{-1} for the year 1992 (Pirrone et al., 1996b). In a most recent study, Pirrone et al. (2010) estimated anthropogenic sources to account for 2320 t a^{-1}. The main types of anthropogenic emission sources may be categorized as shown in Tab. 2-3.

Tab. 2-3 Categories of Anthropogenic Emission Sources (after Porcella et al., 1996).

Category	Type of Anthropogenic Emission
Combustion	fossil fuels (coal, oil, gas, wood), waste (municipal, medical, hazardous), sewage sludge, crematories
High-Temperature-Processes	Smelting, coking, ore roasting, cement and lime production
Manufacturing/commercial	chlor-alkali plants, metal processing, chemical and instruments industry (Hg containing chemicals, paints, batteries, thermometers, process reactants, and catalysts)
Gold Extraction	
Other Sources	fluorescent tube, hazardous and municipal waste sites, mine spoils, land disturbance (e.g. deforestation, reservoir construction)

A summary of atmospheric emissions of mercury from anthropogenic sources in different continents is presented in Fig. 2-5 (AMAP/UNEP, 2008).

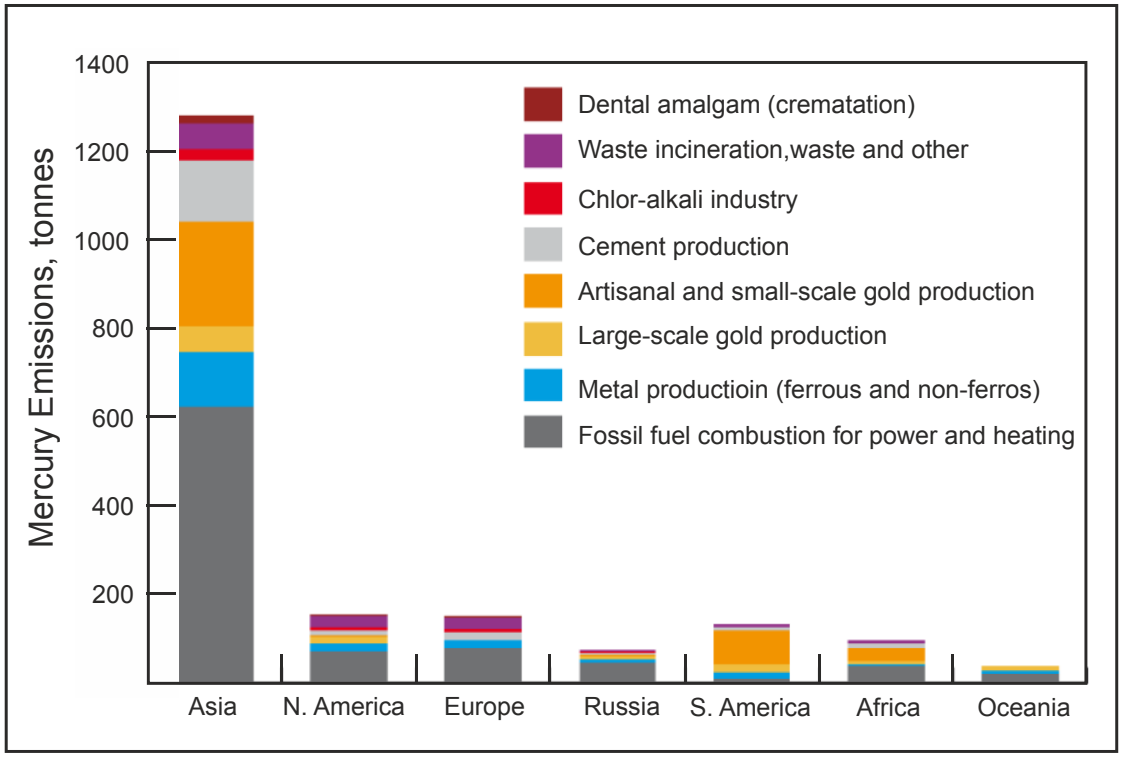

Fig. 2-5 Global anthropogenic emissions of mercury to air in 2005 from different continents by sector (AMAP/UNEP, 2008).

2.4.2 Natural Mercury Sources

The assessment of truly natural mercury sources and their relative importance compared to direct anthropogenic emissions and indirect (re)emissions is a fundamental problem in studying the global balance and cycling of mercury in the environment. There are numerous environmental pathways exchanging Hg with the atmosphere coming to mind when thinking of “natural” processes:

- Hg degassing from Hg containing rock erosion
- Volcanic eruptions and other geothermal activity
- Evasion of Hg from the Earth’s subsurface crust
- Hg degassing from soil erosion
- Hg degassing from oceans and freshwater ecosystems

Among these, however, only the first three are clearly and unambiguously natural and not influenced by anthropogenic activity. They could be classified as geological sources and

are also the only ones that are exclusively sources. The others are all to a certain extend influenced by human activities and are both sources and sinks of atmospheric mercury (Ebinghaus et al., 1999a).

It seems to be the general opinion that whenever elevated mercury concentrations are encountered in any ecosystem compartment in the absence of obvious local or direct anthropogenic sources, this can be interpreted as proof of an anthropogenic influence via atmospheric long-range transport and deposition. While this may be true in many cases, some of these anomalies may be caused, at least partially, by natural local emissions due to underlying geologic anomalies.

The magnitude of natural emissions is not as well-known as the anthropogenic emissions. Mason *et al*. (1994) estimate natural terrestrial emissions to be approx. 5 Mmol per year.

Other measurements and estimations about Hg emissions from different natural sources are given in Tab. 2-4. The great variation in estimations about natural Hg emissions shows that there is still a high demand for more profound knowledge on natural Hg sources and their emissions.

Tab. 2-4 Measurements and Estimations of Hg Emissions from different geological sources.

Source	Hg Amount	Reference
Hg-degassing from soils and rocks		
Mercuriferous belts	1–5 ng m^{-2} h^{-1}	Lindqvist *et al*., 1991
Temperate forest soils	10-50 ng m^{-2} h^{-1}	Lindberg *et al*., 1992, Kim *et al*., 1995
Over seismic zones	10-50 ng m^{-2} h^{-1}	Varekamp & Buseck, 1986
Cinnabar rich soils in Almadén, Spain	330 ng m^{-2} h^{-1}	Lindberg *et al*., 1979
Over geothermal zones in Nevada	50-10000 ng m^{-2} h^{-1}	Gustin & Lindberg, 1997
Siberia (Area: 10^7 km^2)	40 t a^{-1}	Obolensky, 1996
Total Earth's continents	700 t a^{-1}	Lindqvist *et al*., 1991
Evasion from the earth's crust		
Continental crust	3000-6000 t a^{-1}	Rasmussen, 1994
Mid-ocean ridge	1900-3800 t a^{-1}	Rasmussen, 1994
Oceanic crust	7300-14700 t a^{-1}	Rasmussen, 1994
Total geological sources	2500-30000 t a^{-1}	Lindqvist et al., 1984
Total geological sources	3000 t a^{-1}	Nriagu & Pacyna, 1988
Total geological sources	5 Mmol a^{-1}	Mason et al., 1994

Tab. 2-4 continued.

Source	Hg Amount	Reference
Volcanic eruptions and other geothermal activities		
Volcanic eruptions (total)	830 t a^{-1}	Varekamp & Buseck, 1986
Volcanic eruptions (total)	20-90 t a^{-1}	Fitzgerald, 1996
Solfatara-Volcano, Italy	0.3-1.6 kg a^{-1}	Ferrara *et al*., 1994
Kilauea-Volcano, Hawaii	1.5 kg a^{-1}	Varekamp & Buseck, 1986
Kolima-Volcano, Mexico	440 kg a^{-1}	Varekamp & Buseck, 1986
Etna-Volcano, Italy	2700 kg a^{-1}	Varekamp & Buseck, 1986
Volcanic geyser on Iceland	8 kg a^{-1}	Edner *et al*., 1991
Above a geothermal area in the Western USA	10-1000 ng m^{-2} h^{-1}	Gustin & Lindberg, 1997
Global emissions of geothermal sources	60 t a^{-1}	Varekamp & Buseck, 1986
Total volcanoes and geothermal activities	90 t a^{-1}	Mason, 2009

The current estimate of mercury emissions from natural processes, which comprises both primary mercury emissions and re-emissions is shown in Tab. 2-5 (Pirrone et al. 2010).

Tab. 2-5 Global mercury emissions by natural sources estimated for 2008 (Pirrone et al. 2010).

Source	Mercury [t a^{-1}]	Contribution [%]
Oceans	2682	52
Lakes	96	2
Forests	342	7
Tundra/Grassland/Savannah/Prairie/Chaparral	448	9
Desert/Metalliferous/Non-vegetated Zones	546	10
Agricultural areas	128	2
Evasions after mercury depletion events	200	4
Biomass burning	675	13
Volcanoes and geothermal areas	90	2
TOTAL	**5207**	**100**

2.5 Global Mercury Cycle

Mercury is emitted into the atmosphere from a number of natural as well as anthropogenic sources. In contrast to most of the other heavy metals, mercury and many of its compounds behave exceptionally in the environment due to their high volatility. Hence, it is dispersed intra- as well as interhemispherically. This dispersion is mainly contributed by elemental mercury (Hg^0) (Slemr *et al.*, 1985; Nriagu & Pacyna, 1988; Mason *et al.*, 1994), which has a high vapor pressure and a relatively low solubility in water. In this form mercury has an atmospheric residence time of at least a few months, maybe even one or two years, and is uniformly distributed throughout the troposphere (Lindqvist and Rohde, 1985). The global dispersion on Hg and its sources and sinks was modelled by Mason *et al.* (1994). Fig. 2-6 (after Mason *et al.*, 1994) shows Hg contents in different environmental compartments and annual flux rates from present and pre-industrial time.

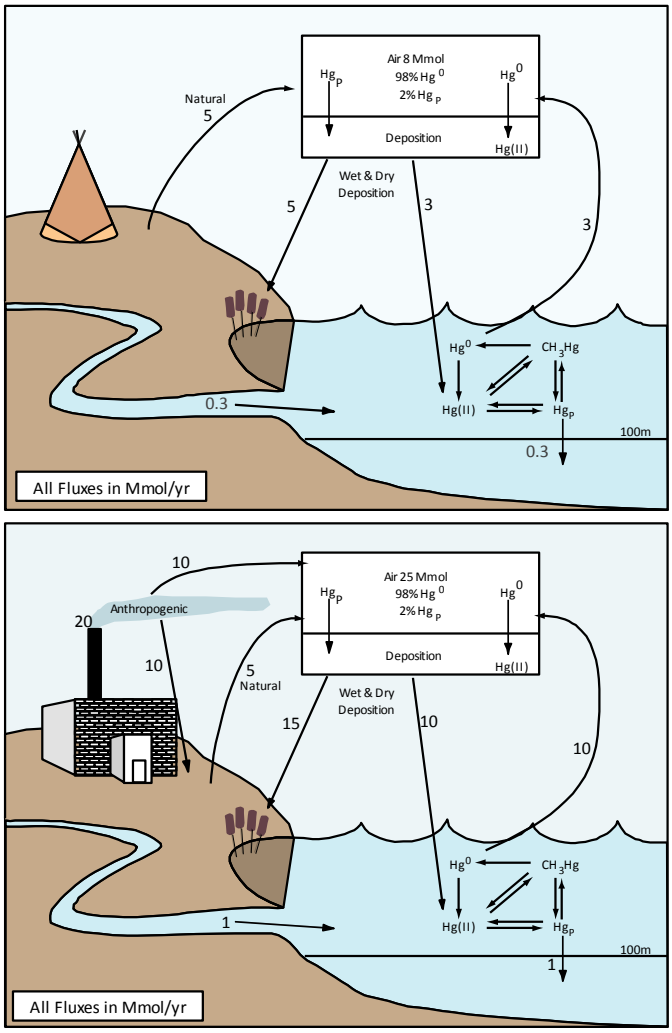

Fig. 2-6 **Global mercury cycle to pre-industrial and recent times (after Mason et al., 1994).**

Due to the anthropogenic influence, the Hg amount in the atmosphere has been tripled. Mean concen trations in the atmosphere are now adays ca. 1.6 ng m^{-3}. Preindustrial concentrations are estimated to be ca. 0.5 ng m^{-3} (Mason et al., 1994). The fraction from anthropogenic sources is estimated to be 70 – 80 % (Mason et al., 1994). Nevertheless, due to the fact that approximately 50 % of anthropo genic emissions are deposited on a local or regional scale they do not contribute to the global cycle.

Fig. 2-6 also shows that the deposition of Hg occurs to 60 % over continents and only to 40 % over oceans – even though the oceans cover 70 % of the earth's surface. Mason et al. (1994) explain this by two different possible

mechanisms of the oxidation of Hg^0 to the deposable Hg(II). Oxidation possibly occurs in clouds (Munthe, 1992; Munthe & McElroy, 1992) as well as with aerosols (Mason et al., 1992). The aerosol bounded oxidation occurs almost exclusively over continents and thus generate the different deposition rates between oceans and continents.

Slemr et al. (1985), Fitzgerald (1989), Slemr and Langer (1992), and Fitzgerald (1995) show a clear gradient of Hg concentration in the atmosphere between the Northern and the Southern Hemisphere (Fig. 2-7). Temme (2003) affirms the same gradient.

This clear difference between the Hg concentrations of the two hemispheres are explained by two arguments. First it results from the arrangement of landmass being the main emission source covering ca. 43 % of the Northern Hemisphere, but only about. 28 % of the Southern Hemisphere. Additionally, it represents the difference in anthropogenic activities between the Northern and Southern Hemisphere.

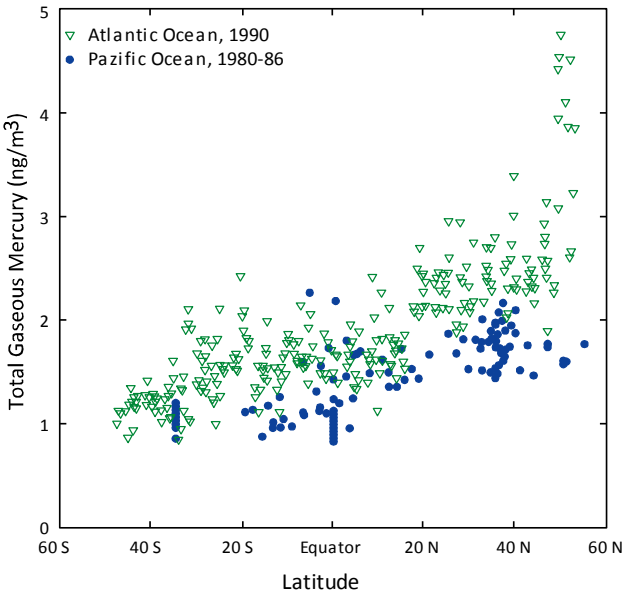

Fig. 2-7 **Distribution of TGM over the Atlantic and Pacific Oceans. Data from Slemr and Langer, 1992 and Fitzgerald, 1989 in Fitzgerald, 1995.**

Mason et al. (1994) show in their study the difference between exchange rates between the atmosphere and oceans on the one hand and between the atmosphere and continents on the other hand. While all into the oceans deposited Hg will be reemitted nearly completely, the terrestrial deposited Hg will be fixed within soils, which are the main sinks for Hg. It will be reemitted to the atmosphere or to waters very slowly (Fig. 2-6). A reduction of anthropogenic Hg emission therefore does not lead to a direct decline of the global contamination.

2.6 Atmospheric Mercury and Transformation Processes

Mercury is an atmospheric pollutant with a complex biogeochemical cycle. The atmospheric cycling includes chemical oxidation/reduction in both gaseous and aqueous phases, deposition and re-emission from natural surfaces in addition to emissions from both natural and anthropogenic sources (Schroeder and Munthe, 1998). In the atmosphere, mercury primarily exists as inorganic mercury in the two oxidation states Hg^0 and Hg(II). Only a small part exists as organic mercury; < 3 % of the total mercury; besides in the direct vicinity of emission sources; (Slemr et al., 1985; Fitzgerald et al., 1991; Lee and Iverfeldt, 1991; Lamborg et al., 1995; St.Louis et al., 1995). Mercurous (Hg(I)) compounds are very instable (Schroeder et al., 1998).

The three dominant forms of mercury in the atmosphere are: gaseous elemental mercury, gaseous divalent mercury (Hg(II)), and particulate phase mercury (Hg(p)). The three different species have different atmospheric behaviour and lifetimes. Hg^0 is relatively inert to chemical reactions with other atmospheric constituents, and is only sparingly soluble in pure water. This gives elemental mercury an atmospheric residence time between 0.5 and 2 years. (Slemr et al., 1985; Lindqvist and Rhode, 1985; Schroeder and Munthe, 1998). Thus, once released to the atmosphere mercury can be dispersed and transported for long distances over hemispheric and global scales. Long-range transport has been shown to be an important source of mercury in many remote regions (Brosset, 1987; Iverfeldt, 1991a; Petersen et al., 1995). It is vertically well mixed in the troposphere (Banic et al., 1997; Ebinghaus and Slemr, 2000; Temme, 2003) and its typical concentration is ~1-4 ng m^{-3} at background sites (Slemr and Langer, 1992; Lin and Pehkonen, 1999).

Hg(II) and Hg(p) are more readily deposited on local to regional scales via wet or dry deposition. Hg(II) has a residence time of only days to weeks (Slemr et al., 1981; Lindqvist and Rhode, 1985). Some of the gas-phase oxidized mercury such as $HgCl_2$ or $HgBr_2$ is highly water soluble, reactive, and less volatile than Hg^0, so is often called reactive gaseous mercury (RGM). The amount of reactive gaseous mercury in the atmosphere is typically less than 5 % of the total mercury concentration, but RGM is very important with respect to mercury deposition (Lindberg and Stratton, 1998).
Mercury deposition occurs either directly as Hg^{2+} and particulate mercury (Hg(p)) or indirectly as Hg^0 after Hg^0 is converted to Hg^{2+} through oxidant mediated reactions mainly in cloud droplets (Finlayson-Pitts and Pitts, 1986; Munthe, 1992; Lin and Pehkonen, 1997).

Tab. 2-6 Comparison of Hg^0 and Hg(II) behavior and reactions in the atmosphere.

	Hg^0	Hg(II)
Fraction of atmospheric Hg	>90 %	<10 % of total Hg < 3 % of total gaseous Hg
Atmospheric Form	Dominant form of the gas phase	Primarily in dissolved form or bond to particles
Residence time	0.5 – 2 years	Days – weeks
Way of transport	> 10000 km	10 – 1000 km
Deposition	Dry	Wet and dry

Due to the different residence times and depositional behaviour of the different species (Tab. 2-6), chemical transformations in the atmosphere are the key factor for the understanding of the global mercury cycle.

The most important reactions that occur in the atmosphere are shown in Fig. 2-8 and are listed in Tab. 2-7.

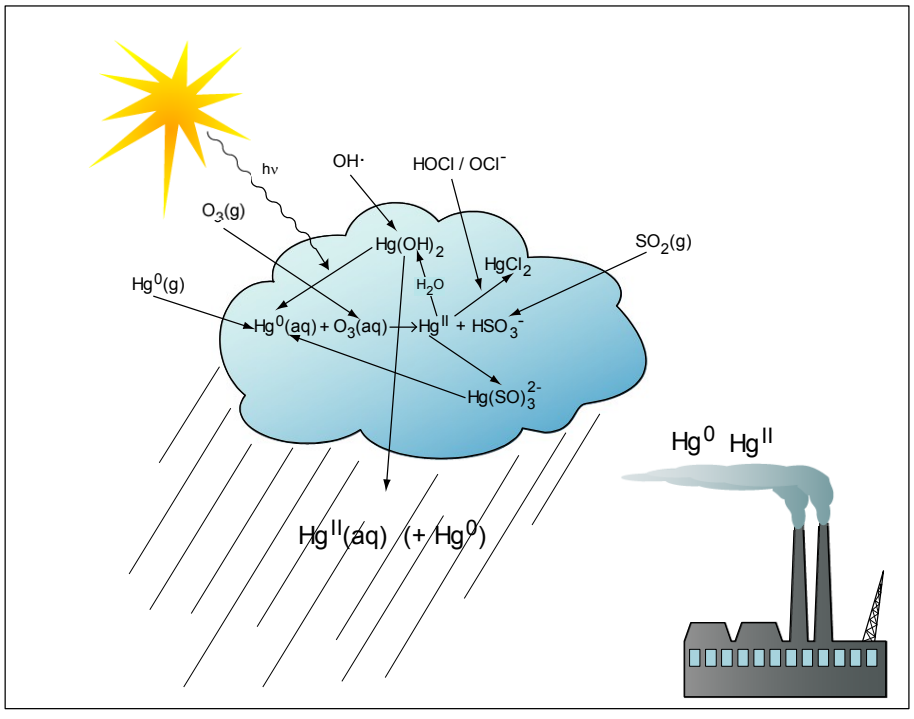

Fig. 2-8 Schematic diagram of the most important transformation processes of mercury in the atmosphere (after Lindqvist, 1991).

Tab. 2-7 Atmospheric reactions (modified after Temme, 2003)

Type of Reaction	Reaction	Literature
Oxidation in the gas phase	$Hg^0(g) + O_3(g) \rightarrow HgO(g,s) + O_2(g)$	Hall, 1995
	$Hg^0(g) + NO_3^{\bullet}(g) \rightarrow HgO(g,s) + NO_2(g)$	Sommar et al., 1997
	$Hg^0(g) + Cl_2(g) \rightarrow HgCl_2(g)$	Stein et al., 1996
	$Hg^0(g) + H_2O_2(g) \rightarrow Hg(OH)_2(g,s)$	Tokos et al., 1998
	$Hg^0(aq) + {}^{\bullet}OH(g) \rightarrow {}^{\bullet}HgOH(g)$ ${}^{\bullet}HgOH(g) + O_2(g) \rightarrow HgO(g,s) + HO_2^{\bullet}(g)$	Sommar et al., 2001
Oxidation in the liquid phase	$Hg^0(aq) + O_3(aq) + H_2O \rightarrow Hg^{2+}(aq) + 2OH^-(aq) + O_2(aq)$	Iverfeldt & Lindqvist, 1986
	$Hg^0(aq) + H_2O_2(aq) + 2H^+ \rightarrow Hg^{2+}(aq) + 2H_2O$	Iverfeldt & Lindqvist, 1986
	$Hg^0(aq) + O_3(aq) + H^+(aq) \rightarrow Hg^{2+}(aq) + OH^-(aq) + O_2(aq)$	Munthe, 1992
	$Hg^0(aq) + {}^{\bullet}OH(aq) \rightarrow Hg^+(aq) + OH^-(aq)$ $Hg^+(aq) + {}^{\bullet}OH(aq) \rightarrow Hg^{2+}(aq) + OH^-(aq)$	Lin & Pehkonen, 1997
	$Hg^0(aq) + HOCl(aq) \rightarrow Hg^{2+}(aq) + OH^-(aq) + Cl^-(aq)$	Lin & Pehkonen, 1999
Reduction in the liquid phase	$Hg^{2+}(aq) + SO_3^{2-}(aq) \leftrightarrow HgSO_3(aq)$ $HgSO_3(aq) \rightarrow Hg^0(aq) + Products$	Pleijel and Munthe, 1995
	$Hg^{2+}(aq) + HO_2^{\bullet}(aq) \rightarrow Hg^+(aq) + O_2(aq) + H^+(aq)$ $Hg^+(aq) + HO_2^{\bullet}(aq) \rightarrow Hg^0(aq) + O_2(aq) + H^+(aq)$	Pehkonen & Lin, 1998
Photoreduction in the liquid phase	$Hg(OH)_2(aq) \xrightarrow{hv} Hg^0(aq) + products$	Xiao et al., 1994
Equilibrium	$Hg^{2+} + 2Cl^- \leftrightarrow HgCl_2$	Lin & Pehkonen, 1999
	$Hg^{2+} + 4Cl^- \leftrightarrow [HgCl_4]^{2-}$	Lin & Pehkonen, 1999
	$Hg^{2+} + 2OH^- \leftrightarrow Hg(OH)_2$	Lin & Pehkonen, 1999
	$Hg^{2+} + SO_3^{2-} \leftrightarrow HgSO_3$	Lin & Pehkonen, 1999
	$Hg_2^{2+} \leftrightarrow Hg^0 + Hg^{2+}$	Munthe and McElroy, 1992

2.6.1 Reactions in the Gas Phase

The dominant reaction of atmospheric mercury is the oxidation of Hg^0 to Hg(II). This transformation allows a subsequent complexation of mercury with different anions, which leads to a better solubility. Increased concentrations of atmospheric oxidants accelerate these reactions (Iverfeldt and Lindqvist, 1986; Lindberg, 1986). The troposphere comprises many potential oxidants, which can react with Hg^0, e.g. O_2, O_3, H_2O_2, and NO_2, but as well radicals like $NO^{\bullet}_3$, $^{\bullet}OH$, $HO^{\bullet}_2$, and $RO^{\bullet}_2$.

Many different reaction mechanisms for the oxidation of Hg^0 to Hg(II) in the gas phase are studied in the last years. However, there are only a few studies about the kinetics of these reaction and many existing data are not verified yet.
The most important gas phase oxidation pathways are the reactions with ozone (Hall, 1995) and $^{\bullet}OH$ radicals (Sommar et al., 2001).
Hall (1995) examined the reaction with ozone (Tab. 2-7) under different conditions in laboratory.
This reaction is slower than some other gas phase reactions, but the relatively high concentrations of ozone found in the troposphere with respect to other oxidant compounds makes it the most important. Only regarding this reaction, Hall calculated a mean residence time of Hg in the atmosphere to be ca. 1.4 years (Hall, 1995).
New data by Sommar et al. (2001) show that it could be reasonable to include $^{\bullet}OH$ as potential oxidant for the modeling of the global atmospheric Hg cycle (Tab. 2-7). Their results show a fast oxidation of gaseous Hg^0 by $^{\bullet}OH$. The calculation with an averaged global $^{\bullet}OH$ concentration (Krol et al., 1998) leads to a residence time of atmospheric mercury of 4 to 7 months (Sommar et al., 2001).
However, as experimentally determined the reaction of Hg^0 with ozone (Hall, 1995) is to slow to be the main mechanism for the removing of Hg from the atmosphere (Bergan and Rhode, 2001) and the simulated reaction with $^{\bullet}OH$ and $^{\bullet}HgOH$ (Sommar et al., 2001) is too fast. The residence time of Hg in the atmosphere is a result of a complex interaction between many compounds and reactions, which still have to be scope of prospective studies. Important atmospheric reactions of mercury are listed in Tab. 2-7.

Oxidation of Hg^0 leads to Hg(II) species which are notably less volatile than Hg^0 and will tend to condense onto atmospheric particulate matter or be deposited to marine or terrestrial surfaces. Some of the listed oxidation reactions might have an important influence on the formation of particulate phase mercury. As mentioned, HgO is the primarily product of the gas phase reaction of Hg with O_3, $^{\bullet}OH$, and other oxidants

(Schroeder et al., 1991; Hall, 1995; Sommar et al., 2001). The vapor pressure of HgO is very low ($9.2 \cdot 10^{-12}$ Pa at 25 °C; Schroeder and Munthe, 1998). Thus, HgO will probably transfer into a solid phase. Due to the low concentration of HgO in the atmosphere the condensation of pure HgO is impossible. Hence, an adsorption on aerosol particles is presumably (Schroeder et al., 1998).

Many atmospheric pollutants can be directly transformed or abolished due to photochemical reaction. Schroeder et al. (1991) examined the absorption of wavelengths > 253.7 nm by elemental mercury by measuring the absorption cross-section (σ). They could not find any absorption and hence no proof for photochemical oxidation of Hg^0. Sunlight of shorter wavelengths (<290 nm) is filtered out by a variety of ionisation reactions within the stratosphere (e.g. in the ozone layer). Hence, Hg^0 cannot be oxidized directly via photochemical reaction in the troposphere.

However, due to the depletion of the stratospheric ozone layer, the intensity of shorter wavelengths (e.g. UV-B) in the troposphere has risen during the last decades. To what extend this circumstance influences a possible photochemical reaction of Hg still has to be examined.

2.6.2 Reactions in the Aqueous Phase

Elemental mercury is present in atmospheric water, whether it occurs as fog or cloud water or the water associated with deliquesced aerosol particles. The Henry's Law constant for mercury is low, so the elemental mercury concentration in atmospheric water should reach equilibrium with the gas phase concentration rapidly, if no particularly rapid reactions of elemental mercury occur in the aqueous phase. The possible Hg^0 concentration in water is calculated to be between 3 and 16 pg L^{-1} (Stein et al., 1996; Lin and Pehkonen, 1999). The measured Hg in precipitation, however, reaches concentrations up to 1000 ng L^{-1}. This implies that mercury species exist in the atmosphere, that are much more soluble in water than Hg^0. These species are products of various reactions in the aqueous phase. These reactions are generally faster by several magnitudes than the accordant reactions in the gas phase (Lin and Pekhonen, 1999).

Possible oxidants for the oxidation of Hg^0 to Hg(II) in the aqueous phase are O_3, H_2O_2 (Iverfeldt and Lindqvist, 1986; Munthe, 1992), $^{\bullet}OH$ radicals (Lin and Pehkonen, 1997), and HOCl (Lin and Pehkonen, 1999). The reaction between Hg^0 and O_3 is supposed to be the most important oxidation process in the aqueous phase (Seigneur et al., 1994).

Oxidised Hg in atmospheric water is usually found complexed with SO_3^{2-}, OH^-, or Cl^- ions, the concentration of the various complexes depending on the origin of the aqueous phases. In most cases, apart from sea-salt aerosol, the concentration of Cl^- ions is low and OH^- and SO_3^{2-} complexes are predominant. The greater solubility and lower volatility of Hg(II) with respect to Hg^0 means that Hg(II) does not generally outgas from the aqueous phase in any significant fashion, although recent research suggests that $HgCl_2$ outgassing from the marine aerosol may be an important process in the marine boundary layer (Hedgecock and Pirrone, 2001).

Hg(II) in fog and raindrops may adsorb to particulate matter scavenged by the droplets. This is particularly likely if the particulate matter is rich in elemental carbon (soot) as the adsorption coefficient for Hg on soot is high (Petersen et al., 1998; Pirrone et al., 2000).
Reduction of Hg(II) in the aqueous phase may occur by the reaction with SO_3^{2-} (Tab. 2-7; Pleijel and Munthe, 1995). SO_3^{2-} exists in the atmosphere due to the elution of the emitted pollutant SO_2. However, because of the short residence time of SO_3^{2-} in clouds or fog, the contribution of SO_3^2 to the Hg^0 production is generally low.
A possible photo reduction of $Hg(OH)_2$ to Hg^0 is shown in Tab. 2-7 (Xiao et al., 1994). However, this reaction is supposed to have only minor effects on the production of Hg^0.

2.7 Definition of the most important Hg Fractions

A particular aspect of mercury is that it exists in the environment in a number of different chemical and physical forms with different behavior in terms of transport and environmental effects (Schroeder and Munthe, 1998). Large research efforts have been put into the identification and quantification of these species over the last decades (e.g. Braman and Johnson, 1974; Brosset, 1982, 1987; Brosset and Lord, 1995; Stratton and Lindberg, 1995).

In the atmosphere, the main three forms of Hg are: elemental Hg vapor (Hg^0), reactive gas phase Hg (RGM) and particulate phase mercury (TPM) (Tab. 2-8). Of these three fractions, only Hg^0 has been tentatively identified with spectroscopic methods (Edner et al. 1989) while the other two are operationally defined species, i.e. their chemical and physical structure cannot be exactly identified by experimental methods but are instead characterized by their properties and capability to be collected by different sampling equipment. RGM is defined as water-soluble mercury species with sufficiently high vapor pressure to exist in the gas phase (Munthe et al., 2001). The reactive term refers to the

capability of stannous chloride to reduce these species in aqueous solutions without pre-treatment. The speciation of RGM is not known in detail but based on laboratory studies and the methods of its collection, it is assumed to consist of gaseous neutral Hg(II) complexes, such as $HgCl_2$, $HgBr_2$, HgClBr, HgClO, HgBrO, and possibly other divalent mercury species (Ariya et al., 2002; Balabanov and Peterson, 2003). TPM consists of mercury bound or adsorbed to atmospheric particulate matter. Several different components are possible. Hg^0 or RGM adsorbed to the particle surface, divalent mercury species chemically bound to the particle or integrated into the particle itself (Brosset, 1987).

Tab. 2-8 Different mainly operationally defined mercury species, their acronyms and definitions.

Acronym	Name	Definition and Species
TGM	Total Gaseous Mercury	GEM + RGM; Species passing through a 0.45 µm filter and which are collected on gold
GEM	Gaseous Elemental Mercury	Hg^0
RGM	Reactive Gaseous Mercury	Water-soluble, reactive Hg(II) compounds with a vapor pressure being high enough to allow the compounds to stay in the gas phase; e.g. HgX_2, $HgSO_4$, CH_3HgCl, $(CH_3)_2Hg$, (HgO) etc.
DGM	Divalent Gaseous Mercury	
GOM	Gaseous Oxidised Mercury	
PHg	Particulate Mercury	Mercury which is chemically bond with or adsorbed on particles
TPM	Total Particulate Mercury	
PPM	Particulate Phase Mercury	
Hg_P	Mercury, particular	
PM	Particulate Mercury	

2.8 Sampling and Analytical Methods

In the last few years, new automated and manual methods have been developed to measure TGM (Tekran, Inc.; Urba et al., 1995), RGM (Tekran, Inc.; Stratton and Lindberg, 1995; Feng et al., 2000), and TPM (Keeler et al., 1995; Lu et al., 1998). These developments offer the possibility to determine both urban and background concentrations of TGM, RGM, and TPM (EU-Position Paper, 2001).

In order to compare different methods used to determine the level of mercury and its compounds in air a number of field intercomparisons have been performed (e.g. Ebinghaus et al., 1999b; Munthe et al., 2001). A major conclusion from these studies is that ambient levels of TGM can be measured with relatively high accuracy whereas TPM and especially RGM are more complex. Although the basic techniques available for measurements of TPM and RGM have proven to be reliable in research projects, further work on standardization is clearly warranted before they can be applied to routine measurements or monitoring.

2.8.1 TGM Measurements

TGM Measurements can either be performed by automated or by manual methods.
The most common automated methods currently available are the Tekran Gas Phase Mercury Analyzer (Tekran, Inc.) and the Gardis Mercury Analyzer (Urba et al., 1995, 1998).

At the Tekran Analyzer (Model 2537A) pre-filtered sample air is passed through gold cartridges where the mercury is collected. The mercury is then thermally desorbed, transferred in an argon stream, and detected by means of atomic fluorescence spectrometry. The instrument utilizes two gold cartridges in parallel, with alternating operation modes (sampling and desorption/analyzing) on a predefined time between 5 and 15 minutes. With a sampling flow between 1 and 1.5 L min^{-1} a detection limit of 0.15 ng m^{-3} is achieved. The accuracy and the precision of the Tekran has been assessed in international intercomparisons (Schroeder et al., 1995a; Schroeder et al., 1995b; Ebinghaus et al., 1999b; Munthe et al., 2001).

The Gardis instrument is based on gold amalgamation and Atomic Absorption Spectrometry detection (Urba et al., 1995). The Gardis operates with ambient air as carrier gas and does not require Argon for detection. The sampling is run at about 1 L min^{-1}, with sampling times of 10 minutes. Under these conditions, a detection limit of about 1 ng m^{-3} is achieved. This instrument has been part of intercomparisons (Urba et al., 1998; Ebinghaus et al., 1999b, Munthe et al., 2001).

The manual methods are based on gold (or silver) trap amalgamation. The samples are manually analyzed using thermal desorption and cold vapor atomic fluorescence spectrometry (Brosset, 1987; Bloom and Fitzgerald, 1988). Samples are collected on a trap consisting of a quartz glass tube containing a mixture of small pieces of gold wire

and quartz glass grains. Alternatively, the adsorbing material may consist of gold-coated quartz glass grains. The airflow is normally > 0.5 L min^{-1}. With 24 h sampling time the detection limit is typically 0.01 ng m^{-3}.

2.8.2 RGM Measurements

The transport and deposition of atmospheric mercury depends strongly on its speciation. Beside elemental (Hg^0) gaseous oxidized Hg-species (defined as Reactive Gaseous Mercury (RGM) are of great importance due to their high water solubility and high deposition velocity. Furthermore models on mercury transport and deposition are highly sensitive to assumptions of the fraction of mercury present as RGM (Petersen et al., 1989).

Due to the fact that the fraction of RGM in the atmosphere is very small (<3 % of total gaseous mercury) and that no reference materials or adequate standards for the collection part of the RGM analytical systems are available, it is crucial to define precisely the methodology used. In the last time, there have been at least three collection methods used for RGM sampling: a multi-stage filter pack method (Bloom et al., 1996), a refluxing mist chamber method (Stratton and Lindberg, 1995; Lindberg and Stratton, 1998; Stratton et al., 2001), and a KCl-coated denuder method (Xiao et al., 1997; Feng et al., 2000; Landis et al., 2002a).

None of these methods are considered standard, as each method has advantages and disadvantages. For the filter pack method, particulate mercury (Hg_p) is removed from the air stream by the first two Teflon filters with the RGM collected by the cation-exchange membranes positioned behind. Therefore, both Hg_p and RGM are collected simultaneously. The main disadvantage of this method is the long sampling time required, usually 24 h, to obtain sufficient RGM for analysis since the flow rate is relatively low. Volatilization of collected Hg_p and its subsequent collection by the cation-exchange membrane is another concern, although it has been demonstrated not to be a problem for other volatile species, such as HNO_3, HCl, and NH_3 (Harisson and Kitto, 1990). If oxidation of Hg^0 by heterogeneous reactions occurred on the filter surface, this would also cause a positive artifact. The extent of this problem is not clear. Adsoprtion of RGM onto the particle-removing filters at low flow rates is also possible. For example, adsorption of $HgCl_2$ onto quartz fiber filters has been observed in the lab (Bloom et al., 1996), but Stratton et al. (2001) found no bias in field measurements with or without filters in front of the refluxing mist chamber. While there is little field evidence to support

adsorption, if these types of artifact did happen in field they would jeopardize almost all filter pack RGM measurements.

The refluxing mist chamber allows higher flow rates and thus shorter sampling time, usually between 30 and 300 min. However, the scrubbing solution (dilute HCl) not only removes RGM from the air stream but also other water-soluble gases, some of which may react with Hg^0 or RGM and cause either positive or negative artifacts. The composition of the scrubbing solution, especially the concentration of chloride, does influence the amount of RGM collected (Stratton et al., 2001). A Teflon filter can be attached to the chamber inlet to remove particles. Again, this filter may cause artifacts that have been discussed above.

The denuder method also allows higher flow rates and shorter sampling time. Two types of denuders have been developed: the tubular denuders (Xiao et al., 1997) and the annular denuders (Stevens et al., 1999; Landis et al., 2002a). For the annular denuders, particles larger than 2.5 µm are removed from the air stream by a cyclone before entering the denuder, and smaller particles pass through without deposition under the proper flow rate because of the laminar conditions inside the denuder. Adsorption of Hg^0 is a potential positive artifact for the denuder method. Xiao et al (1997) determined the Hg^0 breakthrough efficiency by spiking gaseous Hg^0 into the tubular denuder inlet and found that only 98.7 % of the spike was recovered downstream. This non-100 % breakthrough efficiency was interpreted as a result of system error and another experiment was conducted, which demonstrated that the denuder did not adsorb Hg^0 to any degree in the laboratory. The quality of KCl coating is important to collection efficiency and it may change over time when operated in the field, which resultant changes in Hg^0 adsorption. Just 1 % Hg^0 adsorption would be enough to compromise the measured RGM concentration.
In order to estimate whether these methods are directly comparable there have been various intercomparisons (e.g. Munthe et al., 2001, Sheu and Mason 2001).

2.8.3 TPM Measurements

TPM concentrations in ambient air are between less than 1 pg m^{-3} and some hundreds of pg m^{-3}. The low concentrations make the measuring of TPM difficult. The traditional procedure is to sample particles on fiber or membrane filters (Keeler et al., 1995). About 10 m^3 of ambient air is sampled with a sampling rate of 10 L min^{-1}. The filters are

analyzed via acid digestion where the mercury is dissolved as Hg(II). Afterwards the mercury is analyzed by reduction with $SnCl_2$ and measuring with CVAFS or CVAAS.

In recent years an alternative method has been developed by Lu et al. (1998). This mini trap is used both for sampling and for analyzing via pyrolysis. Therefore, the risk of contamination during transport and analysis is low. The trap consists of a small quartz glass fiber filter (Ø: 6 mm), which is held via a Teflon screen support within a quartz glass tube. The flow rate during the sampling is between 3.5 and 5.5 L min^{-1} and the sampling duration is between 12 and 48 hours (Lu et al., 1998). This technique has been tested in intercomparisons (Lu et al., 1998).

2.8.4 Mercury in Precipitation

Mercury in precipitation is determined by collection of precipitation in adequate samplers and subsequent analysis for total mercury concentration.
A summary of sampling techniques used in different monitoring networks is presented in Tab. 2-9. Two alternative materials for funnels and collection bottles are adequate for sampling or precipitation; glass and fluoropolymer such as Teflon (US-EPA, 2002).

Precipitation can be sampled using wide mouth jars or funnels and bottles. The sampling vessels can either be bulk samplers, which are open at all times, or wet-only samplers which are only open during precipitation events (see also Tab. 2-9). Wet-only samplers have the advantage that they avoid particle dry deposition, although the contribution of gaseous or particulate mercury species to the wet deposition fluxes in non-industrialized or non-urban areas is probably not large (Iverfeldt and Sjöberg, 1992; Iverfeldt and Munthe, 1993).

For extended sampling periods it is also necessary to prevent the diffusion of Hg^0 into the precipitation sample collected, since it could contribute to the mercury content of the sample via oxidation to water-soluble forms (EU-Position Paper, 2001). This can be done easily by using a capillary tube between the funnel and the bottle. It is also necessary to shield the sample bottles from light to avoid photo-induced reduction of the mercury in the precipitation sample.

The most reliable technique for the analysis of mercury in precipitation is by oxidation, subsequent reduction, purge and trap, and cold vapor atomic fluorescence spectrometry.

Atomic absorption spectrometry may be used but requires larger sample volumes due to the lower detection limit.

Detailed instructions for the accurate analysis can be found in the Method 1631 (US EPA, 2002), in Munthe, 1996 and in OSPAR, 1997.

Tab. 2-9 Sampling and analytical techniques used in different monitoring networks

Mercury Species	Sampling Techniques	Analytical Techniques	Literature
TGM	Tekran 2537 A Gardis Analyzer	Atomic Fluorescence spectrometry (CVAFS) Atomic absorption spectrometry (CVAAS)	Schroeder et al., 1995a,b Urba et al., 1995 Urba et al., 1998 Ebinghaus et al., 1999b Munthe et al., 2001
	Manual Method with Gold Trap Manual Method with Silver Trap	UV absorption spectrophotometry Atomic absorption spectrophotometry AAS Cold-Vapor techniques, AFS Atomic Emission Spectrometry (AES)	Brosset, 1987 Bloom & Fitzgerald, 1988 Schroeder et al., 1995a,b Ebinghaus et al., 1999b Munthe et al., 2001 Wängeberg et al., 2001
RGM	KCl-coated tubular denuders	Thermal desorption/ AFS (AAS)	Xiao et al., 1997 Sommar et al., 1999
	KCl-coated annular denuders	Thermal desorption/ AFS (AAS)	Sommar et al., 1999 Landis et al., 2002a
	Refluxing Mist-Chamber	$SnCl_2$-reduction/ AAS or AFS	Stratton & Lindberg, 1995 Lindberg & Stratton, 1998 Stratton et al., 2001
TPM	Filter (glass, polypropylene, cellulose, Teflon) AES-Mini-Traps with Quartz filters	Thermal desorption/ Pyrolysis/ amalgamation/ CVAAS or CVAAS	Schroeder et al., 1995a Keeler et al., 1995 Ebinghaus et al., 1995 Lu et al., 1998 Lu & Schroeder, 1999 a,b
Hg in Precipitation	Bulk-Sampler: Glass or Teflon funnel with glass or Teflon bottle	Oxidation, reduction, purge and trap, CVAFS or CVAAS	Iverfeldt, 1991b Jensen & Iverfeldt, 1994 Chazin et al., 1995 Ebinghaus et al., 1995
	Wet only Sampler: Glass or Teflon funnel with glass or Teflon bottle	Oxidation, reduction, purge and trap, CVAFS or CVAAS	Kreutzmann et al., 1995 Bieber & Althoff, 1995 Vermette et al., 1995

2.9 Worldwide Atmospheric Mercury Measurements

In recent years, a great effort has been made to characterize the levels of mercury species in ambient air and precipitation in order to investigate both large-scale (spatial) and short/long-term (temporal) distribution characteristics of atmospheric Hg on a global scale (Sprovieri et al., 2010a). In this context, it was shown that in fast developing countries in Asia mercury emissions are rapidly increasing in a dramatic fashion (Pacyna et al., 2006; Pirrone et al, 2010). However, this development of Asian emissions is neither reflected in both the long-term measurements of TGM and Hg in precipitation in Europe and North America. Even though the reason for this is not yet clear, it was hypothesized that atmospheric Hg cycling is possibly faster than previously thought (Sprovieri, 2010a). The understanding of the way in which mercury is released into the atmosphere, transformed, and deposited is of crucial importance. However, it is extremely difficult to analyze the global long-term trends of mercury in the atmosphere due to the lack of a coordinated monitoring network, especially with regards to the Southern Hemisphere. Already in 1995 Fitzgerald proposed an international research program, AMNET, or Atmospheric Hg Network, to address the important question, "Is Hg increasing in the atmosphere?" (Fitzgerald, 1995). However, this initiative has only partly been accomplished on a regional scale. Indeed, different field intercomparisons (e.g. Ebinghaus et al., 1999b; Munthe et al., 2001) have shown that good agreement of the atmospheric mercury concentrations determined by different laboratories using different techniques (see also Chapter 2.8) makes a combination of datasets from different regions of the world feasible. Nevertheless, a worldwide monitoring network and the need for additional sites is necessary to provide a dataset which can give new insights into Hg cycling on different temporal and spatial scales (Sprovieri et al., 2010a). Keeler et al. (2009) also recommend the establishment of the Coordinated Global Mercury Monitoring Network (CGMMN).

Monitoring networks on regional scales exist for example in Europe (see also 2.9.1) with the programs MAMCS (Mediterranean Atmospheric Mercury cycle System), MOE (Mercury Species Over Europe) and MERMYCS (Mercury Cycling in the Mediterranean Sea Basin); in Canada (see also 2.9.2) with the Network CAMNet (Canadian Atmospheric Mercury Network); and the USA (see also 2.9.2) with NADP-AMNet (National Atmospheric Deposition Program - Atmospheric Mercury Network) and NADP-MDN (National Atmospheric Deposition Program - Mercury Deposition Network).

In addition, there are single background locations, where long-term monitoring is conducted.

In order to understand how the different species in ambient air and precipitation depend on meteorological conditions, many of these baseline monitoring sites are at Global Atmosphere Watch (GAW) stations which are operated by the World Meteorological Organization (WMO) (Fig. 2-9).

Fig. 2-9 **Global atmosphere watch stations (GAW) (yellow dots) and affiliated mercury monitoring sites (red circles). Original image taken from World Meteorological Organization (www.wmo.int).**

The datasets cover terrestrial sites in the Northern Hemisphere (NH) and the Southern Hemisphere (SH) as well as measurements performed over the oceans and seas. The higher spatiotemporal variability of Hg concentrations observed in the NH confirms that the majority of emissions and re-emissions are located in the NH (Sprovieri et al., 2010a). The inter-hemispherical gradient with higher TGM concentrations in the NH has remained nearly constant over the years.

The following sections provide an overview of atmospheric measurements performed at several terrestrial sites in the Northern- and Southern Hemisphere and over the oceans.

2.9.1 Monitoring Networks in Europe

For Europe, continuous monitoring datasets exist for the time period 1998 to 2004 for two coastal background sites, Mace Head, on the West coast of Ireland and Zingst peninsula on the southern shore of the Baltic Sea (Ebinghaus et al., 2002a; Kock et al., 2005). Between 1998 and 2004 the annually averaged TGM concentrations measured at Mace Head (1.72 ng m^{-3}) and Zingst (1.66 ng m^{-3}) remained fairly stable (Kock et al., 2005). At both stations higher concentrations were measured during the winter months and lower concentrations during summer months. They also observed an unexpected West to East gradient. Since Mace Head is located at the European inflow boundary and, therefore considered to be less influenced by continental emissions, these findings are suggesting the important role of enhanced emissions from the sea.

Extensive evaluations of Hg measurements in air and precipitation have been carried out by Wängberg et al., 2007 at EMEP and OSPAR stations in Ireland, Netherlands, Germany, Norway, and Sweden. A decreasing trend in mercury wet deposition with a reduction of 10-30 % can be observed when comparing the two periods 1995-1998 and 1999-2002; probably due to emission controls in Europe. In contrast, no decreasing trend in TGM could be observed during the same periods. The authors suggest that a plausible explanation is that the TGM concentration measured in the OSPAR area to a larger extent than before is dominated by the hemispherical background concentration of TGM.

During the MOE and MAMCS project a comparison of TGM, TPM, and RGM measurements at 10 coastal sites (Fig. 2-10) distributed over Europe was obtained. Four synchronized seasonal field campaigns from 1998 to 1999 were operated at five sites in North Europe and five sites in the Mediterranean Region. It could be shown that TGM was slightly higher and also TPM and RGM were even significantly higher in the Mediterranean region than in Northwest Europe (Wängberg et al., 2001; Pirrone et al., 2003; Munthe et al., 2003; Sprovieri et al., 2010a).

The most probable interpretation is that enhanced reemission fluxes from warm sea surfaces coupled with chemical and physical transformation processes occurring in the Mediterranean MBL lead to local production of RGM and TPM (Sprovieri et al., 2003; Hedgecock et al., 2003, 2005; Ebinghaus et al., 2009; Sprovieri et al. 2010b). These enhanced re-emission fluxes are driven primarily by higher solar radiation, humidity and temperature in the Mediterranean basin when compared to more northern seas.

Tab. 2-10 TGM, RGM, and TPM average values observed at the selected coastal sites during the four seasonal campaigns of the MOE, MAMCS, and MERCYMS projects. NA: data not available; D: day; N: night.

	Location	Season	TGM [ng m^{-3}]	RGM [pg m^{-3}]	TPM [pg m^{-3}]	References
MOE	Neuglobsow, D N53°8'/E13°2'	Fall	2.22	NA	98.83	Wängberg et al., 2001 Munthe et al., 2003 Ebinghaus et al., 2009 Sprovieri et al., 2010b
		Winter	2.14	19.86	21.00	
		Spring	1.98	27.23	46.17	
		Summer	1.58	27.98	30.93	
	Zingst, D N54°26'/E12°43'	Fall	1.60	NA	70.93	
		Winter	1.67	37.48	21.65	
		Spring	1.47	54.61	23.81	
		Summer	1.69	9.15	22.48	
	Rörvik, S N57°8'/E11°56'	Fall	2.69	15.30	18.58	
		Winter	1.40	19.19	4.78	
		Spring	1.54	18.24	7.94	
		Summer	1.39	17.41	7.61	
	Aspvreten, S N58°48'/E17°23'	Fall	1.68	NA	12.37	
		Winter	1.31	11.13	9.99	
		Spring	1.46	13.65	7.00	
		Summer	1.27	9.25	7.48	
	Mace Head, IRL N53°20'/W9°54'	Fall	2.03	28.59	3.99	
		Winter	1.72	25.68	3.51	
		Spring	1.62	31.01	10.18	
		Summer	1.45	27.13	10.58	
MAMCS	Mallorca, E N39°40'/E2°41'	Fall	3.16	1.88	34.40	Wängberg et al., 2001 Pirrone et al.,2003 Ebinghaus et al., 2009 Sprovieri et al., 2010b
		Winter	3.08	99.59	86.12	
		Spring	3.85	76.02	44.11	
		Summer	4.15	NA	33.56	
	Calabria, I N39°25'/E16°0'	Fall	1.30	40.18	26.32	
		Winter	1.86	24.84	28.55	
		Spring	1.42	46.74	22.71	
		Summer	1.09	35.47	45.55	
	Sicily, I N36°40'/E15°10'	Fall	1.34	90.14	5.57	
		Winter	2.37	46.39	8.46	
		Spring	1.89	77.49	11.02	
		Summer	2.18	29.48	9.11	
	Antalya, TR N36°28'/E30°20'	Fall	1.68	NA	14.66	
		Winter	8.71	10.44	14.39	
		Spring	1.34	21.00	25.25	
		Summer	NA	NA	65.25	
	Haifa, IL N32°40'/E34°56'	Fall	1.83	NA	115.39	
		Winter	0.90	36.14	27.30	
		Spring	1.45	34.81	97.89	
		Summer	NA	NA	4.19	
MERCYMS	Cabo de Creus, E N42°19'/E3°19'	Fall	1.60	2.20	9.60	Wängberg et al., 2008 Ebinghaus et al., 2009 Sprovieri et al., 2010b
		Winter	1.50	0.24	9.10	
		Spring	1.60	2.20	9.60	
		Summer	2.10	1.20	11.20	
	Thau Lagoon, F N43°25'/E3°35'	Fall	1.60	8.60	3.00	
		Winter	2.90	41.90	82.00	
		Spring	1.60	8.60	3.00	
		Summer	3.30	191.00	662.00	
	Piran Marine, SLO N45°33'/E13°33'	Fall	NA	4.50	NA	
		Winter	0.80	1.00	18.70	
		Spring	NA	4.50	NA	
		Summer	4.00	15.40	9.40	
	Calabria, I N39°25'/E16°0'	Fall	1.30	1.60	1.00	
		Winter	1.90	4.20	6.10	
		Spring	1.30	1.60	1.00	
		Summer	1.60	NA	NA	
	Haifa, IL N32°40'/E34°56'	Fall	D1.19/N0.78	33.00	89.00	
		Winter	D0.80/N0.50	2.20	3.90	
		Spring	D1.19/N0.78	33.00	89.0	
		Summer	D1.24/N1.21	8.30	22.7	

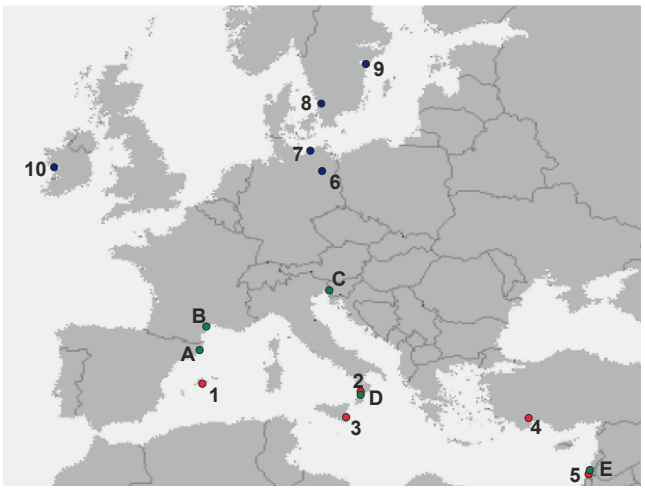

MAMCS
1 Mallorca, E; N39°40'/E2°41'
2 Calabria, I; N39°25'/E16°0'
3 Sicily, I; N36°40'/E15°10'
4 Antalya, TR; N36°28'/E30°20'
5 Haifa, IL; N32°40'/E34°56'

MOE
6 Neuglobsow, D; N53°8'/E13°2'
7 Zingst, D; N52°26'/E12°43'
8 Rörvik, S; N57°8'/E11°56'
9 Aspvreten, S; N58°48'/E17°23'
10 Mace Head, IRL; N53°20'/W9°54'

MERCYMS
A Cabo de Creus, E; N42°19'/E3°19'
B Thau Lagoon, F; N43°25'/E3°35'
C Piran Marine, SLO; N45°33'/E13°33'
D Calabria, I; N39°25'/E16°0'
E Haifa, IL; N32°40'/E34°56'

Fig. 2-10 Sampling sites of the European projects MOE, MAMCS, and MERCYMS.

2.9.2 Monitoring Networks in Northern America

Long-term monitoring of atmospheric Hg with high time resolution started at Alert, Canada in January 1995. This was the first site in the development and set up of the Canadian Atmospheric Mercury Network (CAMNet), which was established in July 1994 by environment Canada (www.ec.gc.ca). In this network 11 sites located between 43° and 82° N latitude and 62° and 123° W longitude have been operated continuously. Long-term monitoring data of TGM concentrations were analyzed for the time period from 1995 – 2005 by Temme et al., 2007 (Tab. 2-11). TGM concentrations at all sites were similar to or slightly lower than those observed at European background sites. Seasonal variations of TGM concentrations were observed for all sites. The study revealed statistically significant decreasing TGM concentrations from rural locations in Canada during the investigated time period, with largest declines close to the urban areas of Toronto and Montreal (17 % and 13 %). This is in good agreement with the overall trend in total mercury concentrations in precipitation observed at co-located or nearby sites, operated by the NADP-MDN, indicating that these changes are mostly driven by local and regional changes in mercury emissions. Other sites reflect hemispherical global background concentrations of airborne mercury, where slight decreases or no statistically significant trend in TGM concentrations exist over the same time period.

More recently, at some sites within CAMNet atmospheric Hg-species concentrations in addition to TGM have been measured. Poissant et al. (2005) reported mean values of GEM, RGM and Hg_p in St. Anicet, Québec for the year 2003 to be 1.65±0.42 ng m^{-3}, 3±11 pg m^{-3}, 26±54 pg m^{-3}, respectively.

And also within the NADP programs AMNet and MDN different species have been measured during various campaigns since the early 1990s. Dividing the sampling sites within these campaigns in the United States into remote, rural and urban location TGM concentrations vary between 1.4-1.8 ng m^{-3} for remote sites and 2.1-8.7 ng m^{-3} for urban sites (Tab. 2-12). RGM concentrations range from 3 pg m^{-3} at remote sites to over 150 pg m^{-3} at urban sites, TPM from 0 to over 197 pg m^{-3} (Tab. 2-12).

Tab. 2-11 Descriptive statistics for TGM data for the 11 CAMNet sites (after Temme et al., 2007)

Site	Mean [ng m^{-3}]	Min [ng m^{-3}]	Max [ng m^{-3}]	SD [ng m^{-3}]
Alert	1.55	0.03	3.12	0.37
Kejimkujik	1.45	0.54	2.30	0.21
St. Andrews	1.42	0.74	2.46	0.23
St. Anicet	1.64	0.92	16.31	0.40
Point Petre	1.78	0.80	4.26	0.34
Egbert	1.67	0.95	6.90	0.27
Burnt Island	1.58	0.99	2.48	0.21
Bratt's Lake	1.53	0.79	2.68	0.24
Esther	1.65	1.19	2.14	0.15
Fort Chipewyan	1.36	0.95	1.77	0.15
Reifel Island	1.67	0.91	2.92	0.19

Tab. 2-12 Summary of Hg^0, RGM and Hg_P measurements made at remote, rural and urban locations in the United States (Sprovieri et al., 2010a and Refs. therein)

Sites	Hg^0 Range of Means [ng m^{-3}]	RGM Range of Means [pg m^{-3}]	Hg_P Range of Means [pg m^{-3}]	Precip.-Hg_T Mean [ng L^{-1}]
Remote Sites	1.4-1.8	2.7-60	0-9	4
Rural Sites	1.3-3.2	1-92	3-50	6
Urban, Industrial, Mining, or Fire Sites	2.1-8.7	7-150	2-197	10

2.9.3 Measurements in the Southern Hemisphere

Representative measurements of atmospheric mercury in the Southern Hemisphere are very scarce. The only long-term dataset of atmospheric TGM in the non-polar Southern Hemisphere is constituted by TGM monitoring at the Cape Point-GAW station, South Africa (Fig. 2-9). During the period form 1995 until June 1999 TGM concentrations were found to be fairly homogeneous over time ranging between 1.2 and 1.4 ng m^{-3} (Baker et al., 2002) (Tab. 2-13). Whilst no significant diurnal variation was observed, a slight seasonal variation was detectable, with minimum concentration during March and May hand highest concentrations between June and August. The most prominent feature of the highly resolved TGM measurements is the frequent occurrence of events with almost complete mercury depletion (Brunke et al., 2010). This has so far not been observed at non-polar stations.

Tab. 2-13 Atmospheric mercury measurements performed at Cape Point, South Africa. NA: data not available; BDL: Below detection limit.

Location	Period	Method	Species	Mean [ng m^{-3}]	Min. [ng m^{-3}]	Max. [ng m^{-3}]	Reference
South Africa							
Cape Point S34°21'/E18°29'	1995-1999	Silver and gold coated quartz wool	TGM	1.2-1.4	NA	NA	Baker et al., 2002
	10/1996-11/1996		TGM	1.258±0.119	NA	NA	Brunke et al., 2010
	03/2007-06/2008	Tekran 2537A	GEM	0.944±0.160	BDL	5.44	Slemr et al., 2008

Few long term measurements dedicated to atmospheric mercury have been performed in Antarctica compared to those performed in the Arctic. First TGM data from the Antarctica region were reported by De Mora et al. (1993), who conducted TGM measurements from 1985 to 1989 at three different sampling sites (Tab. 2-14). They found mean TGM concentrations between 0.23 ng m^{-3} and 0.6 ng m^{-3} and therefore suggested TGM concentrations in Antarctica being substantially lower than those observed elsewhere. In recent years, monitoring of atmospheric mercury in Antarctica has been extended to several coastal locations - German Research Station Neumayer, Italian Antarctic Station in Terra Nova Bay and the US station McMurdo – and to two stations on the Antarctic Plateau – US South Pole Station and the French-Italian Concordia Base. Results and references of these studies can be found in Tab. 2-14. Due to these studies, there is a scientific consensus about the Hg^0 annual mean concentrations in Antarctica which is around 1.0 ng m^{-3}.

Tab. 2-14 Summary of atmospheric mercury measurements performed at different locations in Antarctica. NA: data not available; BDL: Below detection limit. Data are partly taken from Dommergue et al., 2010.

Location	Time	Method	Species	Mean [ng m^{-3}]	Min. [ng m^{-3}]	Max. [ng m^{-3}]	Reference
Antarctica							
Lake Vanda S77°33'/E161°37'	12/1985	Manual-silvered/ golded sand collectors	TGM	0.23	NA	NA	De Mora et al., 1993
Scott Base S77°51'/E166°46'	1987 1988		TGM	0.52±0.14 0.60±0.40	0.16 0.02	0.83 1.85	
Arrival Heights S77°11'/E166°40'	1989		TGM	0.52±0.16	0.11	0.78	
Neumayer S70°11'/W08°15'	2000-2001	Tekran 2537A; 1130 and KCl-Coated Annular Denuders	TGM Hg(0) RGM	1.08±0.29 0.99±0.27 NA	0.27 0.16 $5*10^{-3}$	2.34 1.89 ~$300*10^{-3}$	Ebinghaus et al., 2002b; Temme et al., 2003a
		AESmini Trap	TPM	NA	$15*10^{-3}$	$120*10^{-3}$	
Terra Nova Bay S74°41'/E164°07'	1999-2001	Tekran 2537A; 1130 and KCl-Coated Annular Denuders	TGM Hg(0) RGM	0.81±0.1 0.9±0.3 (116±78)$*10^{-3}$	0.5 0.29 ~$11*10^{-3}$	0.9 2.3 $334*10^{-3}$	Sprovieri and Pirrone, 2000; Sprovieri et al., 2002
		Goldtraps Filter coll.	TPM	(12±6)$*10^{-3}$	$4*10^{-3}$	$20*10^{-3}$	
South Pole S90°00'	11-12/2003	Tekran 2537A; 1130, 1135	Hg(0) RGM TPM	0.54±0.19 (344±151)$*10^{-3}$ (224±119)$*10^{-3}$	0.24 $95*10^{-3}$ $71*10^{-3}$	0.82 $705*10^{-3}$ $660*10^{-3}$	Brooks et al., 2008a
	11/2000-01/2001	Filter collection	TPM	(166±147)$*10^{-3}$	$11*10^{-3}$	$827*10^{-3}$	Arimoto et al., 2004
McMurdo S77°13'/E166°45'	01/2009	Tekran 2537A 1130 1135	Hg(0) RGM TPM	1.20±1.08 (116±45)$*10^{-3}$ (49±36)$*10^{-3}$	BDL 29*10-3 5*10-3	11.16 $275*10^{-3}$ $182*10^{-3}$	Brooks et al., 2008b

A complementary approach to measurements at a few stationary sites for long periods consists of campaign measurements from moving platforms, such as ships. Long-term measurements over the Atlantic Ocean have been performed by Slemr et al. since 1977 (Slemr et al., 1981; Slemr et al., 1985; Slemr and Langer, 1992; Slemr et al., 1995). The TGM concentrations which were measured during these cruises over the southern Atlantic Ocean are summarized in Tab. 2-15. Further data were collected over the Atlantic Ocean by Lamborg et al. (1999) and Temme et al. (2003a,b) and over the Indian Ocean by Witt et al. (2010) and by Xia et al. (2010). The concentrations measured in the Southern Hemisphere are summarized in Tab. 2-15. For the Southern Hemisphere a rather homogeneous distribution of TGM was observed, compared to the data from the Northern Hemisphere. For further information on the cruise part concerning the Northern

Hemisphere, the reader is referred to the references listed in Tab. 2-15 and to Sprovieri et al. (2010a).

Tab. 2-15 Summary of atmospheric mercury measurements performed during cruise campaigns over Oceans in the Southern Hemisphere.

Location	Period	Method	Species	Mean [ng m^{-3}]	Min. [ng m^{-3}]	Max. [ng m^{-3}]	Reference
Over Atlantic Ocean – Southern Hemisphere (South of ITCZ)							
S32°-N11°	10/1977		TGM	1.19±0.25	0.8	1.7	
N18°-N3°	11-12/ 1978		TGM	1.35±0.2	0.86	1.85	
S2°-N4°	01-02/ 1979	Gold or silver coated	TGM	1.26±0.2	1.07	2.09	Slemr and Langer, 1992;
S34°-N11°	10-11/ 1980	quartz wool collectors	TGM	1.5±0.2	1.1	1.9	
S48°-N7°	10-11/ 1990	AAS/AFS	TGM	1.5±0.3	0.9	2.4	
S46°-N6°	10-11/ 1994		TGM	1.2±0.2	0.8	2.1	Slemr et al., 1995
S33°-N8°	05-06/ 1996	Gold coated quartz sand	TGM	1.61 ±0.09	1.17	1.99	Lamborg et al., 1999
			TPM	$(1.9\pm0.2)*10^{-3}$	$1.3*10^{-3}$	$4.8*10^{-3}$	
S37°-N8°	10-11/ 1996	Tekran 2537A	TGM	1.4±0.1	1.0	2.3	Temme et al. 2003b
S71°-N3°	12/1999-01/2000	Tekran 2537A	TGM	1.27±0.09	0.54	1.84	Temme et al. 2003a/b
S71°-S34°	02-03/ 2000	Tekran 2537A	TGM	1.00±0.12	0.24	1.30	
S71°-S54°	02/2001	Tekran 2537A	TGM	1.1±0.1	0.75	1.4	
Over Indian Ocean – Southern Hemisphere (South of ITCZ)							
S7°-S20°	11/2007	Tekran 2537A	TGM	1.2	1.05	1.51	Witt et al., 2010
S0°-S69°	11-12/ 2007	Tekran 2537B	TGM	1.471±0.8	0.30	4.5	Xia et al., 2010

Relatively few observations of atmospheric mercury have been performed in Central and South America. Additionally, these few studies have been carried out near to, or downwind of major Hg emission sources or in urban areas (Hachiya et al., 1998; Amouroux et al., 1999; De La Rosa et al., 2004; Higueras et al., 2005; Fostier and Michelazzo, 2006; García-Sánchez et al., 2006).

Hence, no reliable baseline mercury data can be used yet to establish long-term trends for the region of South America.

3 DEVELOPMENT OF THE EXPERIMENTAL SET-UP

As lined out in previous chapters the sampling and analyzing of different atmospheric Hg species is a challenging task. While TGM can be measured with relatively high accuracy, the measuring of TPM, RGM and Hg in rainwater is more complex. A number of different sampling techniques were employed for these fractions, but they are not yet standardized (Chapter 2.8). On the market, only one fully automated system exists (Tekran Inc., System with the Models 2537A, 1130, and 1135), were the three components TGM, RGM, and TPM are measured concurrently. However, this system is not capable for the remote sampling areas of this study, because Argon is needed as carrier gas for the detector. Different aspects for choosing the optimal combination of sampling and analytical techniques have to be taken into account, especially with regard to determination of Hg in remote sampling areas:

- The accuracy of the methods has to be warranted
- The risk of contamination has to be low
- Due to the low stability of the compounds, a direct analysis of the samples (especially RGM and Hg in precipitation) during the campaigns is indispensable
- The electric power consumption has to be grantable
- The material complexity has to be kept low
- The material has to be safe against breakage
- The material has to be easy to clean and does not have to have memory effects

Taking all these aspects into account the following combination of sampling and analyzing the different species was chosen (Tab. 3-1).

Tab. 3-1 Sampling and analytical techniques used in this study.

Mercury Species	Sampling Techniques	Analytical Techniques	More Information
TGM	Gardis Analyzer	CV-AAS (Gardis−3)	Chapter 3.4
RGM	Mistchamber	Reduction with $SnCl_2$, Purge and Trap, CV-AAS (Gardis−3)	Chapter 3.5
TPM	Minitrap with quartz glass fiber filters	Thermal desorption/ CV-AAS (Gardis−3, AMA−254)	Chapter 3.6
Hg in Precipitation and Snow	Teflon bags PP tubes	Ox. with BrCl; Red. with NH_2OH•HCl and $SnCl_2$, Purge and Trap, CV-AAS (Gardis−3, AMA−254) CV-AFS (MercurPlus)	Chapter 3.7 Chapter 3.8

3.1 Materials and Chemicals

Preventing samples from contamination during the sampling and the analysis process constitutes one of the greatest challenges encountered in trace metals determinations. Samples may become contaminated by different sources, e.g. by contaminated labware, containers, sampling equipment, reagents, reagent water, or laboratory air.
Hence, an accurate pre-treatment of the materials and chemicals is extremely important.

3.1.1 Sampling Equipment

The construction material used for the sampling and the analytical train was either glass of fluoropolymer because mercury vapor can diffuse in or out of most other materials, leading to incorrect results. Only construction parts which did not get into direct contact to the samples were sometimes made of other materials, like e.g. silicone tubings. For the RGM measurements polypropylene centrifuge tubes were taken as sample containers. Studies of Stratton et al. (2001) showed them to be reliable.
Sample collection bottles as well as all material which came in direct contact to the samples were cleaned prior to the campaigns according to the following procedure: The equipment was first rinsed in Milli-Q water for several times. The equipment was put into a polyethylene tub, which was filled with 3 M HCl, making sure that all of the surfaces were submersed in the HCl. The tub was closed and placed in a water bath at 60 °C for three hours in a fume hood. Afterwards, the material was allowed to soak in the HCl for another three days. After the soak in the HCl, the material was removed from the tub and rinsed with Milli-Q water for several times. The material was then soaked in a 2 M HNO_3 for seven days. At the end of the soak the material was rinsed with Milli-Q water for several times and air dried. Finally, the material was double heat-sealed into polypropylene foil, and stored until use.

3.1.2 Chemicals, Reagents, and Standards

Reagent water: Milli-Q water (18.2 MΩ cm^{-1}; Millipore, Milford, MA, USA). This water was used for cleaning the material, for preparing the reagents and standards, and as blank.

Hydrochloric acid: Merck, p.a.; Hg < 0.005 ppm. This acid was used for cleaning the material and for preparing the reagents.
Merck, Ultrapur, 30 %. This acid was used for preparing Bromine monochloride.

3 M hydrochloric acid: concentrated HCl was added to reagent water at a ratio 1 : 3. This acid was used for cleaning the material.

2 M nitric acid: concentrated HNO_3 (Merck, reinst) was added to reagent water at a ratio 1 : 7. This acid was used for cleaning the material.

Stannous chloride: 20 g of stannous chloride -2- hydrate ($SnCl_2 \bullet 2H_2O$; Riedel-de-Haën, purum; or Merck, p.a.) and 10 mL of concentrated HCl were brought to 100 mL with reagent water. The solution was purified by purging overnight with N_2. The solution was stored in a tightly capped brown glass bottle.

Hydoxylamine hydrochloride: 30 g of hydroxylammonium chloride ($NH_2OH \bullet HCl$; Merck, p.a) were dissolved in reagent water and brought to 100 mL. The solution was purified by adding 0.1 mL of $SnCl_2$ solution and purging overnight with N_2. The solution was stored in a brown glass bottle.

Bromine monochloride (BrCl): 110 mg of Potassium bromide (KBr; Riedel-de-Haën, Spectranal ®; or Merck, p.a.) were dissolved in 100 mL HCl in a fume hood. For this, a clean magnetic stir bar was put in the bottle and stirred for approx. one hour. 150 mg of potassium bromate ($KBrO_3$; Merck, p.a.) were added to the acid slowly while stirring. The running reaction can be seen by a change of the color from yellow to red to orange. The bottle was then capped loosely and the solution was stirred for another hour before the cap was tightened.

Stock Hg standard: Standard solution $Hg(NO_3)_2$ in HNO_3 with a mercury concentration of 1000 mg L^{-1}; Merck, CertiPUR. This standard is traceable to SRM and NIST.

Secondary Hg standard A: Approximately 0.5 L of reagent water and 5 mL of BrCl were added to a 1.00 volumetric flask. 100 µL of the stock mercury standard were added to the flask and were diluted to 1 L with reagent water. That solution contained 100 µg L^{-1} Hg. The solution was transferred to a fluoropolymer bottle and capped tightly. The secondary Hg standard was considered stable until the Merck expiration date of the stock Hg standard.

Secondary Hg standard B: 1 mL of the secondary Hg standard A was diluted to 1 L in a volumetric flask with reagent water containing 0.5 % by volume BrCl solution. That solution contained 100 ng L^{-1} Hg. The solution was transferred to a fluoropolymer bottle and capped tightly.

Working Hg standard A: 10 mL of reagent water containing 0.5 % by volume BrCl solution were pipetted directly into a 50 mL centrifuge tube.

3.2 Energy Supply at the Sampling Sites

For the sampling and analyzing within the field, a sufficient energy supply had to be warranted. Particularly, the Gardis−3 Analyzer needed much electric power (40 W during sampling and 90 W during analyzing), but also the computer for controlling the Gardis−3 and the pumps for the RGM and for the TPM sampling had to be fed.

Because of the low natural background Hg concentrations which ought to be measured, a “clean” electric power supply was necessary. Hence, the availability of “clean” energy was a criterion for the choice of a good sampling site. In Spain, wind energy was supplied by a wind-mill company (Acconia Group). In Austria, the research station, were the sampling was carried out, was supplied by a water power plant. In Patagonia, the logistic circumstances not always permitted an ideal energy supply. At Skyring, the sampling was carried out on the area of the Estancia Skyring. There, the power supply was kindly made available by the owners of the farm, who ran a hydroelectric generator for private use. However, at the other two sites no opportunity of a local power supply existed. Hence, the machines were run with car batteries and an electric generator based on fuel. Here, it was made sure, that the emission of the generator did not influence the measurements. This was achieved, by placing the generator far away from the sampling area, behind a knoll, in the downwind direction.

3.3 Analyzers for the Atmospheric Mercury Measurements

The analyzing of the different samples was generally carried out with a Gardis-3 instrument. In addition, the AMA−254 (Advanced Mercury Analyzer; LECO) was used for comparing means for the measurements of TPM and Hg in precipitation. Both analyzers are based on gold amalgamation, thermal desorption, and subsequent atomic absorption spectrometry (AAS) detection.

3.3.1 GARDIS−3

The Gardis−3 is a field analyzer, which is similar to the earlier model Gardis−1A, which is described in literature (Urba et al., 1995; Urba et al., 1998). The Gardis−3 operates with ambient air as carrier gas. Due to the very remote and logistically difficult sampling sites of this study, this was a great advantage over most other AAS or AFS instruments, which require Argon or Helium for detection.

Technical Parameter of the Gardis−3: In this AAS analyzer a low pressure electrodeless discharge Hg lamp (EDL) with λ = 254 nm is used as a light source. As detector a phototube is used, which is sensitive to the spectral region from 220 nm to 330 nm. Due to a two-beam optical system and a mechanical chopper the light is enabled to pass through the sample and reference cells alternatively. The reference cell has the same dimension as the sample cell and is filled with argon to avoid generation of ozone by the UV light.
The gas train consists of the concentration trap, the analytical trap, the sample optical cell and the gas pumping system, connected in series with Teflon tubings. The gas pumping system provides two flow rates: 1 L min^{-1} for sampling and 10 mL min^{-1} for analysis.

Calibration of the Gardis−3: The Gardis−3 was calibrated with saturated Hg gas phase syringe injections prior to the campaign, using a method adopted from Dumarey et al. (1985).
The source for the Hg saturated gas was a closed flask, containing 20-30 mL of mercury. Within the flask the Hg of the headspace is in equilibrium with the liquid. The vapor pressure of Hg is a function of the temperature and can be measured by equation 3-1 (Landolt-Börnstein, 1969). The resulting vapor pressure curve is shown in Fig. 3-1.

$$\log p = -\frac{A}{T} + B + C \cdot \log T \qquad \text{(Eq. 3-1)}$$

p = Hg vapor pressure [Torr]
T = Hg temperature [K]
A = 3332.7 K
B = 10.5457 Torr
C = -0.848

According to the Ideal Gas Law (Equation 3-2) the amount of Hg within the air volume of the syringe can be calculated. The resulting calibration curve is shown in Fig. 3-1.

$$\frac{pV}{T} = const. \qquad \text{(Eq. 3-2)}$$

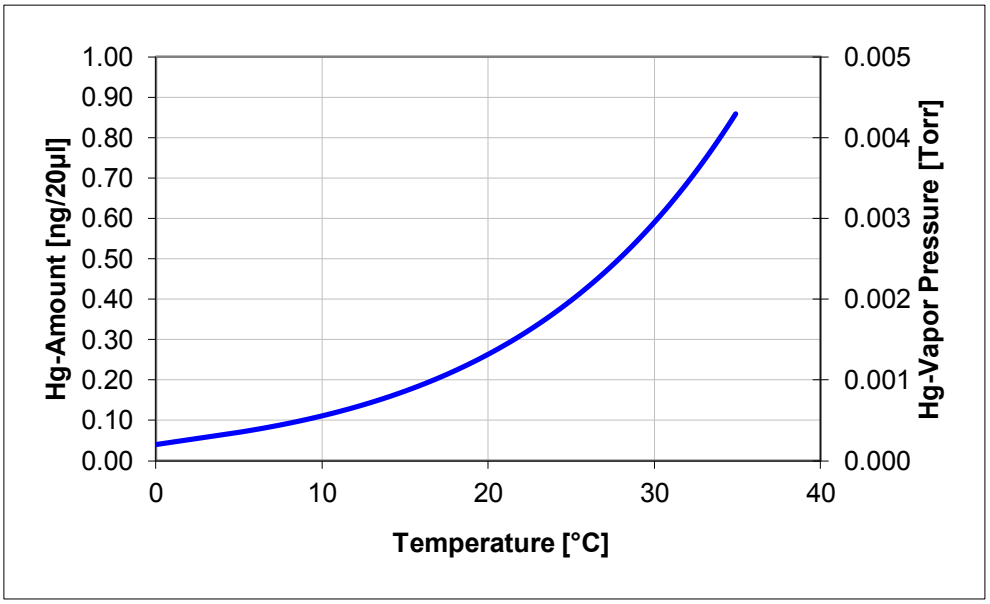

Fig. 3-1 Hg-Vapor Pressure and Hg-Amount versus temperature for calibration of the Gardis.

For the calibration of the Gardis−3, between 10 and 20 µL of Hg-saturated air was removed via a septum by using a gas-tight syringe (Hamilton, # 1700). The air was then injected into the inlet of the Gardis−3. For this, the sampling time was set to be 30 sec.

This procedure was repeated several times (n) to get a reliable average value. If the measured value did not correspond to the calculated value, the calibration constant of the Gardis−3 had to be changed according to equation 3-3.

$$C_n = C_o \cdot \frac{X_c}{\overline{x}_m} \qquad \text{(Eq. 3-3)}$$

C_n: new calibration constant
C_o: old calibration constant
X_c: calculated amount of Hg
$\overline{x}_m$: average measured value

The Gardis−3 was calibrated at regular intervals. Additionally, it was calibrated directly prior to each campaign.

Ageing of the Gold Traps: The gold traps are the most sensitive parts of the Gardis−3 and have to be replaced in regular intervals. Due to the ageing their collection efficiency decreases. This loss in efficiency can be compensated by the calibration constant up to a

certain extend. However, after a certain degree the loss of collection efficiency goes very rapidly (Fig. 3-2).

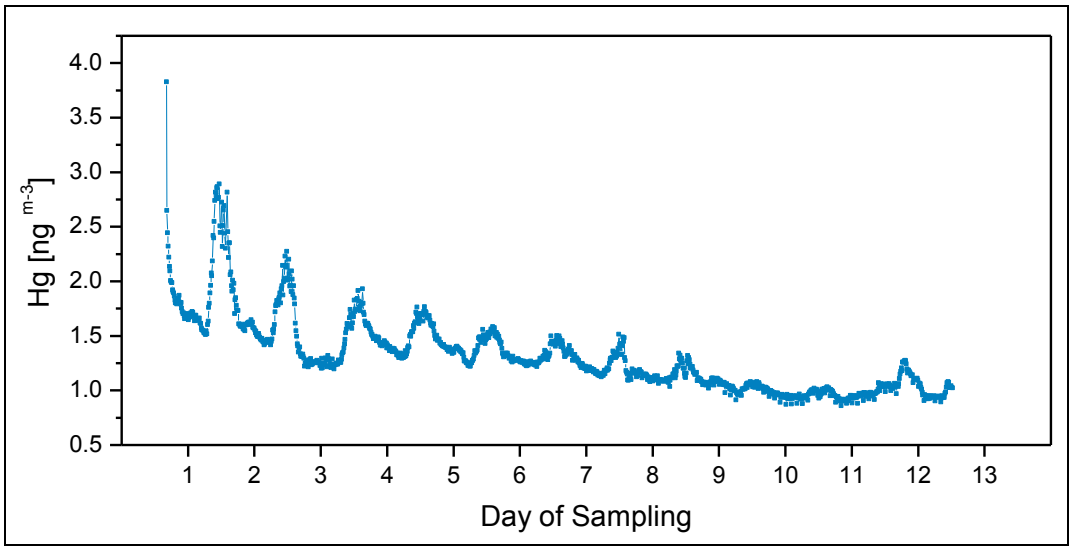

Fig. 3-2 Decrease of the collection efficiency of an old gold trap.

Hence, especially prior to a campaign, it is necessary to check the collection efficiency. One relatively meaningful method to estimate the reliability of the gold trap is the comparison between Hg concentrations depending on different sampling durations. In the ideal case the Hg concentration should be independent from the sampling time. However, the Hg concentration decreases with raising sampling duration. For new gold traps the effect is limited, but for old gold traps this effect is getting worse (Fig. 3-3).

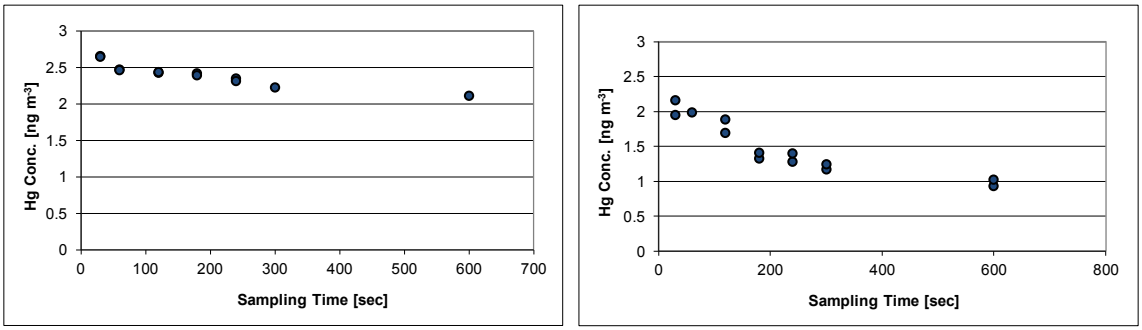

Fig. 3-3 Collection efficiency of a new (left) and an old (right) gold trap, tested with different sampling durations.

3.3.2 AMA−254 for Solid Samples

The AMA−254 is a single purpose atomic absorption spectrophotometer for direct mercury determination in solid and liquid samples without the need of sample chemical pre-treatment. It is fully compliant with the US-EPA method 7473. It is also possible to

measure gaseous mercury by using a gold trap for pre-concentration (see Chapter 3.3.3). The AMA−254 uses a direct atomic absorption cold vapor method with gold amalgamation. The sample is decomposed in a combustion/catalyst tube with oxygen as flue gas. A gold amalgamation trap collects all mercury from the evolved gases and a dual-path length cuvette/spectrophotometer specifically determines mercury over a wide dynamic range.

Technical Parameter of the AMA−254: A low pressure Hg lamp is used (λ = 253.65 nm) as light source and a silicon UV diode as detector. The AMA−254 only provides a one-beam optical system with a serial arrangement of the cuvettes. The gas train consists of the sample holder, the combustion/catalyst tube, the gold amalgamation trap, and the dual-path length cuvette/spectrophotometer. Oxygen is used as carrier gas. In order to avoid interferences a filter for a wavelengths of 254 nm and a half-width of 9 nm is used. The detection limit is at 0.01 ng Hg and the working range covers the range between 0.05 – 600 ng Hg.

Calibration of the AMA−254: The calibration was performed using a liquid standard of 10 ng mL^{-1} prepared from Merck mercury standard solution with 1000 mg L^{-1}. Different amounts of the prepared standard were dosed, getting a 4-point calibration from 0.00 to 15 ng Hg. A typical calibration curve is shown in Fig. 3-4.

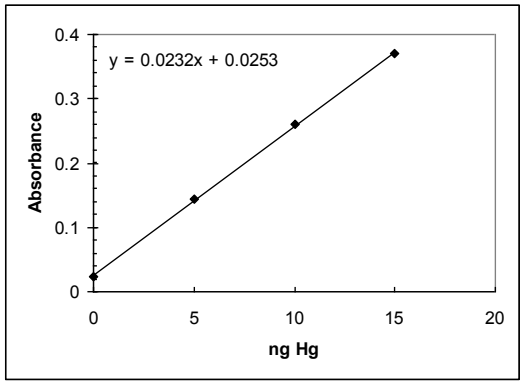

Fig. 3-4 Characteristic calibration curve for the AMA-254.

During a series of measurements three solid standards (NIST 1515, BCR 281, and the internal standard P4) were used to control the proper instrument conditions.

3.3.3 AMA−254 Module for Analyzing Gaseous Mercury

For the control of compartment air, LECO Corp. developed a module for the measuring of gaseous mercury. This module consists of gold traps, a clamp to fix the gold trap to the

analyzing location, a pump with tubes, and the support to mount the gold trap in the analyzer.
The gold trap consists of an 11 cm long stainless steel tube with an outer diameter of 4 mm and an inner diameter of 3 mm. Within this tube there are gold globes, which make up about 4 cm in length. In order to fix the gold globes inside the tube, one end of the tube tapers, leaving an opening of about 1 mm. This opening is packed with quartz wool. On the other side of the gold globes the tube is compressed, leaving only a small crack.

For sampling, the gold trap can be e.g. attached via clamp to the worker's cloths in order to check the exposure of the worker to gaseous mercury. The gold trap is connected via silicon tubes to a pump, whose maximum pump rate lays around 3 L min^{-1}. The air is pulled through the trap at a constant and known flow rate. The gaseous mercury amalgamates on the gold globes and is trapped. For analysis, the gold trap is fixed in a stainless steel cylinder, which is mounted in series with the gas train.

In the framework of this work, it was checked whether this module was probable for the measurement of TGM and mercury in precipitation.
For this purpose, the following aspects considering the traps were examined:

- Determination of the zero value of the traps
- Required thermal purification cycles
- Mercury accumulation on the traps during different types of storing
- Efficiency of mercury accumulation with gaseous standards
- Efficiency of mercury accumulation with liquid standards
- Considerations about general composition stability of the traps

Zero value of the traps and the required thermal purification cycles: First of all, the traps were cleaned due to thermal desorption by repeating the AMA−254 analysis cycle for several times. Through this, both the required purification steps as well as the zero value of the traps were determined. Each trap was measured seven times consecutively. The analysis program was set as recommended for air-dried peat samples by Roos-Barraclough et al. (2002): drying time: 30 s, decomposition time: 125 s, waiting time: 45 s.

Different important results were determined. The zero value of the traps were between -0.018 and −0.025 ng Hg (Fig. 3-5). The absolute values are a result from the then-calibration. The range of variation showed a good accuracy.

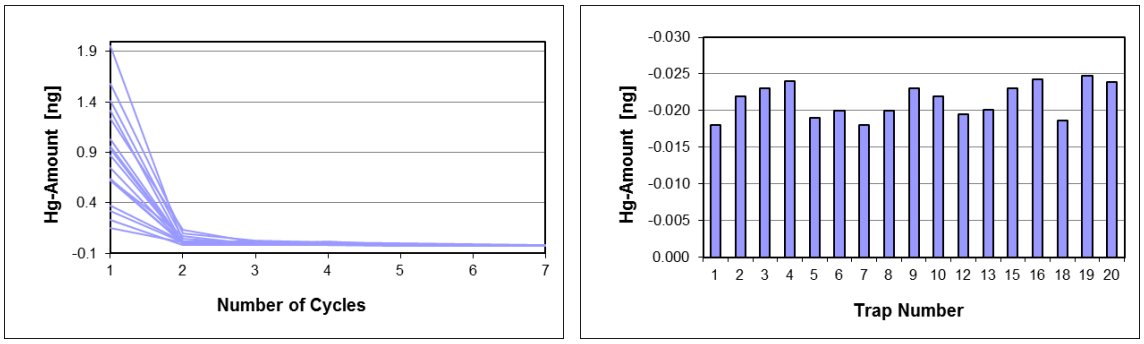

Fig. 3-5 Decrease in mercury during the cleaning of the traps (left) and the mercury amount of the seventh measurement (right).

Furthermore, it was shown, that not all mercury was desorbed during the first run, but three or even four runs were necessary (Fig. 3-5).
That also meant, that the Hg concentrations during a real analyses would have been too low, which is precarious particularly for low Hg concentrations. Hence, the desorption rate was increased to 300 s, in order to assure a total desorption of the Hg from the trap.

Mercury accumulation on the traps during different types of storage: Often, it is not possible to clean or analyze the traps immediately prior to or after sampling. Hence, it was checked how much mercury was accumulated on the traps depending on different type and duration of storage.

After cleaning, all traps were put together in a polyethylene bag with a wire closure. This bag was then put in a glass which was filled with activated carbon. The traps were analyzed after different duration of storage (between 22 and 69 hours). Absolute values varied between 0.2 and 1 ng, resulting in accumulation rates between 0.007 and 0.015 ng h^{-1} or between 0.171 and 0.355 ng d^{-1} (Fig. 3-6).

In a second test, each trap was sealed at both ends with Teflon film and put in a polyethylene bag. All bags were then put together in another polyethylene bag and stored in a glass which was filled with activated carbon. The traps were analyzed after up to 27 days. Absolute values varied between 0.23 ng and 1.12 ng. This resulted in accumulation rates between 0.008 and 0.034 ng d^{-1}, which is less than the accumulation rates in the first test by one order of magnitude.

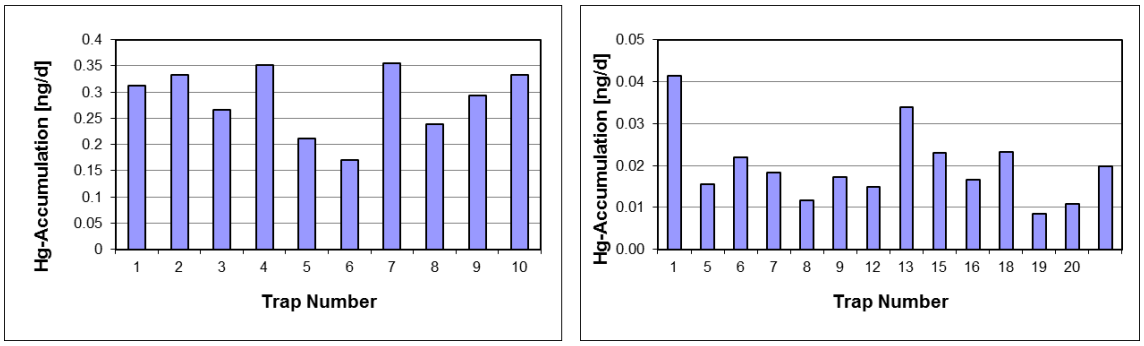

Fig. 3-6 **Mercury accumulation in the gold traps due to storage. All traps packed together (left); each trap packed separately (right).**

The tests show that it is very important to seal the traps carefully, in order to minimize the mercury accumulation from ambient air. Nevertheless, in both test the variation of mercury accumulation between the different traps was very high. Therefore, it is difficult to quantify the blank value after a long period of storage.

Efficiency of mercury accumulation with gaseous standards: To examine the efficiency of mercury accumulation from gaseous samples, the traps were spiked with saturated Hg air (see chapter 3.3.1). Between 20 and 100 µl of Hg-saturated air was injected into the traps. To ensure, that all Hg-saturated air passes the gold trap, an air stream of 1 L min^{-1} was applied.

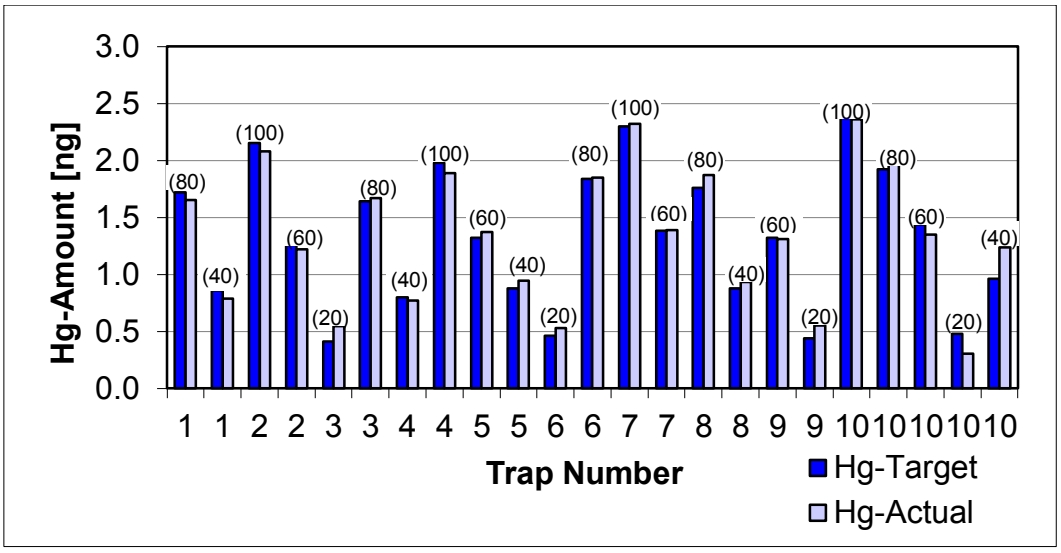

Fig. 3-7 **Mercury accumulation efficiency of the gold traps for gaseous standards.**

The results show, that the accordance between the actual value and nominal value is very high with a correlation coefficient of $R^2 = 0.98$. The largest source of error is probably the uncertainty in the gas volume and in temperature.

Efficiency of mercury accumulation with liquid standards: To examine the efficiency of mercury accumulation from liquid samples, a purge and trap method was developed. A precise amount of liquid Hg standard was poured in a gas washing bottle. 200 µL of $SnCl_2$ solution was added to the liquid to reduce all mercury compounds. The reduced mercury was purged out of the liquid with zero-air and trapped on the AMA−254 gold trap (Fig. 3-8).

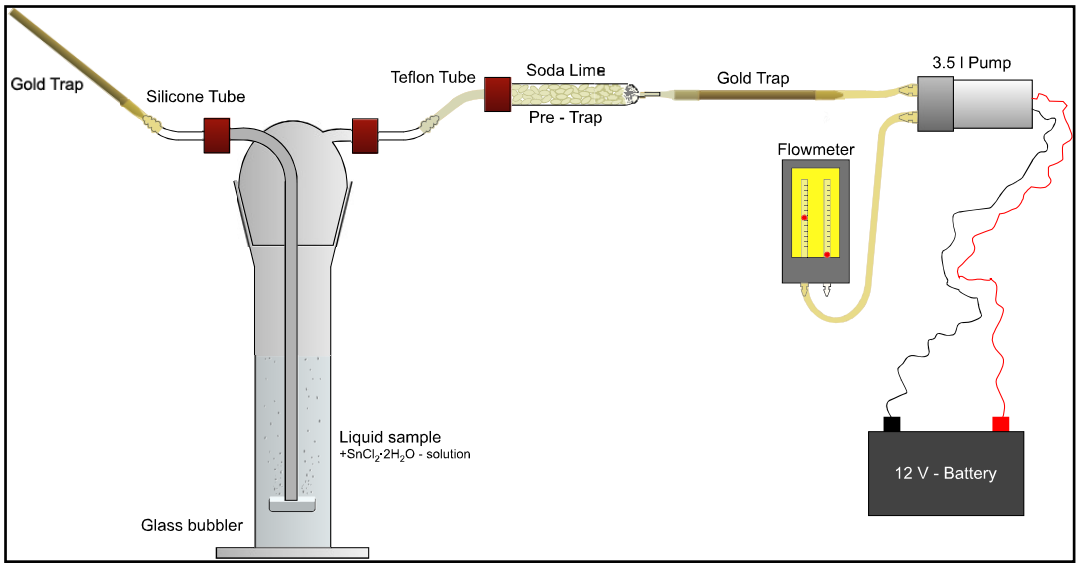

Fig. 3-8 Set-up for the measurement of liquid samples with the AMA−254 gold traps.

For this test, a 100 µL Hg L^{-1} standard was prepared. From this standard, 20, 50, or 100 µL were added to pre-cleaned MilliQ-Water, giving an absolute amount of Hg of 2, 5, or 10 ng, respectively. Purging was done over 20 min. with an air flux of 2 L min^{-1}.

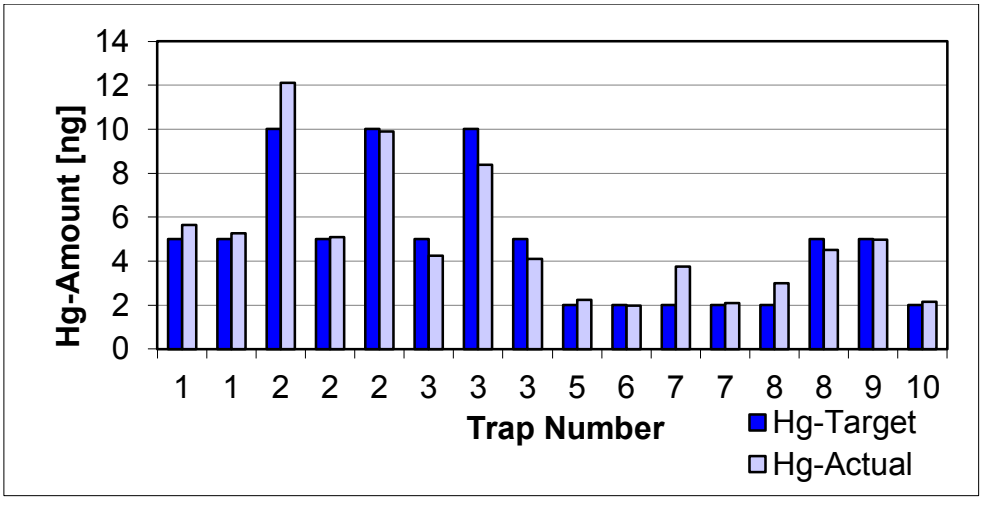

Fig. 3-9 Mercury accumulation efficiency of the gold traps for liquid standards.

The results show, that the mercury accumulation efficiency of the traps is very high for liquid standards with a correlation coefficient of $R^2 = 0.94$.

3.4 TGM Measurements

TGM sampling was carried out using the field analyzer Gardis−3, which is similar to the earlier model Gardis−1A, which is described in literature (Urba et al., 1995; Urba et al., 1998). The method is based on gold amalgamation, thermal desorption, and subsequent atomic absorption spectrometry (AAS) detection. The Gardis-3 operates with ambient air as carrier gas. Due to the remote and logistically difficult sampling sites of this study, this is a great advantage over most other AAS or AFS instruments, which require Argon or Helium for detection.

3.4.1 Sampling Set-Up in the Field

At the sampling sites in Chile as well as in Spain the Gardis−3 was built up inside a tent. In Austria the Gardis−3 was built up inside the research station of the Institute of Limnology of the University of Innsbruck. In each case a 2 to 5 m long Teflon tubing was used as sampling line to lead outside. The inlet of the tubing was protected against rain with a glass funnel and with a PTFE membrane (Sartorius, PTFE membrane filters type 118, 1.2 µm pore size) and installed about 1.5 m above ground level. Aerosol particle filters were added in the sampling line close to the analyzer.

Sampling time was set to 300 sec, which results in a sampling volume of 5 L.
During the first campaign in Chile in October 2002, the Gardis−3 was controlled manually. This was due to the fact of a missing sufficient power supply to run a computer continuously. Hence, for the following campaigns, the power supply was enhanced (see chapter 3.2).

3.5 RGM Measurements

RGM sampling was carried out by using mist chambers. The general procedure of a mist chamber is as follows: Air, at flows of 8-20 L min^{-1}, is aspirated through the chamber and water soluble gases are efficiently absorbed by the nebulized mist. Solution droplets containing scrubbed gases collect and coalesce on the surface of a hydrophobic membrane, then drain back into the chamber.

For analysis the mercury was removed from the solution and made available for the analyzer by purge and trap and then analyzed with the GARDIS−3 or AMA−254.

3.5.1 General Information about the Mist Chamber

RGM measurements were made using a mist chamber (MC) similar to that developed by the group of Stratton and Lindberg (Stratton and Lindberg 1995; Stratton et al. 2001).

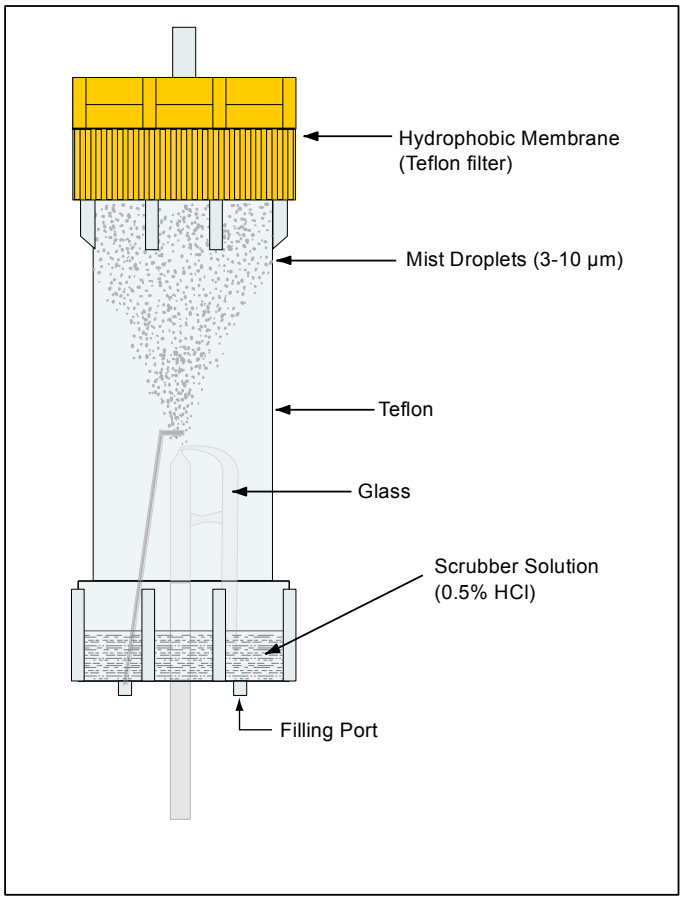

Fig. 3-10 Design of the mist chamber for RGM sampling.

The chamber (Fig. 3-10) was made out of a PFA column with a maximum volume of 150 mL, a height of 12.1 cm and an outer diameter of 47 mm (Savillex®). At the bottom the column was connected to a PFA closure with two ¼" ports (Savillex®). Refluxing was achieved by means of a hydrophobic PTFE-membrane (Sartorius, PTFE membrane filters type 118, 1.2 µm pore size, 50 mm diameter) mounted in a PFA filter holder (Savillex®) which was connected to the top of the column and had an outlet with an inner diameter of 6 mm.

The air inlet was a glass tube with an inner diameter of 6 mm, which was pushed through a hole, which was drilled into the middle of the closure. In order to make sure that the junction between glass tube and closure is tight, the hole was first made a little bit smaller

than the outer diameter of the tube and then the Teflon closure was heated and the tube was fitted into the ductile Teflon.

The mist droplets were produced by a cross-flow nebulizer, which was made out of glass and was connected to the inlet tube.

The mist chamber was filled and emptied through one of the ¼" ports. The other port was used to hold a Teflon impact bead which was supposed to protect the PTFE membrane.

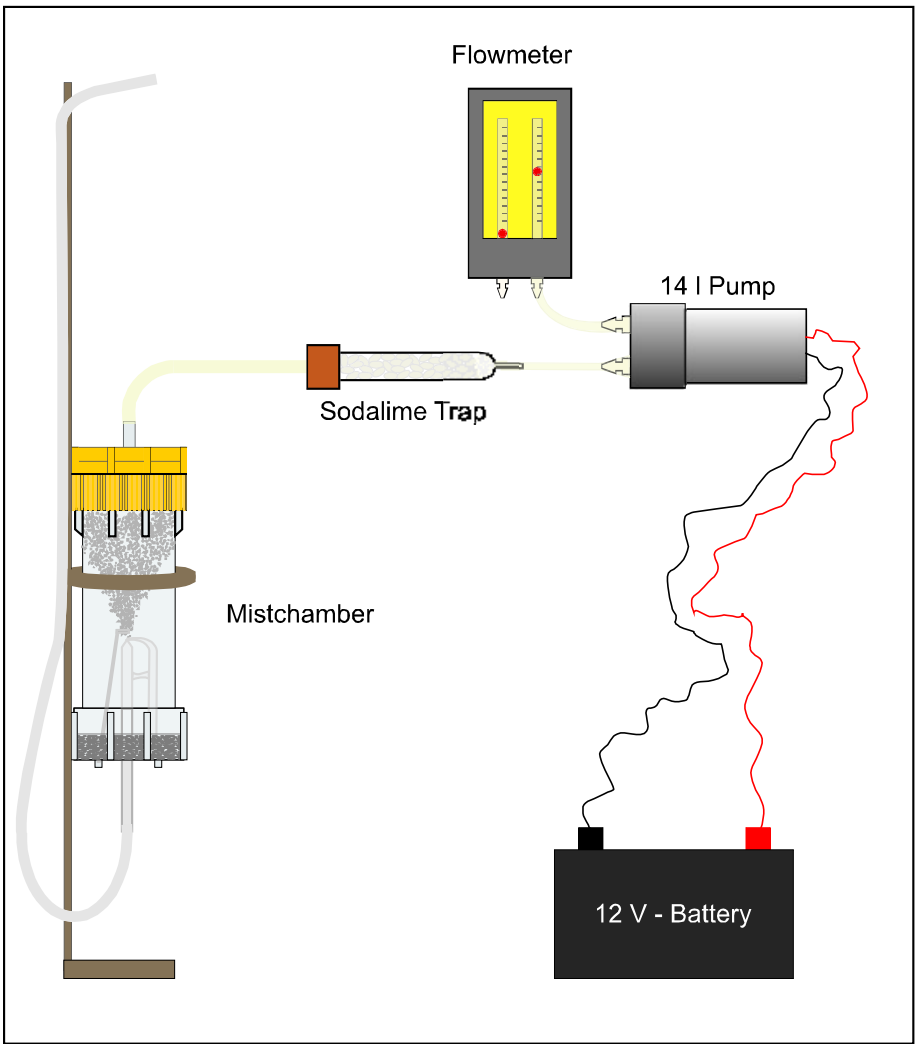

Fig. 3-11 Set-up for the sampling of RGM in the field.

For the sampling (Fig. 3-11), the mist chamber was connected to a vacuum pump (FürGut, model DC12/90S). To save the pump from acidic gases, a soda lime trap was put in line prior to the pump. The flow was monitored by a flow meter (Analyt-MTC, model 102-05C) connected to the pump outlet.

3.5.2 Scrubber Solution

As scrubbing solution diluted HCl was used, prepared by dilution of a special Hg-cleaned HCl (Merck; 1.13386; with Hg < 0.005 ppm) in high quality deionized water.
Stratton et al. (2001) observed that the collection efficiency of the solution was dependent on the concentration of HCl in the absorbing solution. On the other hand, the Hg blank of the diluted HCl was also dependent on the concentration of HCl. To find a good dilution, laboratory air was sampled for 30 min using varying concentrations of HCl.

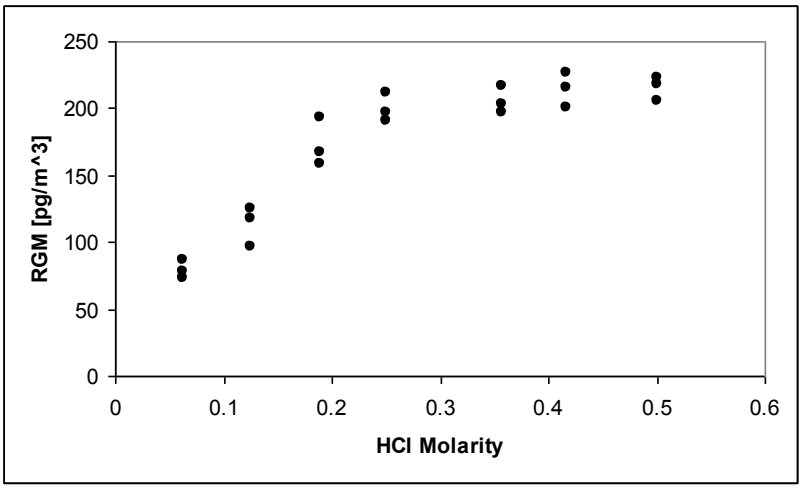

Fig. 3-12 Effect of HCl concentrations on collection of RGM: 30 min mist chamber samples of laboratory air.

The results (Fig. 3-12) showed that the RGM concentration rose linear up to approx. 0.25 M and then formed a slightly rising plateau. The blank rising steadily with HCl concentration, a scrubber solution of 0.25 M HCl was used. Hence, the blank was as small as possible without forfeiting collection efficiency.

3.5.3 Sample Containers

After sampling the scrubber solution was filled into 50 mL polypropylene centrifuge tubes with caps (Falcon, No. 2070). Preliminary tests showed that the blanks of those tubes were negligible. Hence, they were used as received in sealed packages.

3.5.4 Sampling Protocol

Prior to the start of each set of measurements, the mist chamber were rinsed repeatedly in the field using the scrubber solution. The mist chambers were then filled with 25 mL of the scrubber solution. Sample times were between 1 and 5 hours in duration, depending

on location and daytime, with an air flow of 6-10 L min^{-1}. At the end of the sampling time, the solution was transferred to a sampler container. To rinse the mist chamber, 25 mL of scrubber solution were added and the mist chamber was slightly rotated. Afterwards the 25 mL of scrubber solution were added to the sample container.
Two or three additional rinses with DI water or scrubber solution were discarded before the next sample or blank was collected.

3.5.5 Field Sampling Blank

A blank correction was used for all samples. Ideally this should be a “dynamic blank” in which zero-RGM air is sampled for the same time intervals as the samples. Unfortunately, there was no way to devise any suitable method to produce zero-RGM air at a flow of 10 L min^{-1}. Hence, field blanks were obtained by filling the mist chamber with the scrubber solution and aspirating for ca. 30 s. The solution was then collected, stored, transported, and analyzed in the same fashion as the samples. The values for the blanks obtained in this fashion were a combination of the solution blank, the mist chamber blank, the container blank, and the analytical blank.

3.5.6 Analysis of RGM

The analysis of the samples was carried out directly in the field at the end of each campaign.
RGM was measured by means of the purge and trap method (Fig. 3-13). For this, the mercury in solution (as mercuric ions) had to be reduced to elemental mercury (Hg^0) and transferred into the gaseous phase.

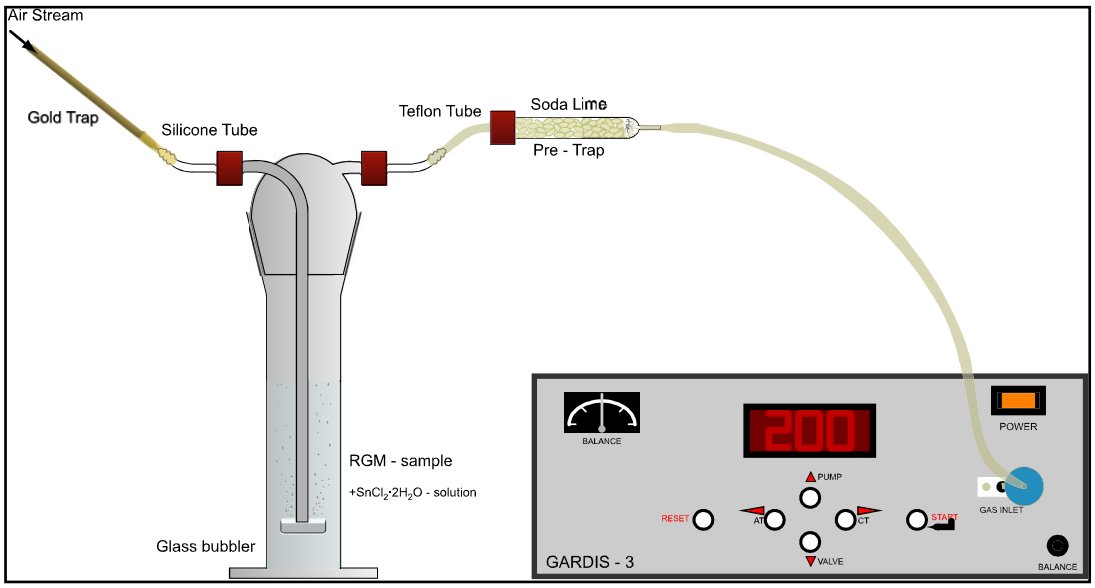

Fig. 3-13 Set-up of the purge and trap method for the RGM analysis.

Hence, the sample was put in a gas wash bottle. 50 µL of stannous chloride was added as a reductant. Mercury-free air passed into the bubbler through a gold trap. The air stream purged the dissolved elemental mercury from the solution and carried it through a soda lime trap, where acid vapor and moisture were removed, into the GARDIS 3. The mercury was absorbed on the gold trap of the GARDIS 3 and was subsequently measured.

3.6 TPM Measurements

TPM Sampling was carried out using a minitrap with a glass fiber filter. Many suggestions about the general built-up were taken from Lu et al. (Lu et al., 1998; Lu and Schroeder, 1999a; Lu and Schroeder, 1999b).

3.6.1 Particulate Trap

The custom-built particulate trap consisted of a quartz fiber filter (6 mm Ø; cut out of a 47 mm Ø filter, Schleicher and Schuell, QF20) held in an arrangement of three quartz glass tubes and a Ni screen support (Fig. 3-14). A 15 cm quartz glass tube (4 mm i.d.; 6 mm o.d.) was put into a 25 cm quartz glass tube (6 mm i.d; 8 mm o.d.) with an overlapping of about 2 cm. At this intersection the two glass tubes were welded together. The quartz fiber filter and a perforated Ni screen as support were positioned at the end of the thick quartz glass tube, so that they got hold by the thin quartz glass tube. Then, another thin quartz glass tube (4 mm i.d.; 6 mm o.d.) was pushed inside the thick glass tube up against the filter. In that way, the filter got hold between the two thin quartz glass tubes and was surrounded by the thick quartz glass tube. The junction between the thick quartz glass tube and the loose thin quartz glass tube was sealed with Teflon band.

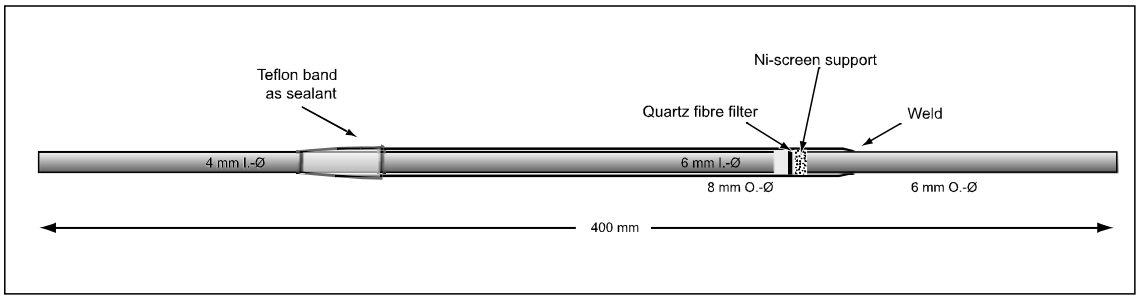

Fig. 3-14 Built-Up of the particulate trap for TPM Sampling.

3.6.2 Pre-Treatment of the Traps

First, the traps were mounted. Then, they were cleaned by heating them up to approximately 400-450 °C with zero-air flowing through. The zero-air was produced by placing a filter and a gold trap in front of the trap. After heating the trap twice for several minutes, they were allowed to cool and afterwards they were double heat-sealed into polypropylene foil, and stored until use.

3.6.3 Sampling Procedure

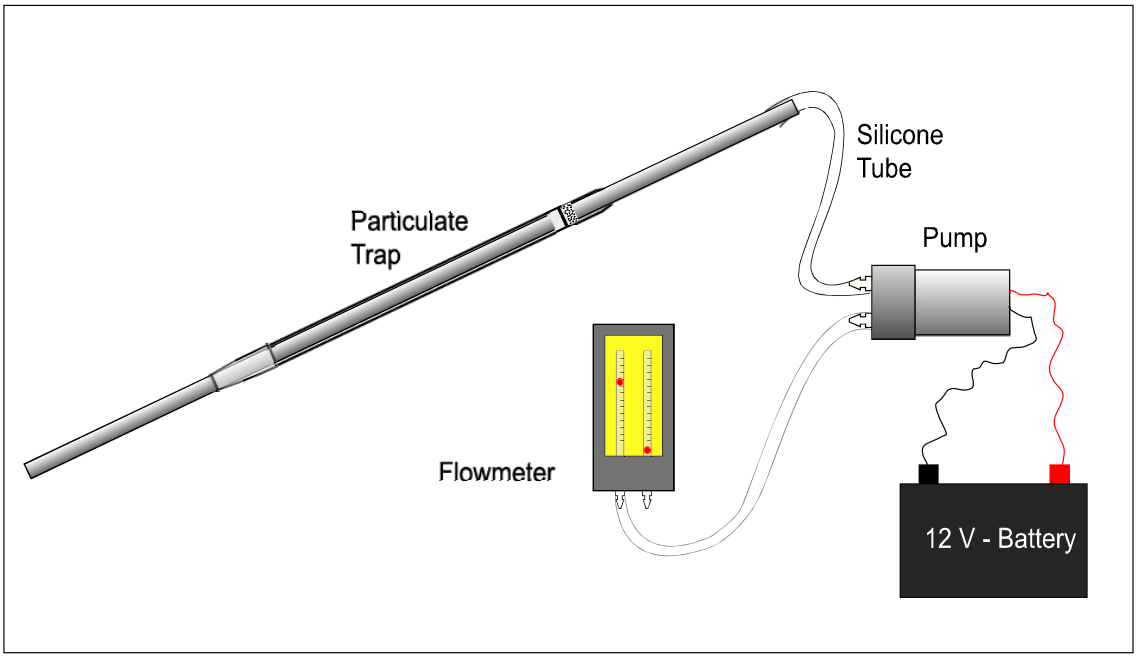

Fig. 3-15 Set-up during the sampling of TPM in the field.

For sampling each trap was connected to pump via silicone tubes. The pumps (FürGut, DC12/18 NK)) had an air flow of approximately 3 L min^{-1}, which however was attenuated due to different resistances like the filters. The exact air flow was measured by a flow meter. The inlet of the trap was about 1.50 m above ground level. In order to avoid the filter getting wet due to the rain, the trap was positioned with an incline of about 30° so that the inlet pointed down.

3.6.4 Dynamic and passive Blanks

Different types of blanks were run parallel to the sampling and analytical procedure. The fashions of these blanks were adopted from Lu et al., 1998.

Two types of blanks were examined; Type D being a dynamic blank and type P being a passive blank.
The dynamic blanks were run parallel to the sampling with the same air flow.
For blank D-1 two particulate traps were connected in series. The upstream trap served as the sampler for TPM, the downstream trap as the blank.
For blank D-2 the inlet of a particulate trap was closed with a Teflon filter (Sartorius, PTFE membrane filters, 0.2 µm pore size).
In both cases of the dynamic blank, it is reasonable to assume that most particles passing through the first trap would also pass through the second one. The signal of the blank is then mainly the sum of adsorbed gaseous mercury and the background signal of the analytical train.
The passive blank traps P were set alongside the sampling line, but no air flow was applied.
The dynamic blanks should mainly be the sum of adsorbed gaseous mercury plus the background signal of the analytical train, whereas the passive blank should be exclusively the background signal of the analytical train.

3.6.5 Analysis of TPM

The determination of TPM was carried out with two different methods; with the atomic absorption spectrophotometer AMA−254 and with the Gardis-3.

Analysis with AMA−254: For analyzing TPM with the AMA−254, the filter was removed from the trap with the help of a Teflon stick and directly dropped into an analyzing boat of the spectrometer. The analytical program was set like described in Chapter 3.3.2.

Analysis with GARDIS-3: The experimental setup for the determination of particulate mercury with the GARDIS-3 is shown if Fig. 3-16.

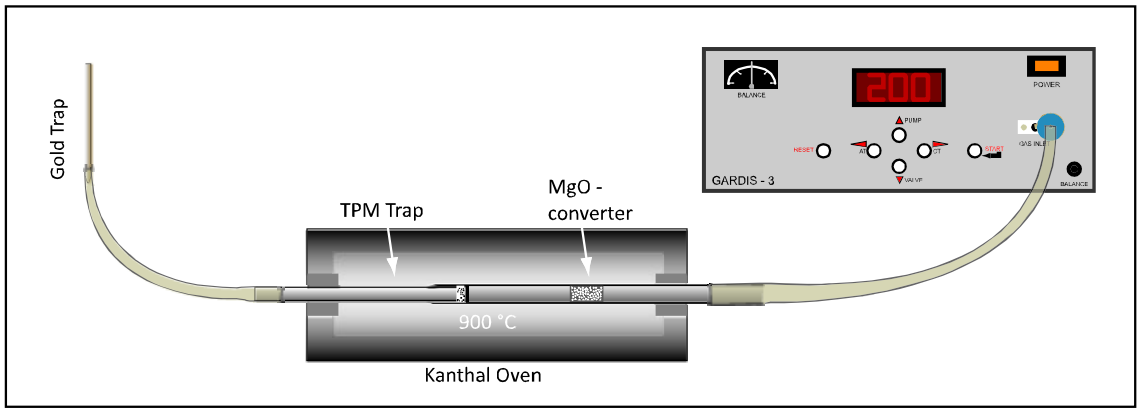

Fig. 3-16 Experimental set-up for the determination of particulate mercury with the Gardis-3.

For the analysis of TPM with the GARDIS-3, the filter remained in the glass tube.
Prior to analysis, a MgO converter was added to the glass housing of the trap. The converter consisted of granular MgO, which was directly put in the quartz glass tube of the trap housing, downstream of the TPM trap. The MgO granules, which finally made up 2 cm of the tube, were held in position with the help of quartz wool. The purpose of the converter was to increase the turbulence and the total resistance time of the gaseous Hg species in the high temperature zone so as to achieve a more complete conversion of Hg compounds into the elemental form (Lu et al., 1998; Lu and Schroeder, 1999a,b).

The whole trap was put in a horizontal Kanthal oven (with exception of the Teflon band, which was removed previously because of its low melting point) so that only the ends of the glass tube extended out of the oven. For a better temperature regulation within the oven both sides of the oven were sealed with quartz wool, only leaving an opening for the trap on each side. Downstream, the trap was directly connected via Teflon tube with the GARDIS-3. For analysis, the Kanthal oven was heated to 900 °C for about 5 minutes. The released Hg species were carried by a stream of Hg-free air at a flow rate of approximately 200 mL min^{-1} to the MgO-converter, to convert all Hg compounds to the elemental form. The resulting Hg^0 was then pre-concentrated on the analytical Au-trap of the GARDIS-3 and then analyzed.

The flow rate during the thermal desorption of Hg was archived by the regulation of the GARDIS-3 pump-rate during sampling.

3.7 Mercury Sampling in Precipitation

The determination of mercury in precipitation was carried out by first obtaining precipitation with the help of custom-made samplers. The mercury was then determined by means of purge and trap and subsequent analysis with help of CV-AAS. Both the GARIDIS-3 and the AMA−254 were taken for analysis.

3.7.1 Sampler Design and Materials

Each custom-made sampler consisted of a collecting pan, which was connected via tube to a sampling bag.

The sampling bag (Bohlender GmbH) was made of PVF (polyvinyl fluoride) which was declared to be non-porous, without plasticizer, absolutely inert, temperature-resistant between -200 and 250 °C, and suitable for the storage of gases and liquids (Bohlender, technical information). The bag was provided with a cylindrical port made of PTFE (OD: 6 mm). The rectangular collecting pan was made of polypropylene. Preliminary tests with a liquid standard showed the material to be suitable for this purpose. Due to the short durance of contact, there seemed to be no interactions between precipitation and pan. In one corner of the pan a cylindrical port like the one of the sampling bag was fitted into a boring.

Both ports, the one of the collecting pan and the one of the sampling bag, were connected to each other via silicone tube. In order to avoid a contact between sample and silicone tube, the distance between the ports was kept against zero. The small inner diameter (ID: 3 mm) of the ports prevented the diffusion of Hg^0 into the precipitation sample collected. This was important because Hg^0 could contribute to the mercury content of the sample via oxidation to water-soluble forms (Munthe, 1996).

The pan was mounted on four stands. During sampling these were plugged into the ground in a fashion to get an adequate inclination for the precipitation to run to the port an in the sampling bag. The inclination was modified regularly to suit the precipitation rate.

To protect the sampling bags against breakaway they were fitted in an open PE can, which was embedded in a hollow in the ground. Additionally, the PE can was wrapped into aluminum foil, shielding it from light to avoid photo-induced reduction of mercury in the sample.

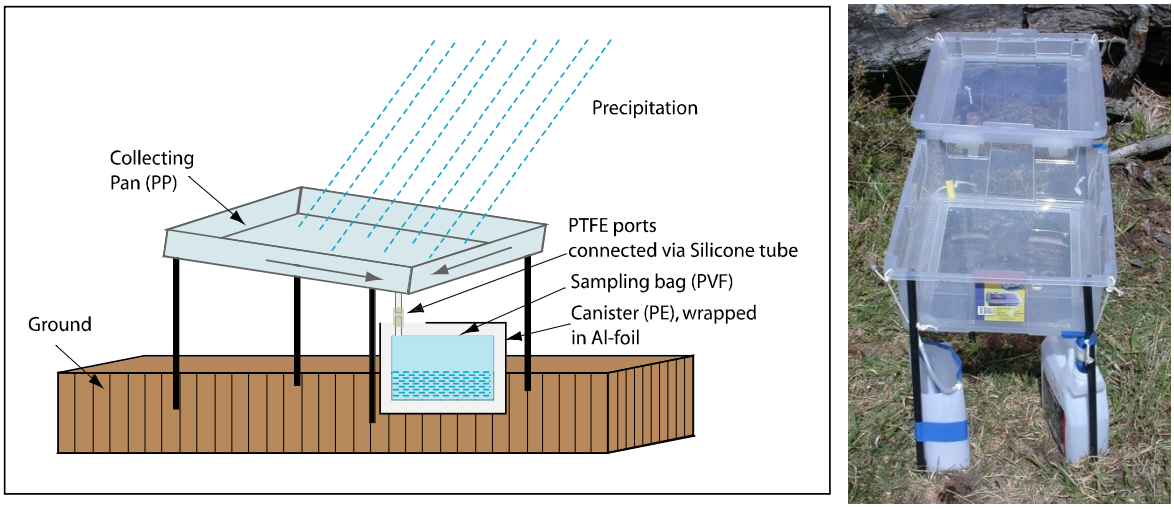

Fig. 3-17 Set-up of the precipitation sampler in the field.

3.7.2 Pre-Treatment of the Samplers

All materials were treated in laboratory as explained in chapter 3.1.1.
Due to the complex assembling of the samplers in the field, the risk of contamination was relatively high. Hence, after the built-up of the sampler, the collecting pan was cleaned with Milli-Q water again. For this, the connection between pan and sampling bag was removed, and the cleaning water was sampled in a PE bottle.

3.7.3 Sampling Procedure

At each sampling site, two or three samplers were run parallel. Sampling periods lay between one and three weeks. Due to the partially heavy precipitation rate, the sample bags sometimes had to be replaced daily.
Only, in Tyrol, Austria, the sampling periods sometimes lasted longer than one month. Hence, the samples were preserved by adding 5 mL HCl.

3.7.4 Quality Control – Quality Assurance

Prior to the sampling in the field, the general design of the samplers was verified being suitable for accurate sampling. This was done with liquid standards. One liter of water, containing 2, 5, or 10 ng Hg, respectively, was poured over the collecting pan and ran through the capillary into the sampling bag. In order to be sure that the total of the liquid standard reached the sampling bag, the collecting pan was rinsed afterwards with 0.5 L of reagent water. This rinsing water was also collected in the sampling bag.

This was done several times in different fashions. The water was poured fast or slowly; continuously or discontinuously with different intervals; inside the laboratory or outside; exposed to sunlight or in the shadow.
The subsequent analysis of the standards showed the sampler to be suitable for this purpose.

The most common causes of sample contamination during the sampling period were insects, bird droppings, or other material in the sampling vessels. The risks of contamination were controlled by using two or three samplers in parallel. Contaminated samples could be identified and discarded and the corresponding data excluded.

Two types of field blank samples were taken at each site: transport blanks and sampling blanks.

Transport blank: A duplicate sampling bag containing diluted HCl was left open at the sampling site during the regular sample exchange procedure. The duplicate bag was as far as possible handled in exactly the same manner as the sample bag. The blank was then analyzed in the same fashion as the samples.

Sampling blank: Two extra sampling bags were brought to the site; one containing diluted HCl and one empty. After removing the regular sample bag the empty bag was installed and the diluted HCl poured in the collecting pan. The blank was then analyzed in the same fashion as the samples.

3.7.5 Sample Storage and Handling

The samples of Patagonia and Spain were mainly analyzed directly during the campaign with the GARDIS-3. Hence, the transportation and storage of those samples were eliminated. However, some samples were transported into the laboratory for comparative studies with the AMA−254. In addition, the samples of Tyrol were not always analyzed directly. Those samples, which had to be transported or stored, were preserved with 5 mL HCl per liter of sample. The sample bags were wrapped in double plastic bags and stored in a refrigerator until analysis. The storage time never exceeded four months.

3.7.6 Analysis of Mercury in Precipitation

The analysis of mercury in precipitation was mainly done using the GARDIS-3. Comparative studies were carried out using the AMA−254.

Sample pre-treatment: For the most common procedure for the analysis of mercury in precipitation a chemical oxidation step should be performed using BrCl. That reagent efficiently converts stable mercury forms to water-soluble species that can be easily reduced by $SnCl_2$. Before analyzing the sample, excess BrCl should then be removed using the mild reducing agent $NH_2OH•HCl$. $NH_2OH•HCl$ often contains high mercury concentrations. This is no problem using it in laboratory, because the mercury can be purged with Hg-free N_2 (see Chapter 3.1.2).

However, in this study it emerged that $NH_2OH•HCl$ also accumulated Hg during the transport by airplane; even if the solution bottle was triple wrapped in PE bags and stored in a plastic container. During the campaign, it was not possible to clean the solution again. Hence, the pre-treatment of the samples was only carried out for the samples, which were analyzed in the laboratory. For the samples, which were directly analyzed in the field, the pre-treatment step was skipped.

Analysis with Gardis-3: Mercury in precipitation was measured by means of the purge and trap method (Fig. 3-13). For this, the mercury in solution (as mercuric ions) had to be reduced to elemental mercury (Hg^0) and transferred into the gaseous phase.
Hence, the sample was put in a gas wash bottle. 50 µL of stannous chloride was added as a reductant. Mercury-free air passed into the bubbler through a gold trap. The air stream purged the dissolved elemental mercury from the solution and carried it through a soda lime trap, where acid vapor and moisture were removed, into the GARDIS-3. The mercury was absorbed on the gold trap of the GARDIS-3 and was subsequently measured.

Analysis with AMA−254: For the mercury determination by means of the AMA−254, the protocol was similar to the mercury determination by means of the Gardis-3. The only difference was that a gold-trap of the AMA−254 was mounted at the oulet of the gas wash bottle (Fig. 3-18). After the purge and trap step, the gold trap was removed and and analyzed with the AMA−254 as described in 3.3.3.

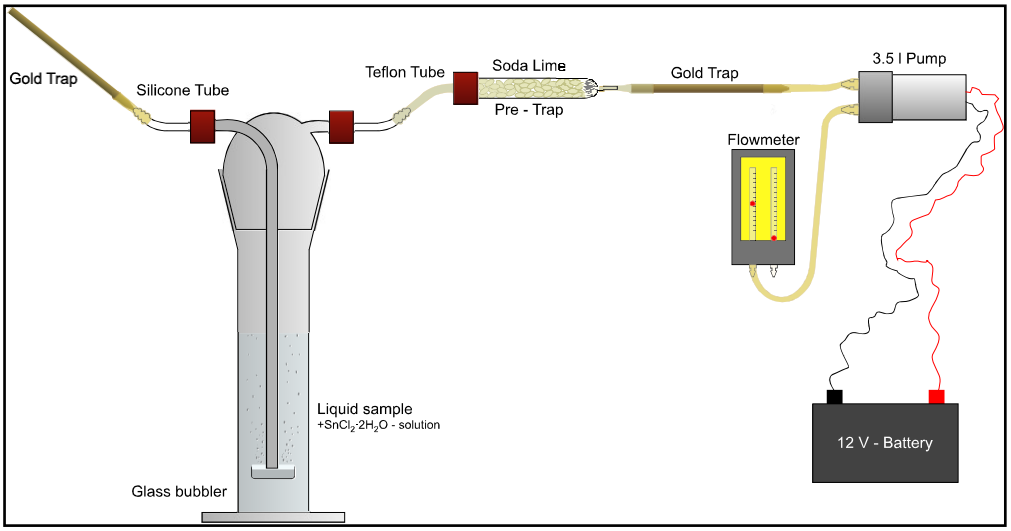

Fig. 3-18 Set-up for the measurement of liquid samples with the AMA−254 gold traps.

3.8 Mercury Analyses in Seasonal Snow

3.8.1 Sampling Procedure, Transportation and Storage

Snow samples were taken at three different altitudes above sea level within the area of Kühtai. At all sites, samples from different depths were taken. The first sample was directly taken from the surface. One other sample was taken from a lower part of the surface stratum which was buried directly due to prolonged snowfall. A third sample was taken from an older stratum. Each sample was taken in triplicates.
Additionally, two depth profiles were taken directly at Lake Gossenkölle. One profile (DP1) was taken on the surface of the lake, in a snow pit, which was excavated a couple of days ago by a research team of the University of Innsbruck. Samples were taken in triplicates at different snow heights. One other profile (DP2) was taken from a freshly excavated snow pit. For this, the pit was excavated using a snow shovel made of PP.

The snow samples were collected into 50 mL polypropylene centrifuge tubes with caps (Falcon, No. 2070). Preliminary tests showed that the blanks of those tubes were negligible. Hence, they were used as received in sealed packages. The tubes were in aluminum foil and the samples were kept cool but not frozen. The samples, which had to be transported and stored, were preserved with 5 mL HCl per liter of sample. During transportation the samples were kept cool and wrapped in the aluminum foil.

The snow strata were identified by characterizing snow cover profiles based on the “International Classification for Seasonal Snow on the Ground” (Colbeck et al., 1985).

3.8.2 Analysis of Snow Samples

The analysis of Hg_T in snowpit samples was performed according to the US EPA Method 1631(version E) (US-EPA, 2002). Due to the expected low mercury concentrations and due to the low amount of material for each sample, the mercury concentrations were analyzed by cold-vapor atomic fluorescence spectrometry using the “MercurPlus” from Analytic Jena at the University of Braunschweig. This instrument is compliant with the EPA norm 1631 and DIN EN 13506.

24 hours before analysis, 5 mL L^{-1} $BrCl_2$ were added to the samples This reagent efficiently converts stable mercury forms to water-soluble species that can be easily reduced by $SnCl_2$. Before analyzing the sample, excess BrCl was then removed using the mild reducing agent NH_2OH•HCl at a concentration of 2 mL L^{-1}. The effective reduction was confirmed by the vanishing of the yellow color of the solution. The final reduction with $SnCl_2$ was automatically done and controlled by the Mercur Plus analyzer.

4 CONCENTRATION AND SPECIATION OF ATMOSPHERIC MERCURY

4.1 Sampling Sites

4.1.1 Patagonia, Chile

Regional variations of atmospheric mercury were analyzed along a west-to-east profile across the Southern Andes (S53°), one of the most pronounced climate-divides in the world.

Climate in southwest Patagonia can be described as cool and windy with a fairly small daily and seasonal temperature cycle (e.g. Zamora and Santana 1979; Casassa, 1985; Endlicher, 1991a; Coronato and Bisigato, 1998). Mean annual air temperature at Punta Arenas on the Strait of Magellan is only 6.5°C (Endlicher and Santana, 1988). Strong westerly surface winds are dominant due to limited friction within the west wind zone of the Southern Hemisphere. Between 40°S and 60°S there are no large continents with high mountain barriers that could generate perturbations of the mean air flow besides the southernmost Andes of South America (Hobbs et al., 1998). The mountain range of the Andes, running north to south, form an orographic obstacle approximately perpendicular to the main air flow (Miller, 1976). The climate on the west side of the mountain range, within the mountains, and in the fjord zone differs significantly from the climate encountered on the lee side to the east. Rainfall shows a dramatic variation between the Pacific west coast and the leeward-side of the mountains (Endlicher, 1991b). Annual precipitation drops from between 6000 mm and 7000 mm at sea level along the main divide of the mountains to only about 1000 mm at the eastern slopes of the Andes and to as little as 430 mm at Punta Arenas (Schneider et al., 2003) (Fig. 4-1).

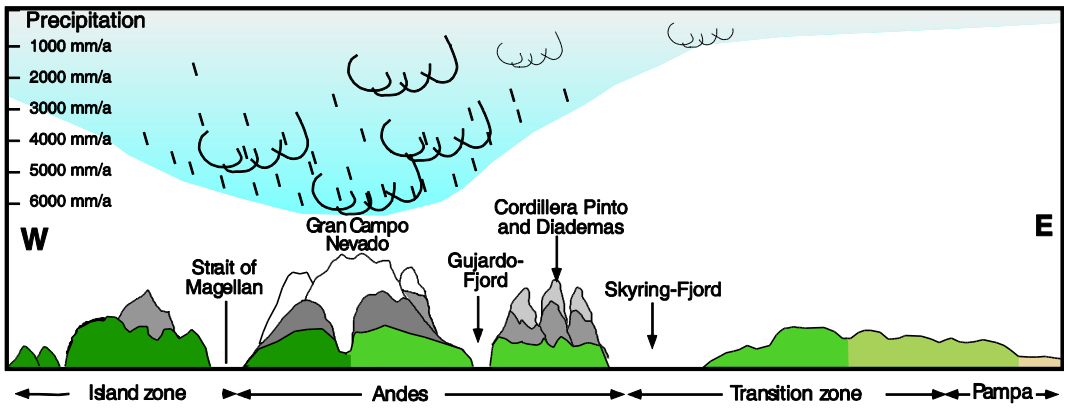

Fig. 4-1 West-East cross section of the annual precipitation across the Andes at S53°.

Fig. 4-2 shows monthly precipitation rates and temperatures for the years 2002 and 2003 at the locations Gran Campo Nevado, Seno Skyring, and Punta Arenas as representative locations for different climatic zones.

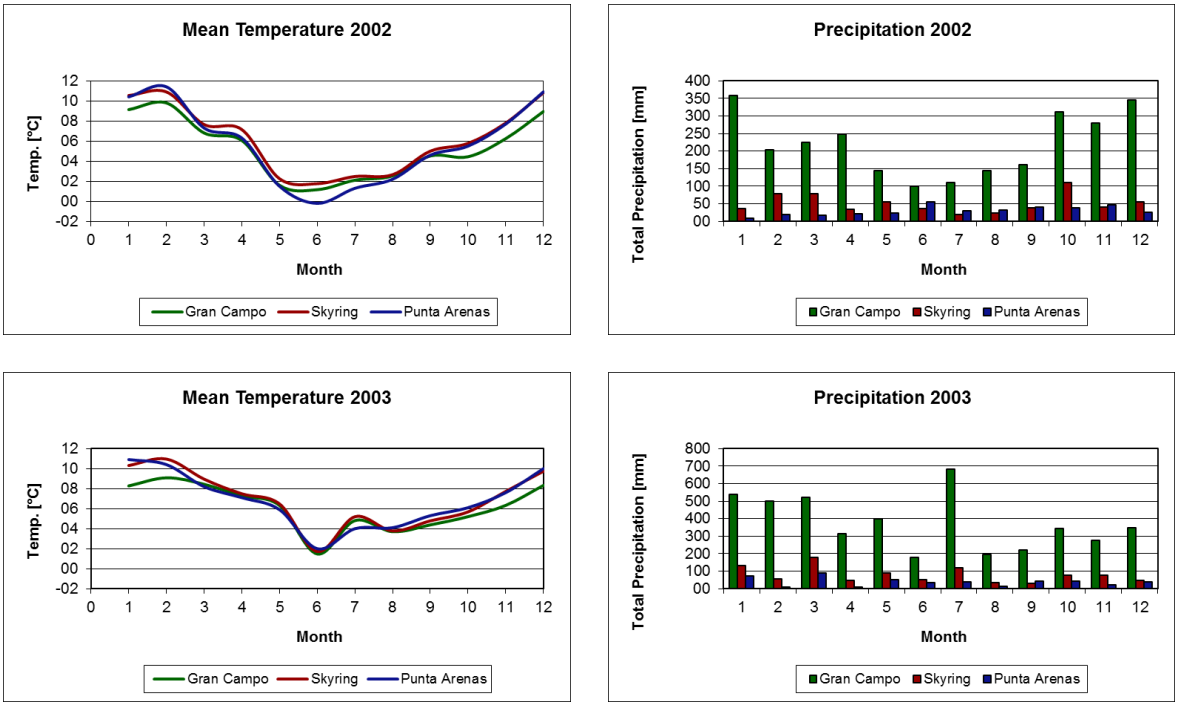

Fig. 4-2 **Mean temperatures (left) and monthly precipitation rates (right) for the years 2002 (top) and 2003 (bottom). Data from weather stations AWS Gran Campo NPB, AWS Skyring and WS Punta Arena JS (for more information see Schneider et al., 2003).**

During the campaigns the climatic conditions were temperate. The air temperatures and precipitation rates at Gran Campo Nevado for September and October of both years are shown in Fig. 4-3.

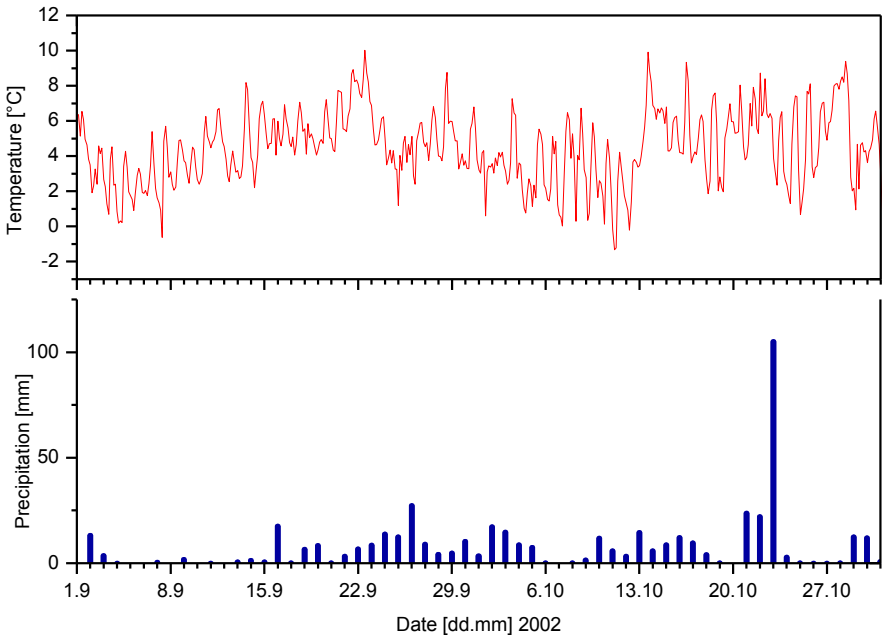

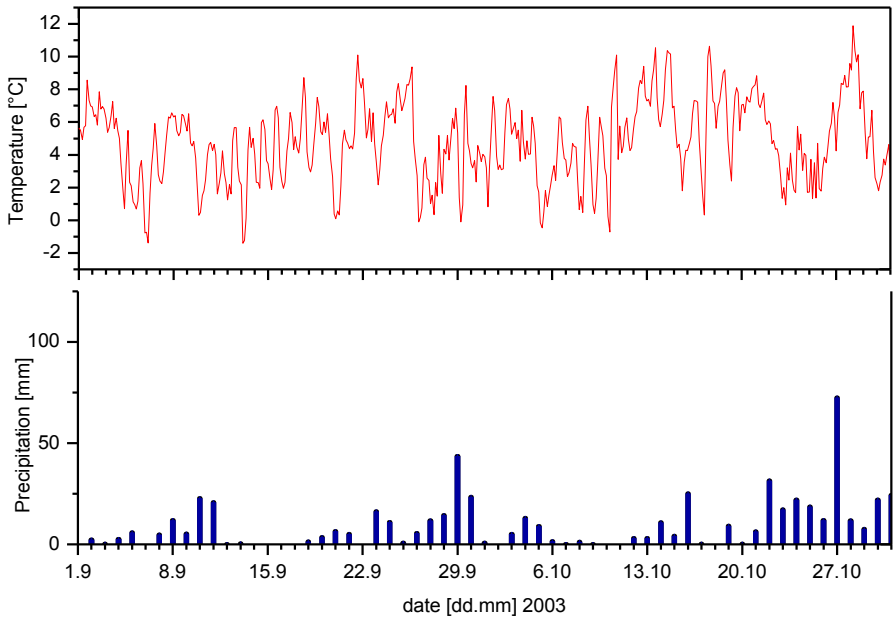

Fig. 4-3 Air temperature and precipitation rates at GC for September and October 2002 and 2003.

Samples for this study were collected from three sites (GC, Sky, and PBr; Fig. 4-4) located in different climatic zones of Patagonia, southernmost Chile. The data presented and discussed here are part of an interdisciplinary research. Thus the sampling sites refer to many other investigations of that area as well (e.g. Biester et al., 2002; Koch et al., 2002; Biester et al., 2003; Schneider et al., 2003; Kilian et al., 2007.)

The Gran Campo Nevado (GC) site (S52°48'24"/W72°56'24") is located in the transition zone between the Magellanic Moorlands and the Evergreen Forest on the Gran Campo Nevado Island. This site is characterized by high precipitation rates of more than 6000 mm yr^{-1} (Schneider et al. 2003) and intense atmospheric deposition of sea-salt aerosols due to the strong yearly westerlies. The sampling site is mostly covered by peat (ombrotrophic and minerogenic) with the typical peat forming *Carex* species and the cushion plants *Donatia fascicularis* and *Astelia pumilia*. The surrounding area is furthermore characterized by the evergreen *Nothofagus betuloides* forests, glaciers and phyllite, argillaceous schist, granodiorite, rhyolite, and andesite as bedrock.
The site at Seno Skyring (Sky) (S52°32'55"/W71°57'33") is located within the Evergreen Forest. Precipitation rates at the Sky location are much lower than at the GC location and vary between 1000 and 1500 mm yr^{-1}. To some extent the area is covered by peatlands. However, most of the area is grassland and *Nothofagus betuloides* forest.

The site at the south-eastern region of the Peninsula Brunswick (PBr) (S53°37'47"/W70°55'08") is located within the national monument museum “Fuerte Bulnes” at the Strait of Magellan. The site is situated in the transition zone between the Evergreen Forest and the Deciduous Forest with *Nothofagus pumilio* and *Nothofagus antartica*. Bedrocks are metamorphic schists covered by Cambisols. Precipitation amounts to 650-800 mm yr^{-1} (Heusser et.al. 2000).

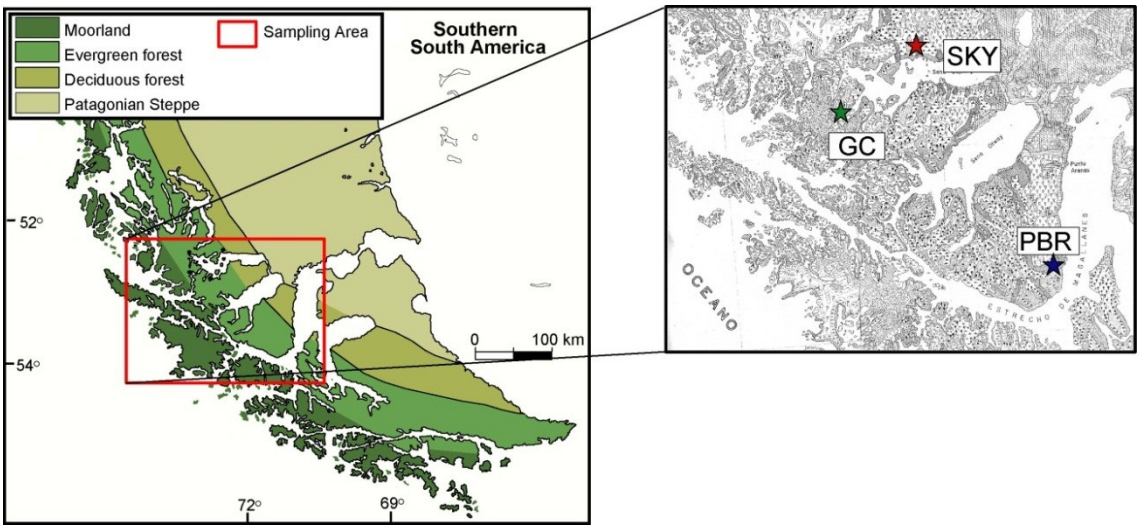

Fig. 4-4 **Map of the climatic zones of Southern South America with the sampling area in Patagonia, Chile and the sampling sites GC, Sky, and PBr.**

Fig. 4-5 **Exemplary set-up of part of the sampling equipment. Here at the location Skyring (Sky).**

4.1.2 Galicia, Spain

Galicia, Spain was chosen as a comparative sampling site to Patagonia. Even if the climatic conditions like e.g. precipitation depths and wind speed in Galicia are not as extraordinary as in Patagonia, for European values they are still most closely to the ones in Patagonia. The climate of Galicia is dominated by the Atlantic with mild temperatures and rainfalls throughout the year. The mean annual temperature in the area ranges from 10 to 7.5 °C, and annual precipitation from 1400 to 1800 mm (Martínez-Cortizas et al., 2002). Snow is only occasional in the area, with most winters free of snow (Olid et al., 2010). Sampling in Galicia was carried out at a station of a wind farm within the mountains of “O Xistral” at the mountainside of “Pico de Cuadramón” (1065 m a.s.l.) at a height of approx. 780 m a.s.l. (N43°28'09"/W07°32'04). The area is mainly covered with grassland and partly with peat. The basal lithology is composed of quartzite and paragneis.

An important coal mining area (As Pontes) is situated 25 km west of the Serra do Xistral. Mining started at the beginning of the 19th century (Olid et al., 2010). Since 1976, a coal power plant has been running with a power capacity of 1,400 MW.

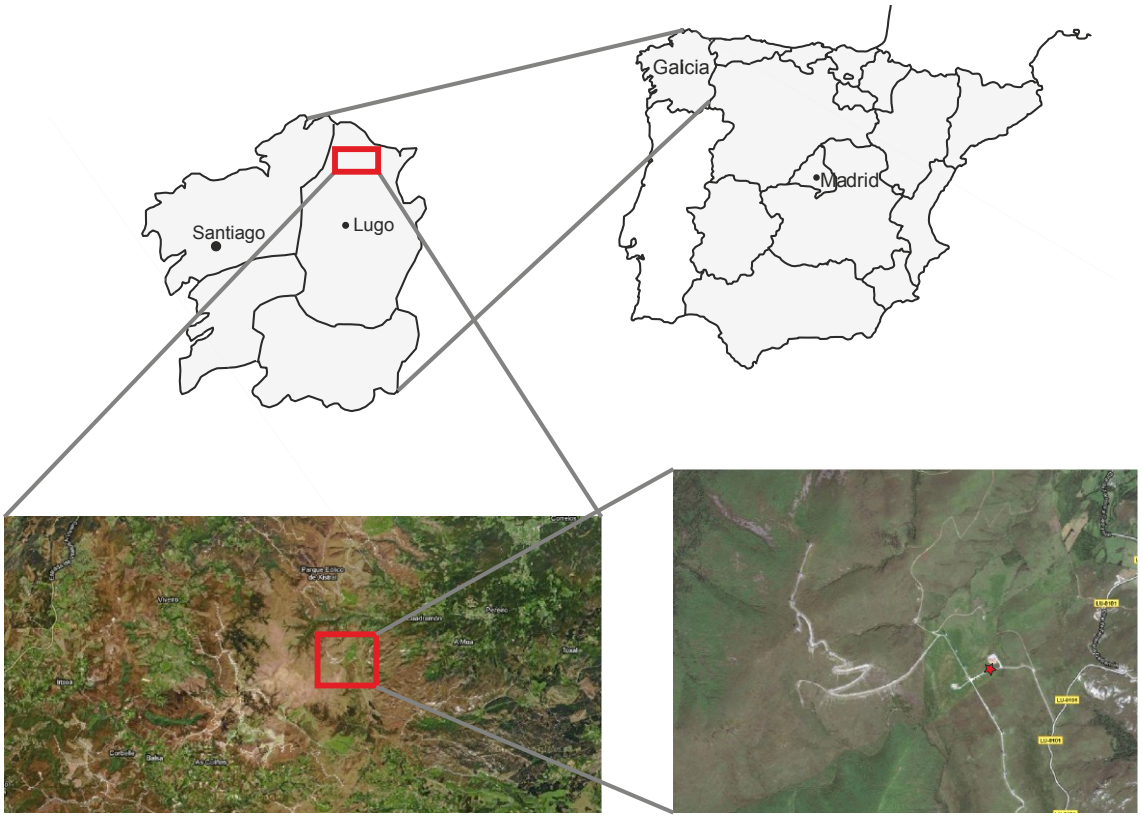

Fig. 4-6 Sampling Site in Galicia, Spain (satellite photograph taken from Google Maps).

4.1.3 Lake Gossenkölle, Kühtai, Austria

In order to determine the oceanic influence on mercury species in Patagonia and Galicia, an additional sampling area without any oceanic influence was chosen for comparative purposes. This inland site is located at the Biosphere Reserve “Gossenköllesee”. The Lake Gossenkölle (N47°13'47"/E11°00'50") is a high-alpine lake (2417 m a.s.l.) at the foot of the Pirchkogel (2828 m a.s.l.) (Kamenik et al., 2000). It is situated in the Stubaier Alps above the small village Kühtai (13 inhabitants) about 30 km west of Innsbruck, Austria.

The Stubaier Alps belong to the Central Alps, which enjoy a predominately continental climate. The precipitation is with about 1200 mm yr^{-1} relatively low compared to the more humid Alpine fringes. Roughly half of the precipitation is in form of snow. Cold snowy winters alternate with warm and dry summers. The mean temperatures range between 0 and 1 °C; with increasing trend.

Eight months of the year Lake Gossenkölle is covered by ice and snow.
Granites, gneisses, and crystalline slates make up the bedrock of the area. Only 10 % are covered with soil and vegetation (alpine grass, heather; Heisberger 1988).
There is no land use directly within the reserve. Occasionally sheep graze within the surroundings.

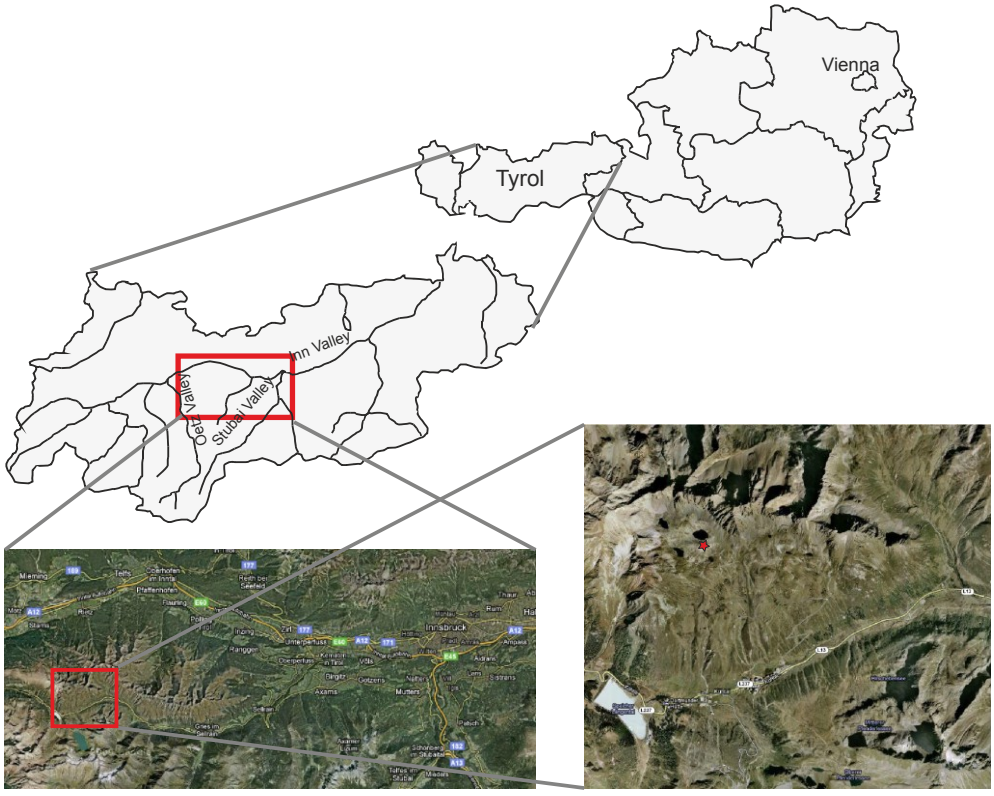

Fig. 4-7 Sampling Site Lake Gossenkölle, Kühtai, Austria (satellite photograph taken from Google Maps).

Fig. 4-8 **Sampling of atmospheric mercury at the limnological station of the University of Innsbruck at Lake Gossenkölle. In front: Inlet for TGM; on the roof: measurement of meteorological data and precipitation sampling.**

4.2 Results

4.2.1 Total Gaseous Mercury in Patagonia, Chile

TGM concentrations were measured at the three sites consecutively. In 2002, a screening was done with single measurements distributed throughout the day (Fig. 4-9). In 2003 a continuously measurement was performed over several days at each site (Fig. 4-10).

The statistical summaries of TGM measured in 2002 and 2003 are listed in Tab. 4-1 and Tab. 4-2, respectively. Average concentrations of TGM were in the same range at the three sites GC, Sky, and PBr with mean concentrations of 1.06 ng m^{-3}, 1.26 ng m^{-3}, and 1.36 ng m^{-3}, respectively for the sampling period in 2002 and 1.02 ng m^{-3}, 0.87 ng m^{-3}, and 1.29 ng m^{-3} for the sampling period in 2003.

Tab. 4-1 Statistical summary of TGM measurements in 2002.

TGM	GC	Sky	PBr
Minimum [ng m^{-3}]	0.17	0.79	0.50
Maximum [ng m^{-3}]	2.56	1.71	4.57
Mean [ng m^{-3}]	1.06	1.26	1.36
Median [ng m^{-3}]	0.86	1.19	0.87
SD	0.69	0.26	1.07
Number of Samples	33	27	19

Tab. 4-2 Statistical summary of TGM measurements in 2003. For the mean concentration at Sky two values were calculated. The first is the total mean value; the one in brackets is the mean value for the stable period (see chapter 4.3.9 for more information).

TGM	GC	Sky	PBr
Minimum [ng m^{-3}]	0.01	0.08	0.45
Maximum [ng m^{-3}]	2.40	3.49	2.57
Mean [ng m^{-3}]	1.02	0.87 (1.16)	1.29
Median [ng m^{-3}]	0.92	0.95	1.28
SD	0.36	0.51	0.20
Number of Samples	244	583	258

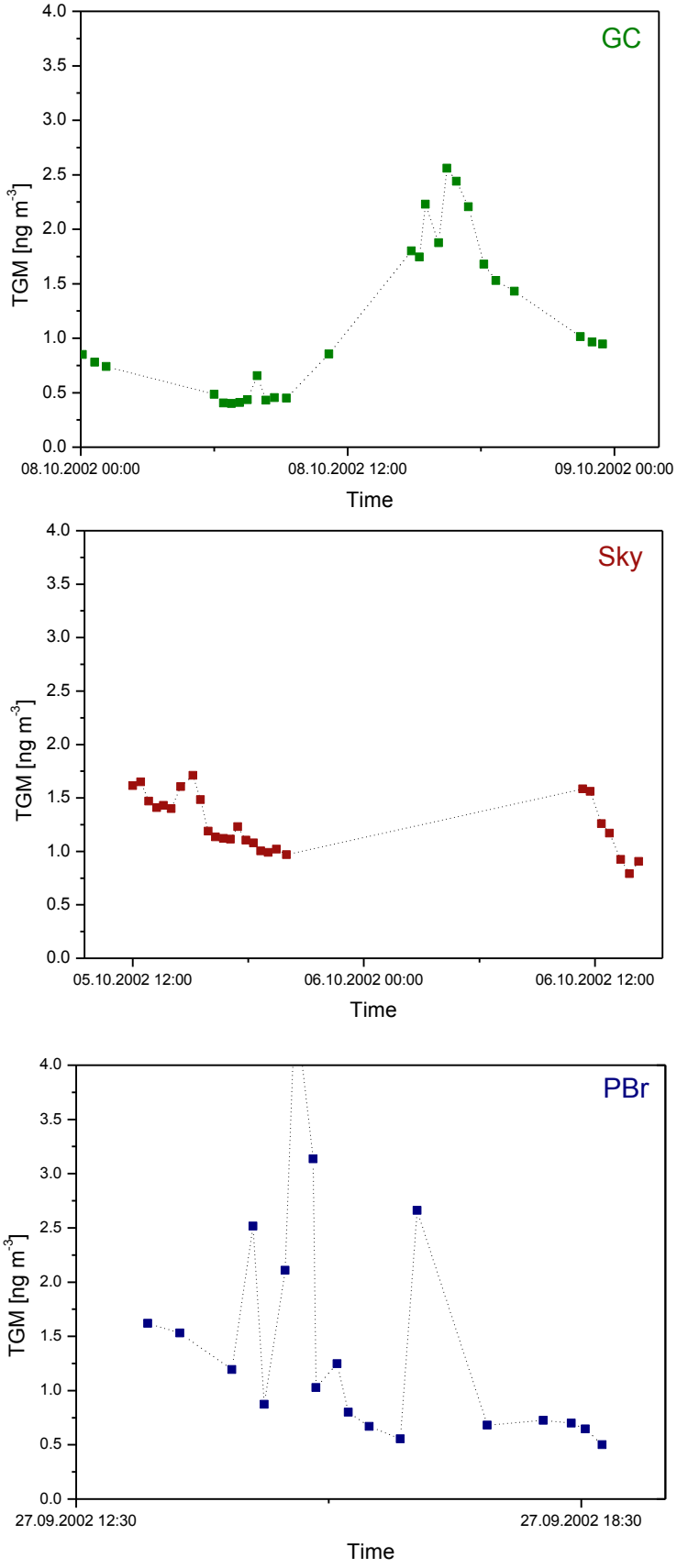

Fig. 4-9 **TGM measurements at the three sites GC (top), Sky (middle) and PBr (bottom) in 2002.**

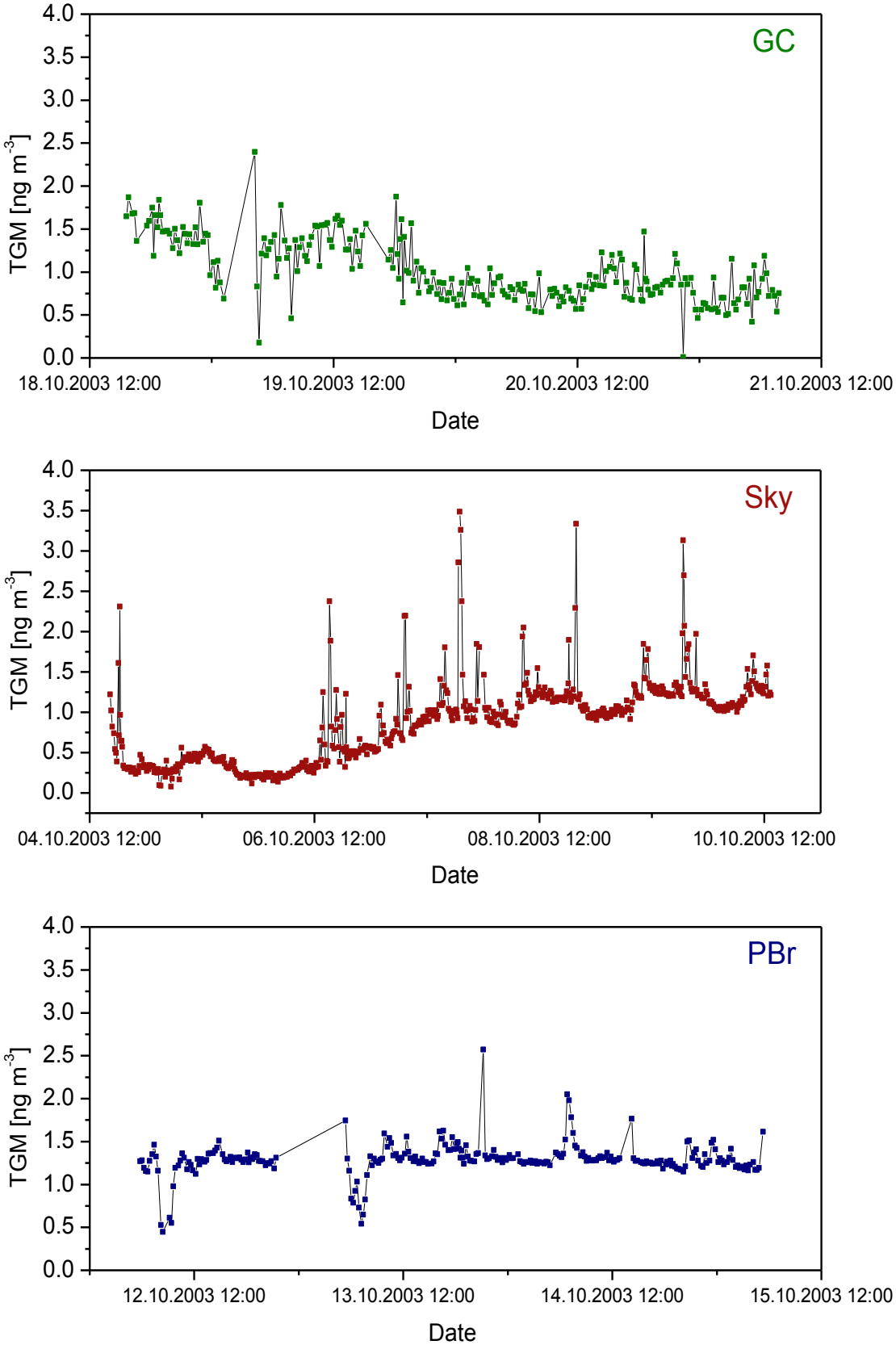

Fig. 4-10 TGM measurements at the three sites GC (top), Sky (middle) and PBr (bottom) in 2003.

4.2.2 Reactive Gaseous Mercury in Patagonia, Chile

RGM concentrations were measured at the three sites consecutively. In 2002, four samples were taken in duplicates at each site. In 2003 a continuously series of sample-duplicates was taken over several days at each site.

The RGM values ranged from 25 pg m^{-3} to 122 pg m^{-3}. Mean concentrations were 73 pg m^{-3}, 80 pg m^{-3}, and 83 pg m^{-3} at GC, Sky, and PBr, respectively. The statistical summary of RGM measured in 2002 and 2003 is listed in Tab. 4-3 and plotted in Fig. 4-11.

Tab. 4-3 Statistical summary of RGM measurements in 2002 and 2003.

RGM	GC	Sky	PBr
Minimum [pg m^{-3}]	25	28	29
Maximum [pg m^{-3}]	95	122	111
Mean [pg m^{-3}]	73	80	83
Median [pg m^{-3}]	78	85	88
SD	20	26	25
Number of Samples	21 (x2)	23 (x2)	20 (x2)

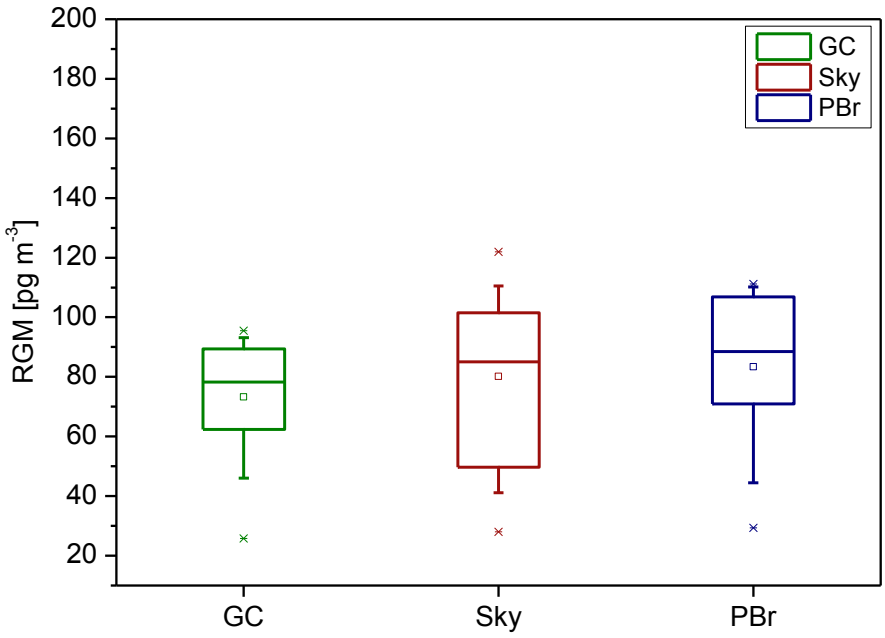

Fig. 4-11 Box Plots of RGM at the three locations GC, Sky, and PBr in 2002 and 2003.

4.2.3 Total Particulate Mercury in Patagonia, Chile

TPM values were taken in duplicates at all three sites in 2002 and 2003. TPM concentrations varied between 52 pg m^{-3} and 367 pg m^{-3} with average concentrations for the three sites of around 63 pg m^{-3} (GC), 357 pg m^{-3} (Sky), and 97 pg m^{-3} (PBr) for the campaign in 2002 (Tab. 4-4 and Fig. 4-12) and 91 pg m^{-3} (GC), 283 pg m^{-3} (Sky), and 187 pg m^{-3} (PBr) for the campaign in 2003 (Tab. 4-4 and Fig. 4-13).

Tab. 4-4 TPM concentrations for the three sites in 2002 and 2003.

TPM	GC	Sky	PBr
2002a [pg m^{-3}]	52.3	366.9	76.7
2002b [pg m^{-3}]	73.4	346.1	117.6
Average 2002 [pg m^{-3}]	62.9	356.5	97.2
2003a [pg m^{-3}]	103.4	297.5	175.6
2003b [pg m^{-3}]	78.6	267.4	196.3
Average 2003 [pg m^{-3}]	91.0	282.5	187.0

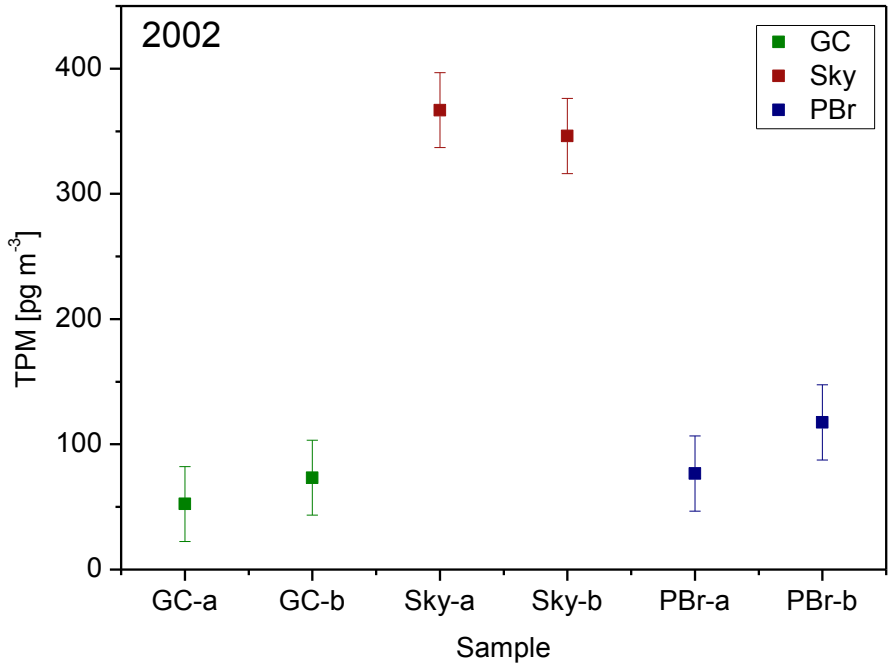

Fig. 4-12 TPM concentrations at the three sites GC, Sky, and PBr in 2002.

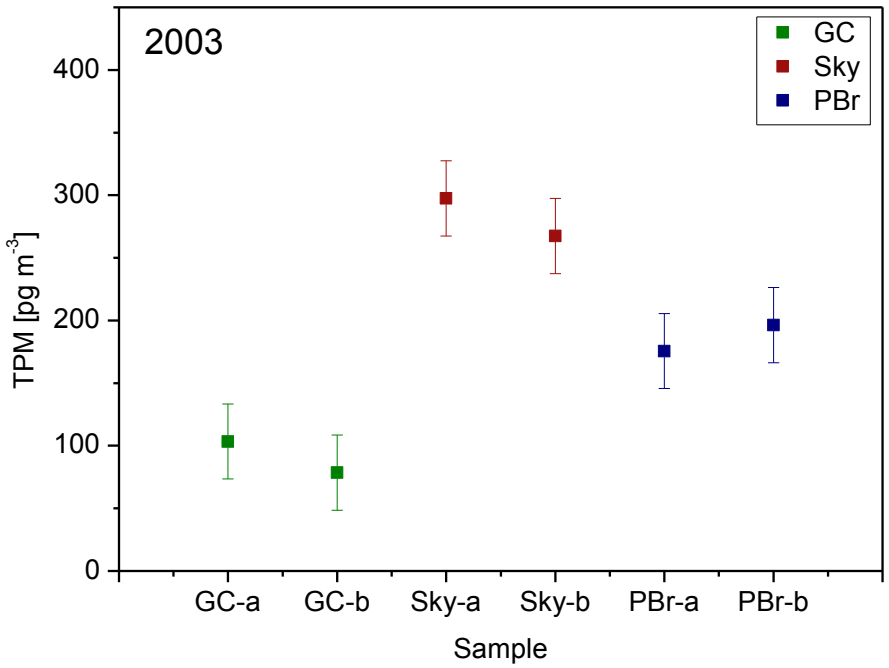

Fig. 4-13 TPM concentrations at the three sites GC, Sky, and PBr in 2003

4.2.4 Mercury in Precipitation in Patagonia, Chile

The total Hg concentrations in precipitation at the three sites were in general very low with volume-weighted mean (VWM) concentrations of 0.48 ng L^{-1} and 0.39 ng L^{-1} for GC and Sky in 2002 and 0.77 ng L^{-1}, 0.60 ng L^{-1}, and 0.83 ng L^{-1} for GC, Sky and PBr in 2003 (Tab. 4-5 and Fig. 4-14).

Tab. 4-5 Summary of Hg concentrations in precipitation at GC and Sky in 2002 and 2003 (ND: no data).

Hg in Precipitation 2002	**GC**	**Sky**	**PBr**
Minimum [ng L^{-1}]	0.40	0.27	ND
Maximum [ng L^{-1}]	0.61	0.59	ND
Mean [ng L^{-1}]	0.48	0.39	ND
Number of Samples	7	7	ND
Hg in Precipitation 2003	**GC**	**Sky**	**PBr**
Minimum [ng L^{-1}]	0.68	0.47	0.66
Maximum [ng L^{-1}]	0.89	0.68	1.09
Mean [ng L^{-1}]	0.78	0.60	0.83
Number of Samples	5	5	5

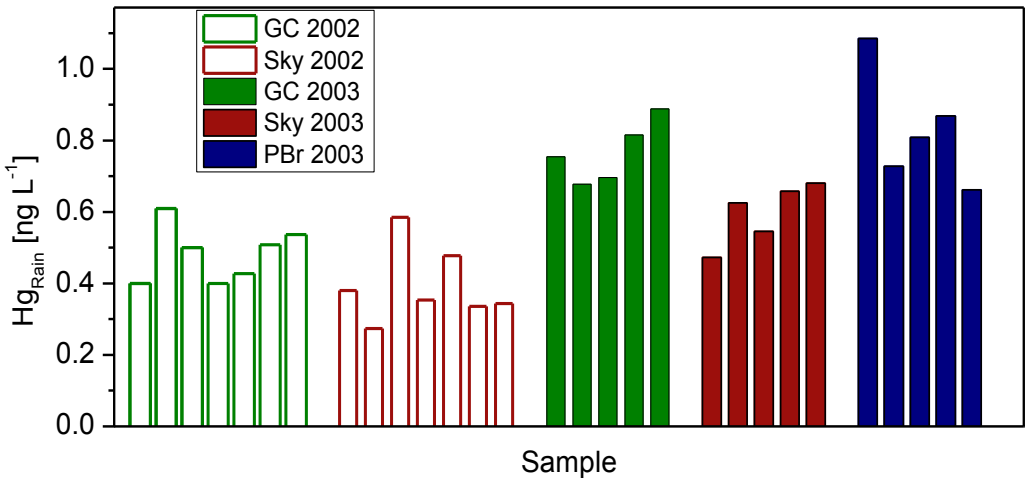

Fig. 4-14 Mercury concentrations in precipitation at GC, Sky and PBr in 2002 and 2003.

4.2.5 Total Gaseous Mercury in Galicia, Spain

TGM concentrations were measured continuously for three days in February 2003 and for five days in July 2003. The statistical summaries of TGM are listed in Tab. 4-6. TGM concentrations varied from 0.289 ng m^{-3} to 4.811 ng m^{-3}. Average concentrations of TGM were in the same range at both campaigns with mean concentrations of 1.003 ng m^{-3} in February and 1.066 ng m^{-3} in July 2003.

Tab. 4-6 Statistical summary of TGM measurements in February and July 2003.

TGM	02/2003	07/2003
Minimum [ng m^{-3}]	0.657	0.289
Maximum [ng m^{-3}]	2.869	4.811
Mean [ng m^{-3}]	1.003	1.066
Median [ng m^{-3}]	0.866	0.795
SD	0.363	0.798
Number of Samples	285	480

4.2.6 Reactive Gaseous Mercury in Galicia, Spain

RGM concentrations varied between 13 pg m^{-3} and 77 pg m^{-3}. The mean concentrations were 55.56 pg m^{-3} and 38.51 pg m^{-3} for February and July, respectively. The statistical summaries of RGM are listed in Tab. 4-7. The individual samples and the deviation in RGM is shown in Fig. 4-15.

Tab. 4-7 Summary of RGM measurements in February and July 2003.

RGM	02/2003	07/2003
Minimum [pg m^{-3}]	33.45	12.94
Maximum [pg m^{-3}]	76.62	73.57
Mean [pg m^{-3}]	55.56	38.51
Median [pg m^{-3}]	56.59	38.00

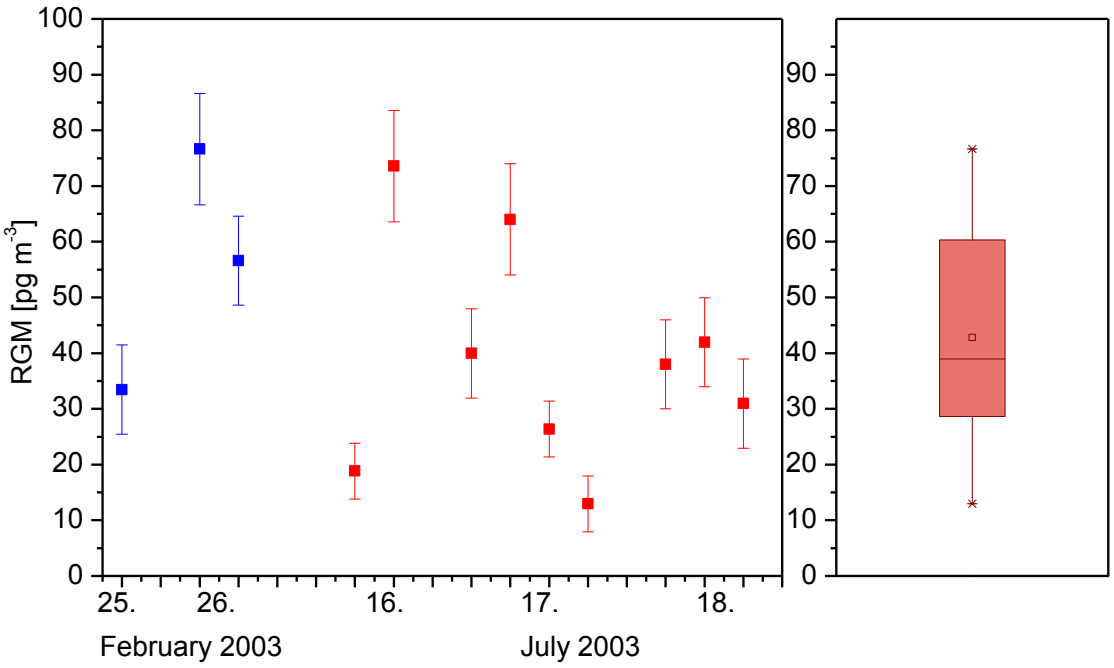

Fig. 4-15 RGM measurements in Galicia in February and July, 2003.

4.2.7 Total Particulate Mercury in Galicia, Spain

TPM concentrations have been determined during the campaign in July, 2003. The concentrations varied between 38 pg m^{-3} and 74 pg m^{-3} and were all in a similar range (Fig. 4-16).

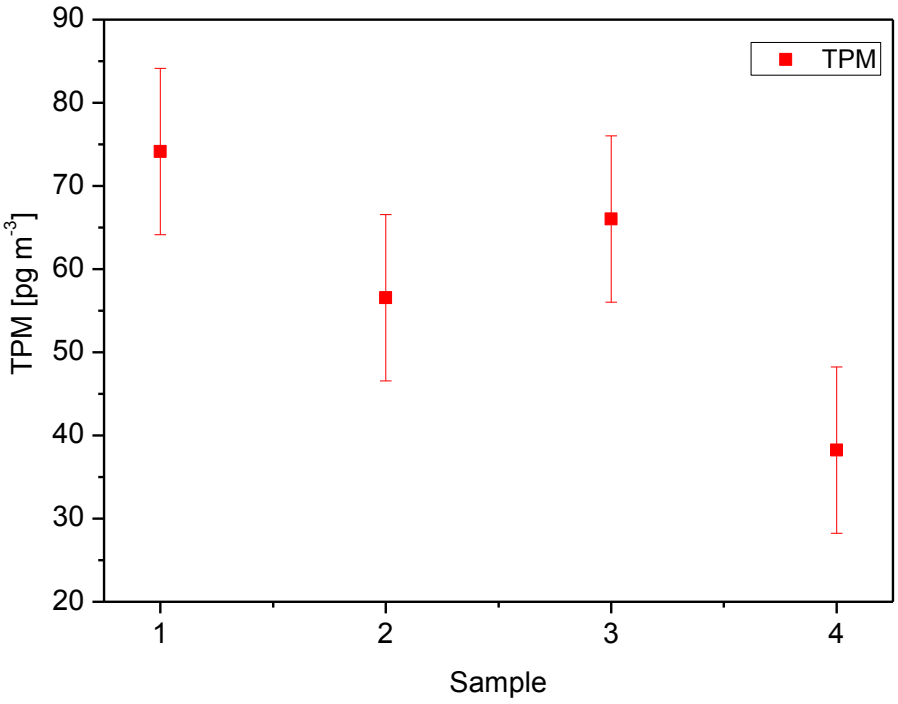

Fig. 4-16 TPM measurements in Galicia in July, 2003.

4.2.8 Mercury in Precipitation in Galicia, Spain

The VWM Hg concentrations in precipitation varied between 1.30 ng L^{-1} and 2.27 ng L^{-1} (Tab. 4-8 and Fig. 4-17).

Tab. 4-8 Summary of Hg in Precipitation in February and July 2003.

Hg in Precipitation	02/2003	07/2003
Minimum [ng L^{-1}]	1.18	1.39
Maximum [ng L^{-1}]	1.56	2.27
Mean [ng L^{-1}]	1.32	1.89
Median [ng L^{-1}]	1.30	2.02
Number of Samples	7	5

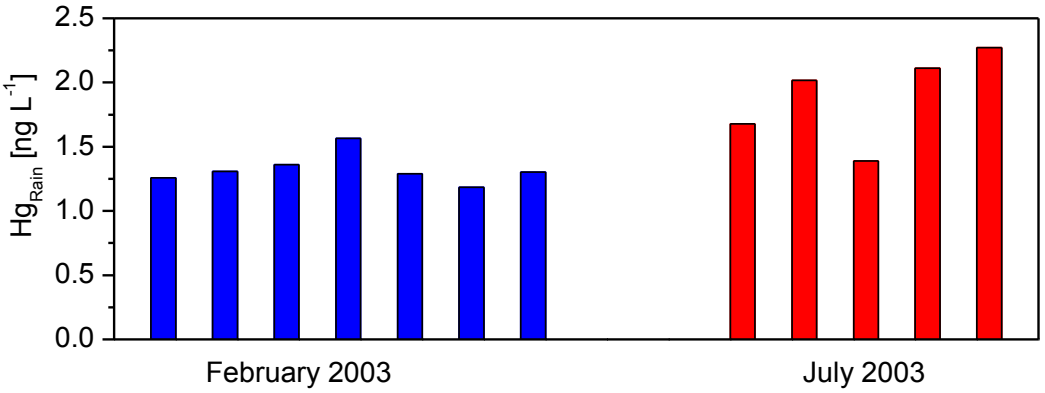

Fig. 4-17 Hg in Precipitation in Galicia in February and July, 2003.

4.2.9 Total Gaseous Mercury at Lake Gossenkölle, Austria

Atmospheric mercury species were measured in April and June 2003. In April 2003 the complete surroundings were covered by snow. In June 2003, the snow was melted completely and the underlying ground - bedrock and to a minor extent grassland - was in direct contact to the atmosphere.

TGM concentrations were measured continuously for several days in April 2003 and in June 2003. The statistical summaries of TGM are listed in Tab. 4-9. Average concentrations of TGM were in the same range at both campaigns with mean concentrations of 1.83 ng m^{-3} in April and 2.03 ng m^{-3} in June 2003.

Tab. 4-9 Statistical summary of TGM measurements in April and June 2003.

TGM	04/2003	06/2003
Minimum [ng m^{-3}]	1.26	1.39
Maximum [ng m^{-3}]	3.83	5.98
Mean [ng m^{-3}]	1.83	2.03
Median [ng m^{-3}]	1.68	1.89
SD	0.42	0.56
Number of Samples	1276	643

4.2.10 Reactive Gaseous Mercury at Lake Gossenkölle, Austria

RGM samples were taken in a continuously series of sample-duplicates in April as well as in June over several days.

The RGM concentrations varied between 3 pg m^{-3} and 58 pg m^{-3} (Tab. 4-10). The mean concentrations were 22.37 pg m^{-3} and 27.84 pg m^{-3} for April and June, respectively.

Tab. 4-10 Summary of RGM measurements in April and June 2003.

RGM	04/2003	06/2003
Minimum [pg m^{-3}]	3	9
Maximum [pg m^{-3}]	49	57
Mean [pg m^{-3}]	22	27
Median [pg m^{-3}]	22	27
SD	10	10
Number of Samples	54	56

The variation of the RGM concentrations was quite high in April as well as in June. However, no daily pattern could be observed (Fig. 4-18 and Fig. 4-19).

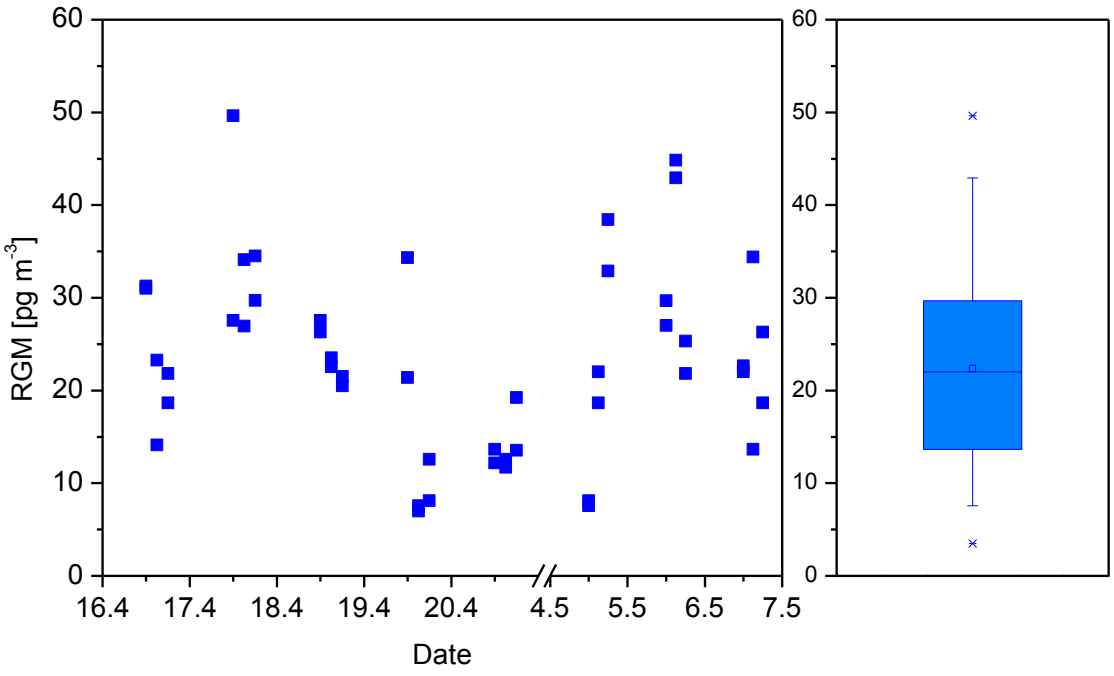

Fig. 4-18 RGM measurements at Lake Gossenkölle, Kühtai, Austria in April, 2003.

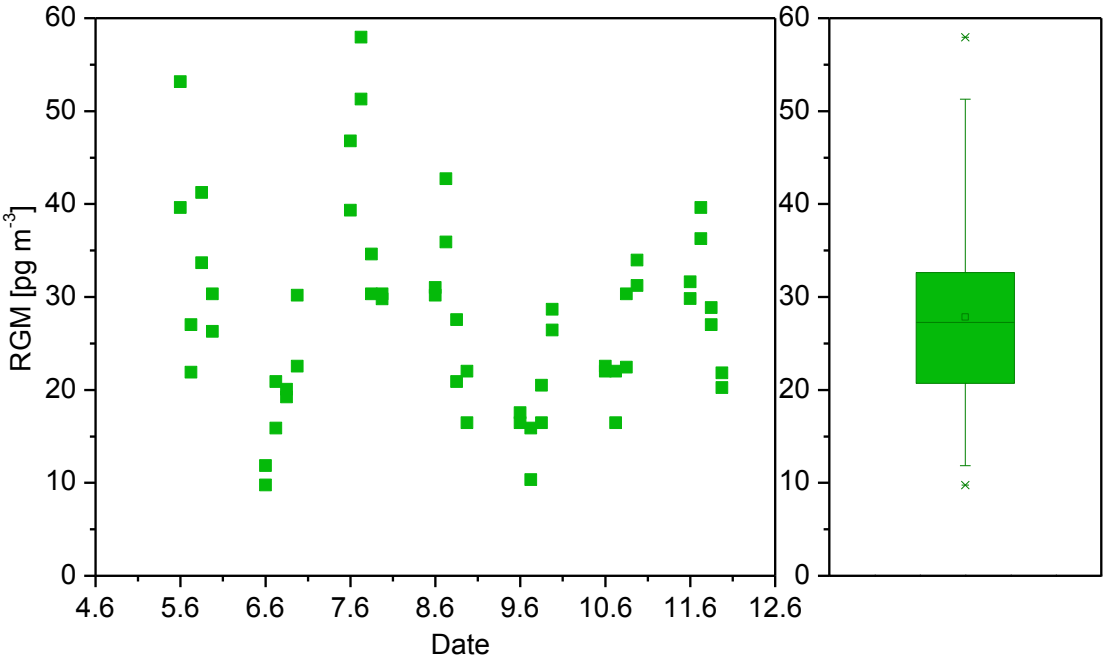

Fig. 4-19 RGM measurements at Lake Gossenkölle, Kühtai, Austria in June, 2003.

4.2.11 Total Particulate Mercury at Lake Gossenkölle, Austria

TPM concentrations have been determined during the campaigns in April and June, 2003 at each with two duplicates. The concentrations varied between 20 pg m^{-3} and 66 pg m^{-3}, whereby the duplicates always showed similar values (Fig. 4-20)

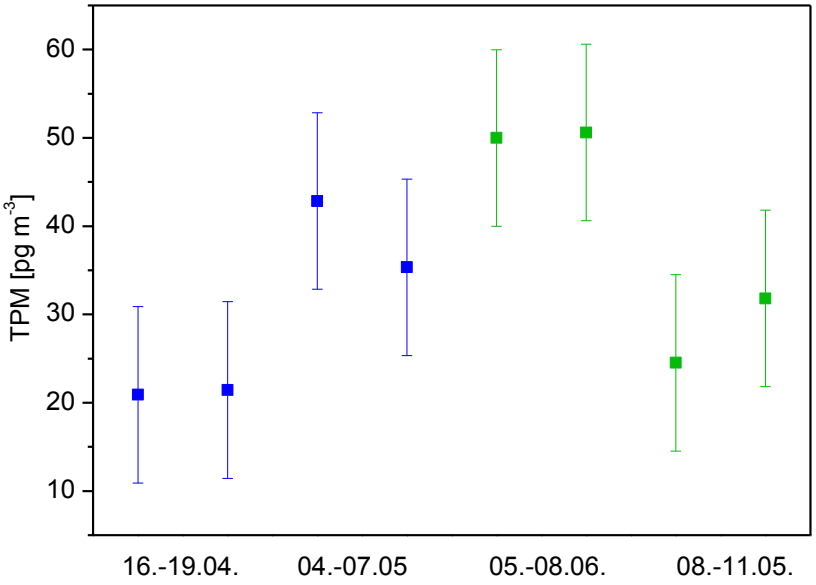

Fig. 4-20 TPM measurements at Lake Gossenkölle, Kühtai, Austria in April and June, 2003.

4.2.12 Mercury in Precipitation at Lake Gossenkölle, Austria

Mercury in Precipitation was only sampled during the campaign in June. During the campaign in April only little precipitation occurred and this precipitation was in form of snow. However, due to the low density of snow the collection of enough material would have taken too long. Especially, when taking into account the fast photo-induced Hg(II) reduction in snow (Lalonde et al., 2003), the comparison of Hg in snow and Hg in rain would have been very challenging and defective. For more information about mercury concentration and Hg(II) reduction in snow the reader is referred to Chapter 6.

The VWM Hg concentrations in precipitation varied between 3.65 ng L^{-1} and 6.15 ng L^{-1} (Tab. 4-11 and Fig. 4-21).

Tab. 4-11 Summary of Hg in Precipitation in April and June 2003.

Hg in Precipitation	04/2003	06/2003
Minimum [ng L^{-1}]	ND	3.65
Maximum [ng L^{-1}]	ND	6.15
Mean [ng L^{-1}]	ND	4.52
Median [ng L^{-1}]	ND	4.38
Number of Samples	ND	10

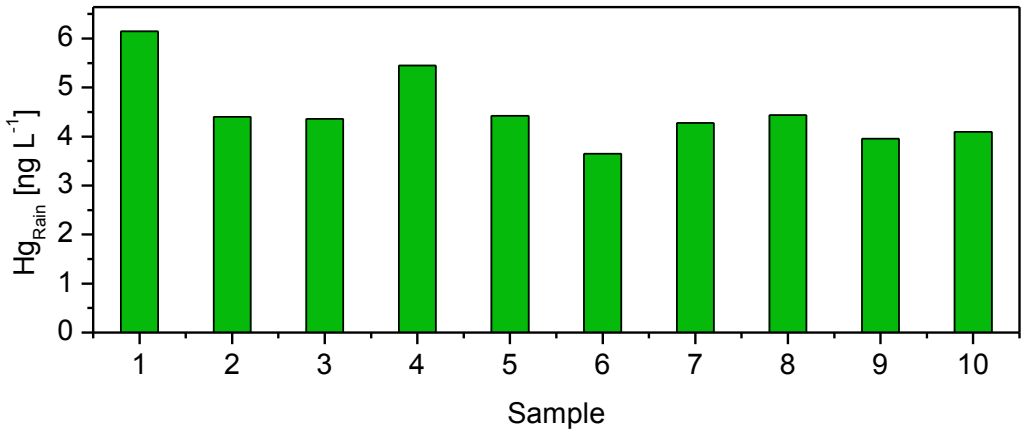

Fig. 4-21 Mercury in Precipitation at Lake Gossenkölle, Kühtai, Austria in June, 2003.

4.3 Discussion

4.3.1 Mercury Data from Patagonia in Comparison with other Locations

The TGM concentrations (mean: 1.09 ng m^{-3}) are in good agreement with average Southern Hemisphere background TGM concentrations (see also Chapter 2.9.3) from previous studies (Slemr et al., 1995; Baker et al., 2002; Ebinghaus et al., 2002b; Slemr et al., 2003; Temme et al., 2003a; Brunke et al., 2010; Slemr et al., 2011). Temme et al, (2003a) found a mean TGM concentration of 1.1 ng m^{-3} over the South Atlantic Ocean between the Neumayer Station and Punta Arenas. The mean TGM concentration at the Neumayer Station is given with 1.08 ng m^{-3} during Antarctic Summer between December 2000 and February 2001 (Temme et al., 2003a). Between August and November 2000 the arithmetic mean was calculated with 0.958 ± 0.278 ng m^{-3} (Ebinghaus et al., 2002b). Slemr et al. (2011) state that TGM concentrations in the Southern Hemisphere decreased from about 1.35 ng m^{-3} around 1996 to about 0.9 ng m^{-3} around 2008.

The relatively high concentrations of RGM (mean: 79 pg m^{-3}) are in good agreement with previous studies in the Southern Hemisphere. RGM concentrations at the Neumayer Station, Antarctica varied between 5 pg m^{-3} and maximum levels of more than 300 pg m^{-3} during the summer period of 2000/2001 (Temme et al., 2003a). Similar values have been reported in the Antarctic at Terra Nova Bay where concentrations ranged from 10.5 to 334 pg m^{-3}, with an average of 116.2 pg m^{-3} (Sprovieri et al., 2002) and at McMurdo where concentrations ranged from 29 to 275 pg m^{-3} with an average of 116 pg m^{-3} (Brooks et al. 2008b). Comparably high values were found at the South Pole with concentrations between 95 and 705 pg m^{-3} and an average of 344 pg m^{-3} (Brooks et al., 2008a). On the Northern Hemisphere similar values were found with e.g. RGM concentrations up to more than 900 pg m^{-3} in the Arctic (Lindberg et al., 2002) and RGM concentrations of 0−386 pg m^{-3} in southern Québec, Canada (Poissant et al., 2005).

TPM data (mean: 180 pg m^{-3}) are intermediate compared to other data from the Southern Hemisphere (compare with Tab. 2-14) were TPM concentrations ranged from 4 pg m^{-3} to 827 pg m^{-3} (Sprovieri et al., 2002; Arimoto et al., 2004; Brooks et al., 2008a,b).

Mercury concentrations in precipitation (mean: 0.64 ng L^{-1}) are extremely low. Especially when compared to data obtained by NADP-MDN, the low mercury concentrations in Patagonian precipitation get obvious. Within the NADP-MDN mean annual concentrations in precipitation in 2002 were between 5 ng L^{-1} for Maine and 26 ng L^{-1} for New Mexico (NADP, 2003) and in 2003 between 3 ng L^{-1} for Oregon and 27 ng L^{-1} for New Mexico

(NADP, 2004). The extremely low mercury concentrations are a result of a diluting effect of the already very clean air in Patagonia due to the very high precipitation rates.

4.3.2 Mercury Data from Galicia in Comparison with other Locations

The TGM values in Galicia (mean: 1.03 ng m^{-3}) are relatively low compared to other measured TGM values in the Northern Hemisphere (compare to Tab. 2-10, Tab. 2-11, and Tab. 2-12). Also TGM measurements over the Atlantic Ocean showed higher TGM values immediately west of Galicia (Temme, 2003). However, within the MAMCS and the MERCYMS programmes (compare to chapter 2.9.1) some other locations also showed such low or even lower mean values, namely Calabria, Italy; Haifa, Israel and Piran, Slovenia. The reason for these quite low TGM concentrations might be the precipitation rate in this region, which is with 1400 to 1800 mm (Martínez-Cortizas et al., 2002) quite high and leads to a Hg washout from the atmosphere. A second reason is probably a low reemission from the surface, due to the waterlogged surface (bog)(compare to section 4.3.4).

The dispersion of the RGM data (13 pg m^{-3} and 77 pg m^{-3}) during the campaigns in Galicia (Fig. 4-15) are in a normal range and do not show any distinctive pattern.
The RGM concentrations match with RGM data collected within other studies at different coastal European sites (compare to chapter 2.9.1) where mean RGM concentrations generally varied between 10 pg m^{-3} and 70 pg m^{-3} with only few outliers.

Also the TPM data (mean: 59 pg m^{-3}) match with TPM data collected within other studies at different European sites (compare to chapter 2.9.1) where mean TPM concentrations generally varied between 10 pg m^{-3} and 100 pg m^{-3} with only few outliers.

Concerning Hg concentration in precipitation (mean: 1.56 ng L^{-1}), unfortunately for discussion, no robust data from comparable regions in Europe could be found in literature. Thus, the data are compared to data obtained by NADP-MDN for the USA. The Hg concentrations in precipitation are quite low in Galicia, Spain. Within the NADP-MDN mean annual concentrations in precipitation in 2003 varied between 3 ng L^{-1} for Oregon and 27 ng L^{-1} for New Mexico (NADP, 2004).
The low mercury concentrations are interpreted as a result of a diluting effect of the already very clean air in Galicia due to the very high precipitation rates.

4.3.3 Mercury data of Lake Gossenkölle in Comparison with other Locations

TGM values at Lake Gossenkölle (mean: 1.93 ng m^{-3}) are higher than those measured in Patagonia, Chile and Galicia, Spain. Compared to other measured TGM values at remote sites in the Northern Hemisphere (compare to Tab. 2-10, Tab. 2-11, and Tab. 2-12), these values are more or less intermediate ones. For the mean TGM values given in the MOE, MAMCS, and MERCYMS projects (Tab. 2-10), the average of the different mean concentrations is about 2.01 ng m^{-3}.

RGM concentrations at Lake Gossenkölle (mean: 25 pg m^{-3}) are lower than in Patagonia (see Chapter 4.2.2) and Galicia (see Chapter 4.2.6). The concentrations were in general slightly lower in April than in June. The variation of RGM concentrations were in the same range for April (Fig. 4-18) and June (Fig. 4-19) with a slightly higher IQR in April. However, this difference is not significant enough to allow any conclusion about differences in transformation processes during the two campaigns.

TPM concentrations (mean: 37 pg m^{-3}) are much lower at Lake Gossenkölle than in Patagonia (see Chapter 4.2.3) and in Galicia (see Chapter 4.2.7). No significant differences between the measurements in April and June could be seen.

Mercury concentrations in precipitation (mean: 4.52 ng L^{-1}) are significantly higher than those in Patagonia, Chile and Galicia, Spain. However, compared to data obtained by NADP-MDN for the USA, the Hg concentration in precipitation are still at the lower range. Within the NADP-MDN mean annual concentrations in precipitation in 2003 varied between 3 ng L^{-1} for Oregon and 27 ng L^{-1} for New Mexico (NADP, 2004).

4.3.4 Diurnal Variation of Total Gaseous Mercury

An examination of time-resolved TGM concentrations reveals significant differences in diurnal variations between the different sites.
In Patagonia, no clear diurnal trend is evidenced. Especially at the GC site, the up- and down-turns are very flat (Fig. 4-10). However, the own studies in Spain (Fig. 4-23, Fig. 4-24) and Austria (Fig. 4-26, Fig. 4-27) and studies of others (e.g. Dommergue et al., 2002; Feng et al., 2003, 2004; Stamenkovic et al., 2007) show a clear TGM dependency on diurnal variations. For the locations Sky and PBr, intraday variations in TGM concentrations can be observed (Fig. 4-10). However, they are not as significant and periodical as in Galicia or Kühtai (see chapters 4.3.6 and 4.3.7) or other studies (Dommergue et al., 2002; Feng et al. 2003, 2004, Stamenkovic et al., 2007).

4.3.5 Factors suppressing the Diurnal Variation of TGM in Patagonia

Variations in TGM concentrations mainly result from Hg re-emission from soils. Factors supposed to be most important in controlling Hg emissions from soils are radiation (Gustin et al., 2002; Bahlmann et al., 2006), temperature (Poissant et al., 1999; Zhang and Lindberg, 1999; Schlüter, 2000), and soil moisture (Gustin and Stamenkovic, 2005; Poissant et al., 1999; Bahlmann, 2004), with short−term spikes in emissions after precipitation events (Lindberg et al., 1999; Poissant et al., 1999).

Regarding those parameters it is explicable, that the diurnal variations of TGM concentrations are insignificant for GC. The range of both temperature and solar radiation is comparably small due to the mostly completely overcast sky during the sampling period. In the context of radiation it is important to mention that particularly the transmission of UV and especially of UV-B radiation is attenuated by clouds (López et al., 2009). The light-induced mercury emission flux from soils shows a strong spectral response to UV-B radiation (Bahlmann et al., 2006). Moore and Carpi (2005) as well showed that soil fluxes under UV and under full spectrum radiation were significantly elevated over dark fluxes, whereas fluxes were not significantly different from dark fluxes when UV light was removed from incident radiation.

In addition to the meteorological parameters the composition of the soil is responsible for the level of Hg emission. Bahlmann (2004) showed that the moisture of the soil influences the Hg release. Wet soils release more Hg than completely dry soils. However, above critical moisture, the Hg emission decreases again with increasing water content. The water content at which the maximum of Hg emission occurs is hereby dependent on the type of soils and varied in the study of Bahlmann (2004) between 10 % and 35 %.
In the presented study the atmospheric measurements at GC were conducted above a minerogenic fen. The water content of this fen varies between 78 and 94 % (Hertel, 2001). Hence, if the conjecture is accurate, that the findings of Bahlmann (2004) are also true for the peat in Patagonia, the re-emission should be very low. Additionally, it is well known, that Hg in soils mainly exists in the oxidized state and forms stable complexes with organic matter (OM) (e.g. Andersson 1979; Kerndorff and Schnitzer, 1980; Xu and Allard, 1991; Schuster, 1991; Johansson et al., 1991; Meili, 1991b). Several studies also show that the mercury flux from soils decreases with higher OM contents (Yang et al., 2007; Edwards and Howard, 2012) and increases with increasing pH value of soils (Yang et al., 2007; pH range: 4.8-7.1). Thanabalasingam and Pickering (1980) showed that the maximum sorption of Hg(II) onto humic acid takes places in a pH range of pH 4 to pH 5.

The upper part of the minerogenic fen at GC above which the atmospheric measurements were conducted had a pH value of 4.6 and an OM content between 50 and 90 % (Hertel, 2001; Franzen et al., 2004).

Due to the fact that the entire area surrounding GC mainly consists of peatland and also the weather in the upwind direction is affected by mostly overcast sky, the Hg reemissions from surrounding soils should be very low, resulting in an overall low diurnal variation of TGM in this region.

For the location Sky, intraday variations in TGM concentrations can be observed (Fig. 4-10). However, they are not as significant and periodical as in Spain (Fig. 4-23, Fig. 4-24) and Austria (Fig. 4-26, Fig. 4-27) or other studies (Dommergue et al., 2002; Feng et al. 2003, 2004, Stamenkovic et al., 2007). Concentration peaks can always be found in the afternoon. However, in addition there are several TGM peaks which are not evenly distributed throughout the day. An explanation for the trend being observed at Sky but not at GC is that first the underlying soil at Sky was not peat but rather organic rich soil and grassland, which in addition was not as wet as the GC peat. Here, the re-emission of Hg is expected to be generally higher. Secondly, the weather during sampling was different. In the time, where the TGM measurements were conducted, it only fairly rained and the sky was not as much overcast as at GC. Hence, the UV-radiation enhanced reduction of the divalent mercury in soil was higher. During the campaign it could be seen that the response time of the TGM concentrations to changes in radiation was very fast and that there are short−term spikes in emissions due to short breakthroughs of the sun.

For PBr a very flat deviation with some single concentration peaks is observed (Fig. 4-10). In this region, the underlying soil was similar to the one of the Sky, namely organic rich soil and grassland. However, in contrast to the Sky-campaign, in the period, in which the Hg-measurements were conducted at PBr, the sky was overcast all along and it rained most of the time. Hence, the changes in Hg reemissions from soils were very low.

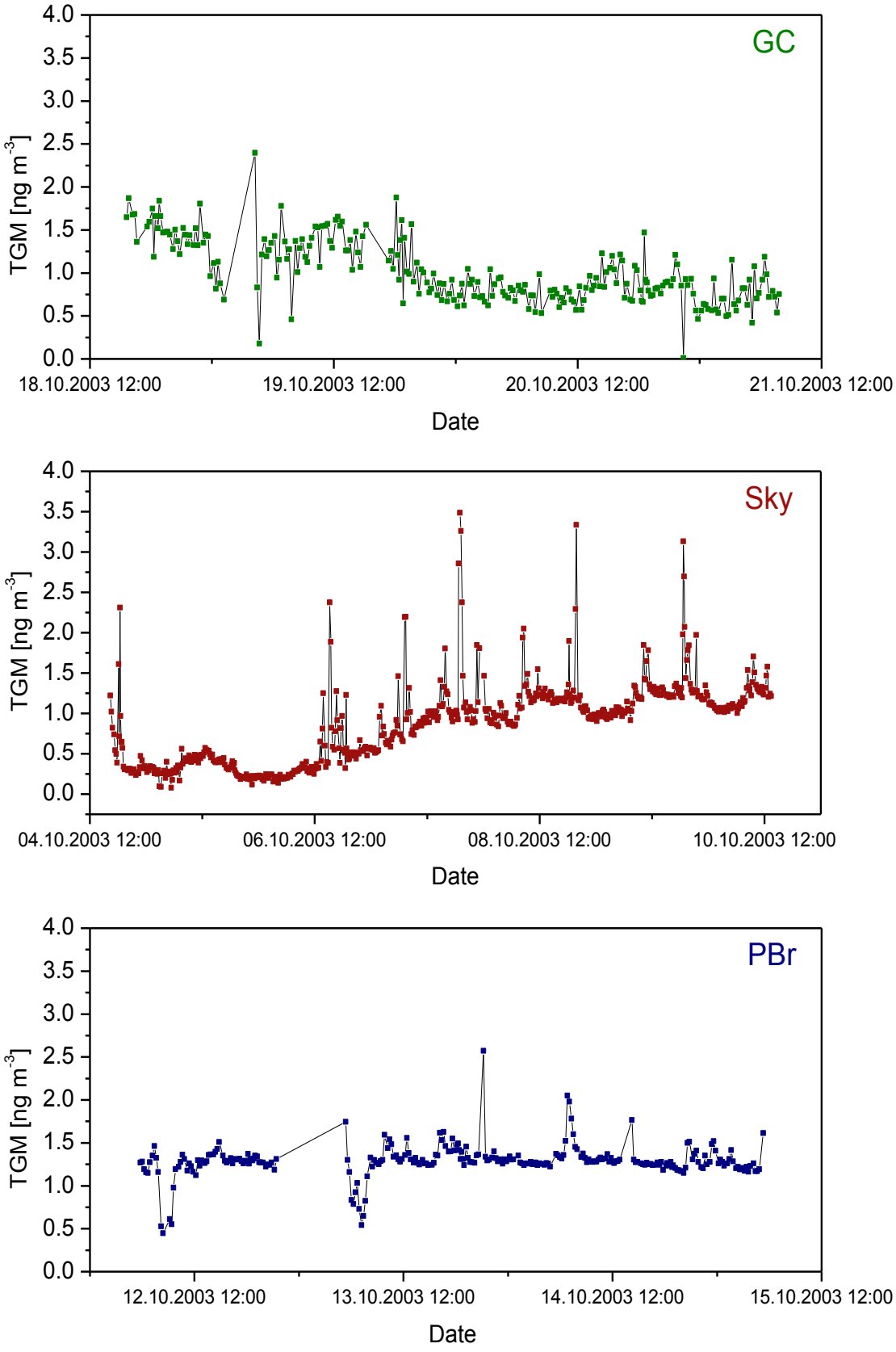

Fig. 4-22 TGM measurements at the three sites GC (top), Sky (middle) and PBr (bottom) in 2003.

4.3.6 Diurnal Variation of TGM as a Result of Insolation

The diurnal variation of TGM is much more pronounced in Galicia and in Kühtai than in Patagonia. Highest TGM concentration in Galicia could be observed during the early afternoon (Fig. 4-23, Fig. 4-24). Lowest concentration could be observed during the night.

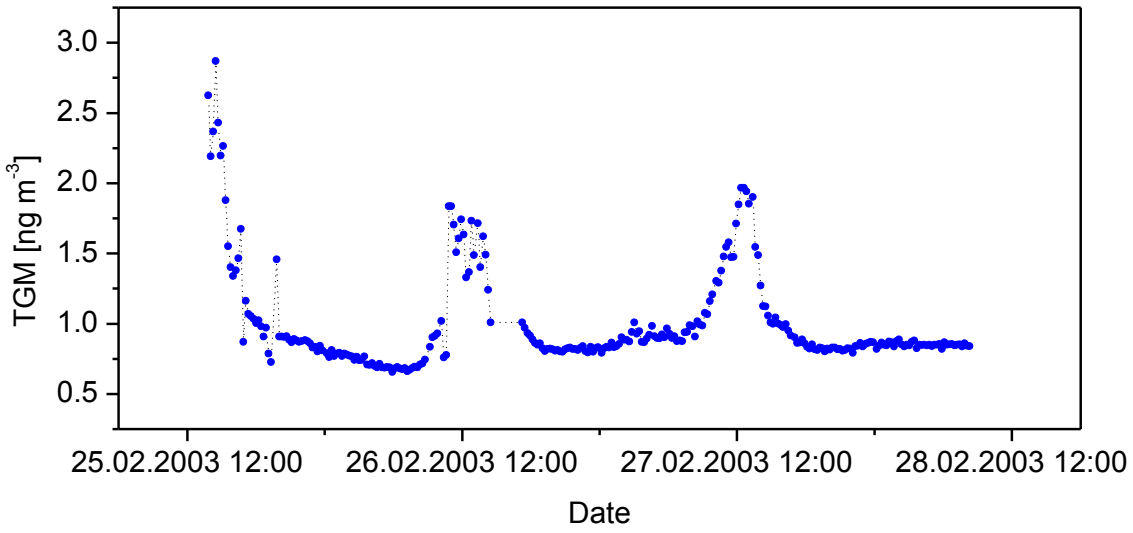

Fig. 4-23 Diurnal variation of TGM in Galicia in February, 2003.

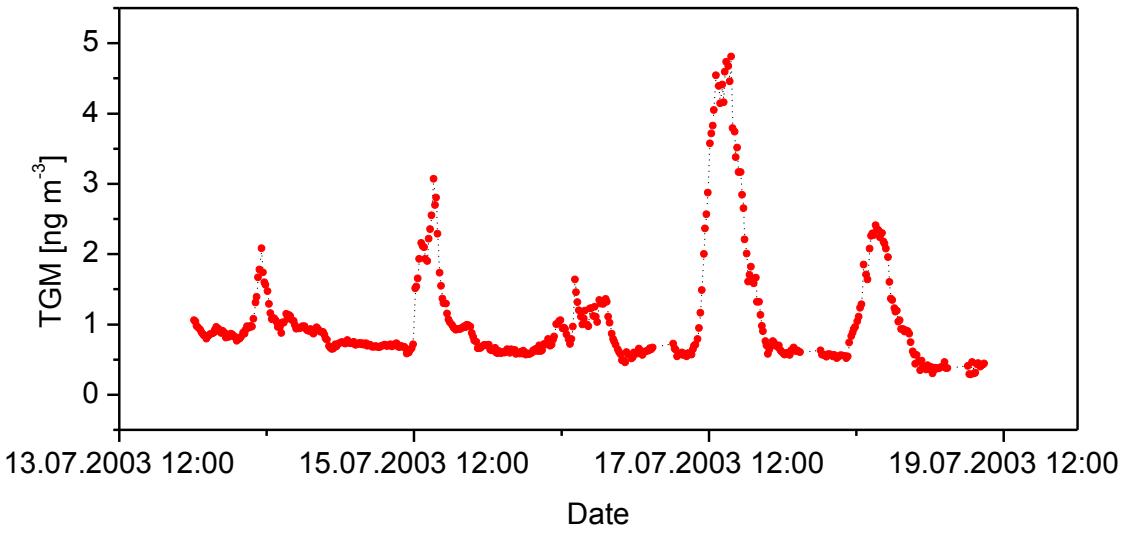

Fig. 4-24 Diurnal variation of TGM in Galicia in July, 2003.

The soil characteristics are similar for both locations, being water saturated bogs. Hence, higher Hg re-emissions are not a result of soil chemistry or water content. On the other hand, the weather and especially the duration and intensity of sunlight were substantially different than in Patagonia. Especially during the campaign in July, the influence of sunlight and associated therewith the influence of UV radiation on the TGM

concentrations could be observed. On the 16th of July the sky was completely overcasted and it rained the entire day. In contrast, on the 17th of July the sky was cloudless for the entire day. On the other days, the weather was variable cloudy with occasional rain.
This different weather conditions are reflected in the diurnal TGM trends, with the highest concentration peak on the sunny day and no distinctive peak on the rainy day.

An evidence for radiation and temperature controlling the TGM concentration is obtained by comparing the TGM time course to the time course of temperature and UV radiation at Kühtai (Fig. 4-25). It can be seen, that the correlation between both temperature and UV radiation on the one hand and TGM concentrations on the other hand is very high on all days. Especially on the 23th of April, where the degree of cloud coverage was very changeable, the dependency of the TGM concentration on temperature and UV radiation gets obvious (Fig. 4-25, lower diagram). Most notably is the very fast response of TGM concentration on chances in temperature and UV-radiation. This implies a very fast reduction of Hg(II) to Hg^0 and subsequent re-emission from the ground or, more explicity, in this case from snow.

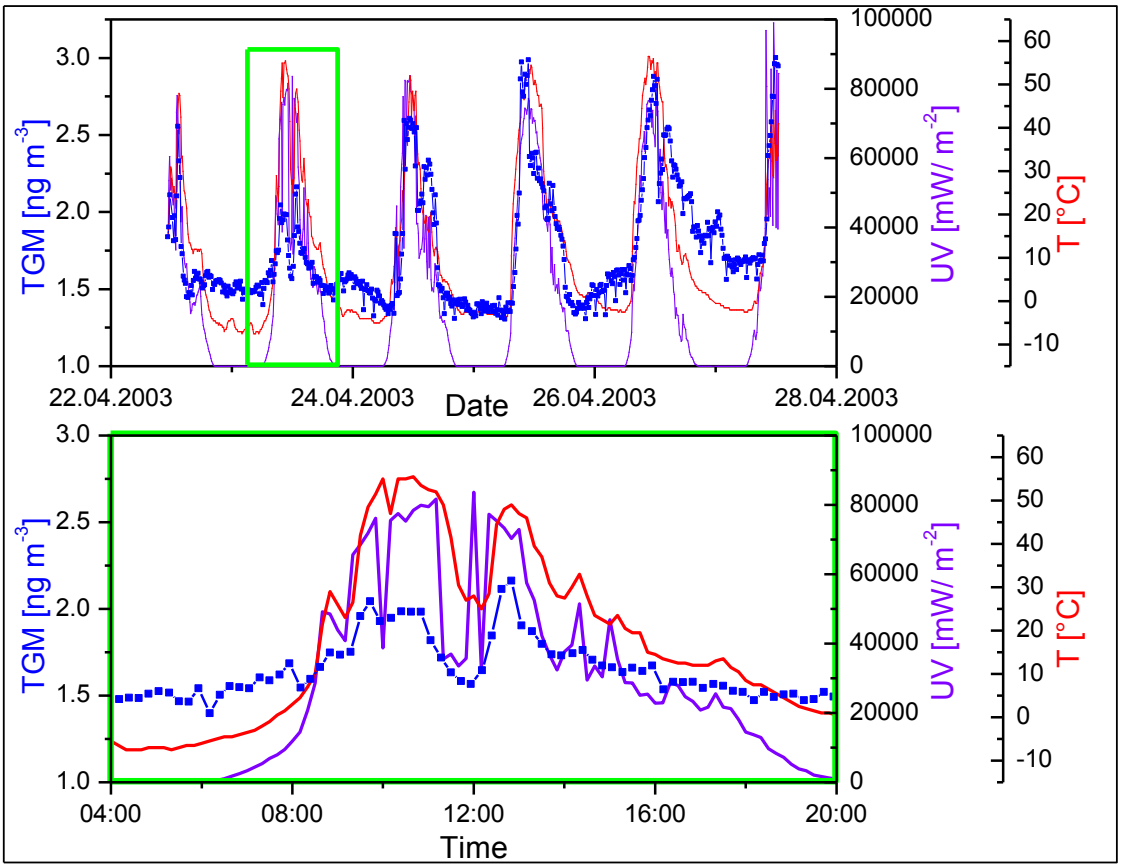

Fig. 4-25 **Diurnal progress of TGM, temperature, and UV radiation at Lake Gossenkölle, Kühtai, Austria in April, 2003. The upper diagram shows a 6 day interval; the lower diagram shows the time-resolved TGM concentrations, temperature and UV radiation of the 23.04.2003.**

4.3.7 Diurnal Variation of TGM above Soil and Snow

The diurnal variation of TGM at Lake Gossenkölle, Kühtai, is much more pronounced than in Patagonia and generally similar to the ones in Galicia. Highest TGM concentration could be observed during midday or in the late morning (Fig. 4-26, Fig. 4-27). Lowest concentration could be observed during the night. While the night-time TGM concentrations in June (Fig. 4-27) were generally slightly higher than in April (Fig. 4-26), the midday peaks were in general slightly lower in June than in April.

A significant difference between the diurnal progresses in TGM concentrations in April and June is the span of highest concentrations. In April, on most days, the time course of TGM concentrations showed a definite and narrow peak during the midday. This fits to different studies about Hg emission from snow packs where it was shown that emission maximizes near midday (Steffen et al., 2002; Ferrari et al., 2005, 2008; Faïn et al., 2007, 2008), with 45 % of daily emission occurring during the 3 h midday interval (Johnson et al., 2008). In contrast, in June, the TGM concentrations rose already during the morning hours and first maximum values were achieved at 9:00 am. Additionally, no distinct concentration peak could be observed, but rather a longer time span in which the concentrations stayed high before they decreased again in the early afternoon. One reason for the earlier TGM increase in the morning was probably because of an earlier sunrise in July than in April. However, in Galicia no temporal differences in TGM increase were found between February and June. The differences in the TGM progress could therefore also be a result from the different underlying ground. While the mercury chemistry in snow packs is mainly isolated and the various mercury compounds do not have many different reaction partners, the chemistry of mercury and its reactions within the soil subsequent to deposition are more complex. Hence, the irradiation mediated reduction of Hg(II) phases is more variable within the soil and different reaction kinetics result in different response speeds of photo induced Hg emission. This finally results in a smearing of the TGM concentrations in time direction.

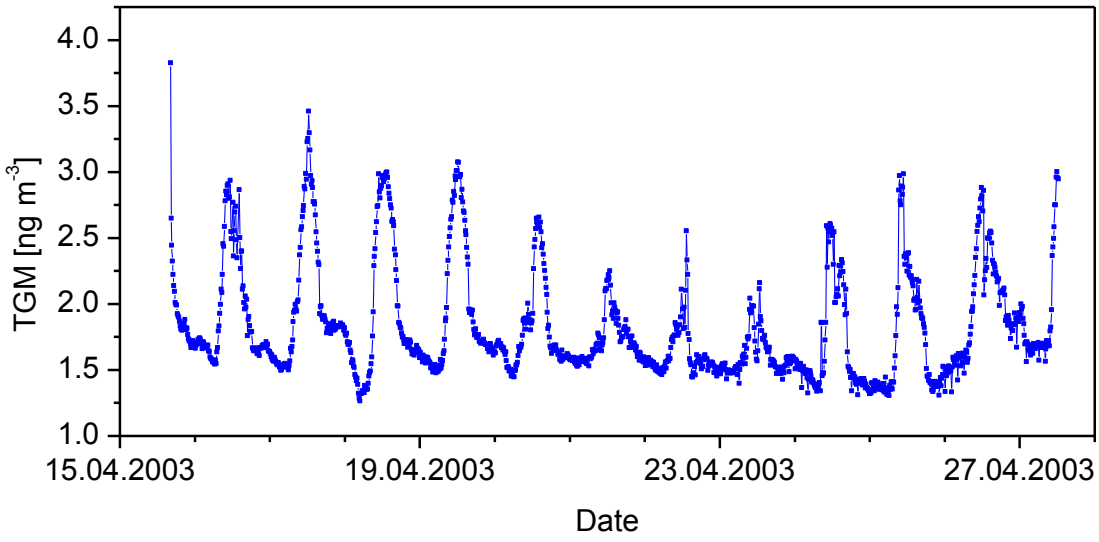

Fig. 4-26 Diurnal variation of TGM at Lake Gossenkölle, Kühtai, Austria in April, 2003.

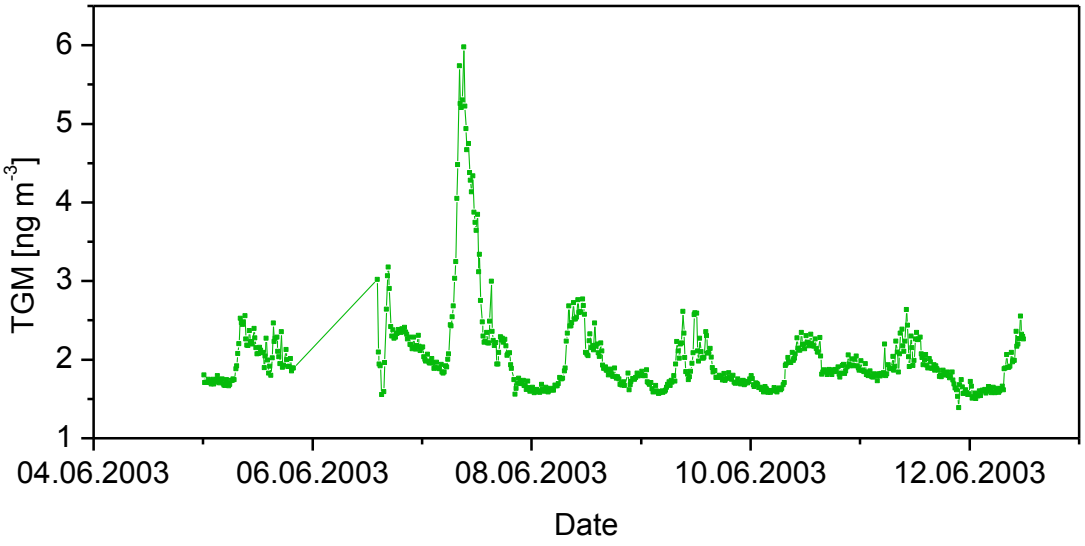

Fig. 4-27 Diurnal variation of TGM at Lake Gossenkölle, Kühtai, Austria in June, 2003.

4.3.8 Contribution of RGM to the Total Gaseous Mercury

The RGM concentrations show a much higher standard deviation than TGM, indicating faster reactivity and lower residence time of these mercury species compared to TGM (Junge, 1972).

Under the assumption of a mean TGM concentration of approximately 1.02 ng m^{-3}, 1.16 ng m^{-3}, and 1.29 ng m^{-3} for the locations GC, Sky, PBr, respectively, the percentage of RGM relative to TGM (Tab. 4-12) is somewhat high compared to the general statement that RGM does not exceed 5 % of TGM.

Tab. 4-12 Statistical summary of percentaged RGM (relative to TGM) in 2002 and 2003.

$RGM_{relative}$	GC	Sky	PBr
Minimum [%]	2.5	2.4	2.3
Maximum [%]	9.4	10.5	8.6
Mean [%]	7.2	6.9	6.5
Median [%]	7.7	7.3	6.9
SD	1.97	2.99	1.9
Number of Samples	21	23	20

These quite high relative RGM concentrations are a result of the oceanic influence with high Hg emission rates from the Sea and active photochemical processes in the Marine Boundary Layer (MBL). High Hg(II) concentrations have been observed in the MBL by various groups (Hedgecock et al., 2003; Laurier et al., 2003; Slemr et al., 2003; Temme et al., 2003b; Soerensen et al., 2010; Sprovieri, 2010c). In addition, the oxidation processes due to the halogen-containing sea salt aerosols play an important role. It is generally known, that the oxidation is promoted by halogen chemistry both above and below the water/air interface (Sheu and Mason, 2004; Lalonde et al., 2001).

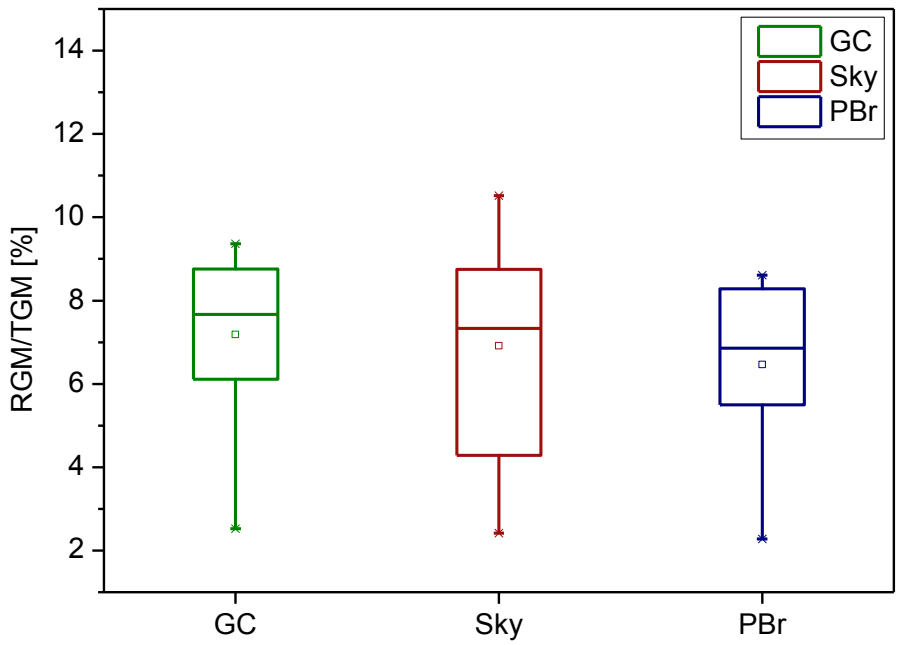

Fig. 4-28 Box Plots of the contribution of RGM to TGM at the three locations GC, Sky, and PBr in 2002 and 2003.

Literature data suggests that the variation of relative RGM concentrations is generally very high. Several studies of atmospheric mercury in the Southern Hemisphere show similar or even higher relative RGM concentrations than in Patagonia. Taking the data shown in Tab. 2-14 the following relative RGM concentrations can be calculated: Terra Nova Bay (Sprovieri and Pirrone, 2000; Sprovieri et al., 2002) 14.32 %, McMurdo (Brooks et al., 2008b) 9.67 %, and South Pole (Brooks et al., 2008a) 63.7 %. In the Northern Hemisphere much lower relative RGM concentrations are found: in Southern Québec, Canada: 0.2 % (Poissant et al., 2005), in Halifax, Canada: 0.26 % (Ebinghaus et al., 2009), in Cheeka Peak, Washington: up to 2 % (Weiss-Penzias et al., 2003), in ambient air of Tennessee and Indiana, USA: 3 % (Lindberg and Stratton, 1998).

4.3.9 Spatial variation of atmospheric mercury in Patagonia

In general, an increasing trend in TGM can be observed from West to East; with 1.06 ng m^{-3} (GC), 1.26 ng m^{-3} (Sky), and 1.36 ng m^{-3} (PBr) in 2002 and 1.02 ng m^{-3} (GC), 0.87 ng m^{-3} (Sky), and 1.29 ng m^{-3} (PBr) in 2003. Only in 2003, the mean TGM concentrations of Sky don't fit into the trend. However, the TGM concentrations were exceptionally low at the beginning of the measurement series (Fig. 4-10). During the first three days the daily average TGM concentration raised steadily before it got stable at the fourth day. If the mean TGM concentration is only determined for the stable time period, a value of 1.16 ng m^{-3} is calculated, which is in good

agreement to the general trend observed. As mentioned in chapter 4.3.4, the TGM concentrations are mainly a direct result of re-emission from soil. Therefore, the sources for the differences in the diurnal variations of TGM (chapter 4.3.4) contribute just as well to the increasing TGM concentrations from West to East. Namely, the differences in soil conditions and in meteorological parameters as already described in chapter 4.3.4.

Comparing the RGM concentrations of the different sites, it can be seen that the mean concentrations are very similar with 73 pg m^{-3}, 80 pg m^{-3}, and 83 pg m^{-3} at GC, Sky, and PBr, respectively. However, an inspection of the interquartile range (IQR) reveals that this is quite higher for Sky than for the other two locations. This shows that at this location there is a faster transformation of the different mercury species. This is probably a result from the variable meteorological conditions mentioned in 4.3.4

TPM concentrations in 2002 were in a similar range at GC and PBr with values of around 63 pg m^{-3} and 97 pg m^{-3}, respectively. The TPM concentrations at Sky were much higher with values around 357 pg m^{-3}. A similar trend could be seen for 2003 where the concentrations at Sky were again the highest ones with values around 283 pg m^{-3}. However, at this campaign the concentrations at Sky were lower than 2002, whereas the concentrations at GC and PBr were higher than in 2002, resulting in a difference in 2003 which was not as big as in 2002.
One reason for the higher TPM concentrations is that at Sky generally more particulate matter was present. This was due to the fact that first the aerosols were not washed out by the rain and second that the active husbandry at the Estancia Skyring yielded a significant amount of particulate matter.

4.4 Conclusion

In this study, different mercury species were investigated in order to obtain a better understanding of the global mercury cycle. At three different sampling areas, namely Patagonia, Chile, Galicia, Spain and Kühtai, Austria the mercury species TGM, RGM, TPM and Mercury in Precipitation were analyzed during several field campaigns. Of these locations, one (Patagonia) was a remote area in the Southern Hemisphere, whereas the other two (Galicia and Kühtai) were remote areas in the Northern Hemisphere.

Concerning the TGM concentrations, the values were in a similar range for Patagonia and Galicia, which is not in agreement with the generally stated significant difference between the Southern and Northern Hemisphere. Based on the existing data within the mercury community, there is a scientific consensus about the current global background concentration of airborne Hg which is considered to be in the range of 1.5 to 1.7 ng m^{-3} in the Northern Hemisphere and between 1.1 and 1.3 ng m^{-3} in the Southern Hemisphere (Lindberg et al., 2007). However, the reason for these low TGM concentrations in Galicia might be the precipitation rate in this region, which is with 1400 to 1800 mm (Martínez-Cortizas et al., 2002) relatively high and leads to a Hg washout from the atmosphere. A second reason is probably a low reemission from the surface, due to the surface (bog) having a high water content (compare to 4.3.4). Nevertheless TGM concentrations in Galicia showed a pronounced diurnal variation, similar to the TGM trend in Austria. This was not observed for Patagonia. The reasons for this difference are on the one hand different underlying soils with water saturated bogs in Patagonia, slightly dryer bogs in Galicia and grassland and bedrock in Austria. On the other hand reasons are the meteorological parameters, first and foremost temperature and UV radiation, with much higher variations for Austria and Galicia than for Patagonia. Comparing the diurnal variations of TGM in Galicia and Kühtai, as most significant should be mentioned the different daytimes in which the TGM concentration peaks occurred. In Galicia highest concentrations were observed in the early afternoon for both campaigns in February and July. In Kühtai, in April TGM concentrations maximized near midday with a short interval of maximum concentrations. In June, TGM concentrations rose already in the morning hours and the concentrations peak was generally much broader than in April.

Tab. 4-13 Comparison of the Mercury Species TGM, RGM, TPM, and Hg in Precipitation between the different locations. For Patagonia, concentrations of all three sampling sites (GC, Sky, and PBr) were averaged. TGM_{AvD} − TGM_{AvN}: Difference between averaged daytime peaks and averaged nighttime concentrations.

Location	TGM [ng m^{-3}]	TGM_{AvD}− TGM_{AvN}	RGM [pg m^{-3}]	$RGM_{rel.}$ [%]	TPM [pg m^{-3}]	$Hg_{Prec.}$ [ng L^{-1}]
Patagonia, Chile	1.09	0	79	7.24	180	0.64
Galicia, Spain	1.03	1.22	43	4.17	59	1.56
Kühtai, Austria	1.93	1.20	25	1.30	37	4.52

Concerning RGM and TPM concentrations, the values were with 79 pg m^{-3} and 180 pg m^{-3} highest for Patagonia, with 43 pg m^{-3} and 59 pg m^{-3} intermediate for Galicia and with 25 pg m^{-3} and 37 pg m^{-3} lowest for Austria. This is a result of the mutual interference between reduction and oxidation processes. In Patagonia higher emission rates from the Sea and more active photochemical processes in the Marine Boundary Layer (MBL) result in a generally more rapid Hg cycling. High Hg(II) concentrations have been observed in the MBL by various groups (Hedgecock et al., 2003; Laurier et al., 2003; Slemr et al., 2003; Temme et al., 2003b; Soerensen et al., 2010; Sprovieri2010c) Additionally, the oxidation processes are the dominant ones, probably mainly due to the halogen-containing sea salt aerosols. It is generally known, that the oxidation is promoted by halogen chemistry both above and below the water/air interface (Sheu and Mason, 2004; Lalonde et al., 2001). In Galicia the halogen promoted oxidation probably also plays an important role. However, due to the higher solar radiation, the photo-reduction of Hg(II) counteracts, resulting in intermediate RGM and TPM concentrations. In Kühtai no enhanced oxidation processes like the ones with sea salt aerosols exist, resulting in lower RGM and TPM values.

Mercury concentrations in precipitation were generally quite low. However, a significant difference could be seen between the three sites. The lowest concentrations were found in Patagonia, with an average of 0.54 ng L^{-1}. In Galicia the average concentrations (1.56 ng L^{-1}) were higher by a factor of 2.5 and in Austria the concentrations (4.52 ng L^{-1}) were higher compared to Patagonia by a factor of 7. The low concentrations in Patagonia are a result of the combination of generally low atmospheric mercury concentrations and the extremely high precipitation depths.

5 DO HG ACCUMULATION RATES IN ARCHIVES REFLECT ATMOSPHERIC DEPOSITION RATES?

Mercury is removed from the atmosphere through both wet and dry processes acting on Hg^0, Hg(II) and Hg(p) species (Schroeder and Munthe, 1998). However, a quantification of these processes to get a precise Hg deposition rate is very challenging. Additionally, only recent deposition rates can be calculated or modeled by knowing the processes and the atmospheric Hg chemistry. However, in order to estimate human impacts on the biogeochemical cycling of mercury, it is necessary to compare recent deposition rates with preindustrial deposition rates. For this, historical records of mercury accumulation in lake sediments (e.g. Aston et al., 1973; Swain et al., 1992; Gobeil et al., 1999; Bindler et al., 2001; Kamman and Engstrom, 2002) and peat bogs (e.g. Pheiffer-Madsen, 1981; Martínez-Cortizas et al., 1999; Biester et al., 2002; Bindler, 2003; Shotyk et al., 2003; Roos-Barraclough and Shotyk, 2003; Givelet et al., 2004) have often been used.

However, many processes controlling time-resolved mercury accumulation in peat and sediments are still poorly understood. Hence, it still has to be specified under which postulates the accumulation rates in the archives are reliable for calculating the atmospheric deposition rates (Franzen and Biester, 2003; Biester et al., 2007).
In this chapter the atmospheric mercury data obtained in this study and mercury accumulation rates in peat bogs and lacustrine sediments obtained in previous studies are collated.

5.1 Sampling Sites of Mercury Records in Peat Bogs and Lake Sediments

In previous studies the mercury accumulation rate in three peat cores (GC1, Sky1, PBr2) and one lacustrine sediment core (LMP1) were investigated (Biester et al., 2002; Biester et al., 2003; Franzen and Biester, 2003). All three bogs were raised bogs situated at the same sites, where the atmospheric mercury measurements presented in Chapter 4 were conducted (Fig. 5-1). The lacustrine sediment core LMP1 was taken from a tarn (Lago Muy Profundo, informal name), which has developed in a cirque excavated by a glacier. The surface area of the lake is approximately 0.5 km^2 and the catchment-to-lake-ratio is approx. 10. It is situated 3 km west of Gran Campo Nevado ice field and hence in the same region as GC1. Therefore, recent atmospheric Hg deposition rates should be similar for GC1 and LMP1. More information on the sampling site and the lacustrine

sediment cores can be found in Baeza Urrea, 2005. More information on the peat bogs can be found in Biester et al., 2002 and Biester et al., 2003.

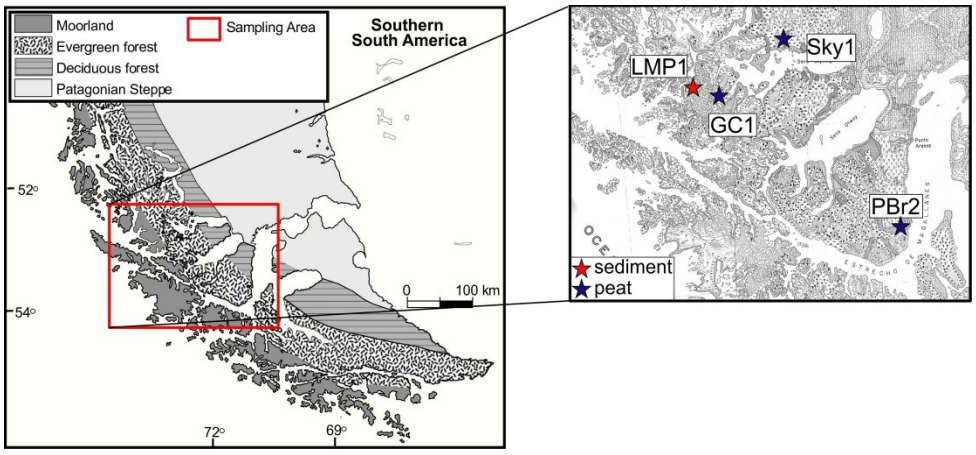

Fig. 5-1 **Map of the study area and locations of sampling sites of three peat cores PBr2, Sky1, and GC1 and of one lacustrine sediment core LMP1.**

5.2 Mercury Accumulation in the Raised Bog GC1 and the Sediment LMP1

Using the generally accepted equation for mercury accumulation in peat (Eq. 5−1) pre-industrial mercury accumulation rates in the bog GC1 ranged between 2.5 and 3.9 µg m^{-2} a^{-1} (Biester et al., 2002).

$$AR_{Hg} = C_{Hg} \cdot \rho_P \cdot AR_P \cdot 10 \qquad \text{(Eq. 5−1)}$$

AR_{Hg} = Accumulation Rate of Mercury [µg m^{-2} a^{-1}]
C_{Hg} = Concentration of Mercury in Peat [µg kg^{-1}]
ρ_P = Density of the Peat [g cm^{-3}]
AR_P = Accumulation Rate of Peat [cm a^{-1}]

In the past 100 years, mercury accumulation rates increased 18−fold from about 3 µg m^{-2} a^{-1} to a maximum of 62.5 µg m^{-2} a^{-1}. In the uppermost section of the bog, the accumulation rates were still around 20 µg m^{-2} a^{-1} (Fig. 5-2).

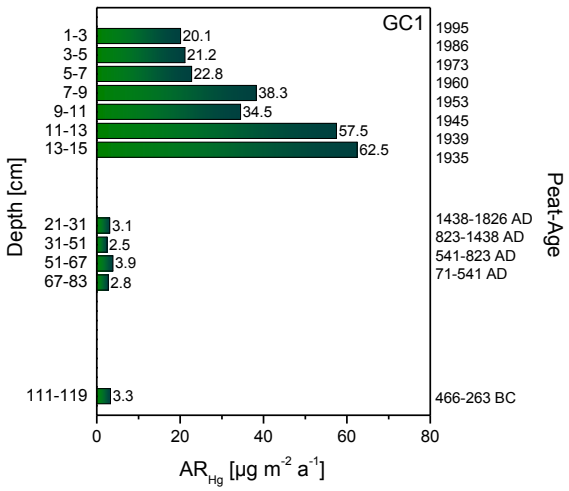

Fig. 5-2 **Uncorrected net accumulation rates of Hg in selected sections of core GC1. Ages of the uppermost 20 cm were calculated based on ^{210}Pb activity (CRS model); other ages were obtained by means of ^{14}C AMS dating (Biester et al., 2002).**

However, since this area not being influenced by any recent local point source of mercury emission, this 18−fold increase is not consistent with the three-fold net increase in globally dispersed atmospheric Hg estimated for the same period (Mason et al., 1994). Also Selin et al. (2008) suggested an average increase in Hg deposition by a factor of 2 to 3 for southernmost South America.

This raises questions about the reliability of peat bogs to reflect true atmospheric mercury fluxes and the magnitude by which the fluxes have changed.

In Biester et al. (2002; 2003) is shown already, that comparability of Hg accumulation rates form different peat sections within one core is not given, when calculated from density, peat accumulation rates, and Hg concentration (Eq. 5−1). Peat formation is a dynamic process accompanied by intense mass loss and alteration of the organic material. During this peat evolution differences in net mass accumulation rates are not compensated by linear changes in density, peat accumulation, or Hg concentrations. Therefore, in order to achieve comparability of Hg accumulation rates derived from differently altered peat sections, Hg accumulation rates have to be normalized to peat humification and subsequent mass loss. By this method, explained in Biester et al. (2002; 2003) maximum Hg accumulation rates in the upper part of the GC1 core, representing industrial ages were downscaled from 60 µg m^{-2} a^{-1} to 7.9 µg m^{-2} a^{-1} which revealed only a 2.5−fold increase compared to the lower part of the core, representing preindustrial ages (Fig. 5-3). These corrected accumulation rates and the resulting enrichment factors are much more consistent with the net increase in globally dispersed atmospheric Hg.

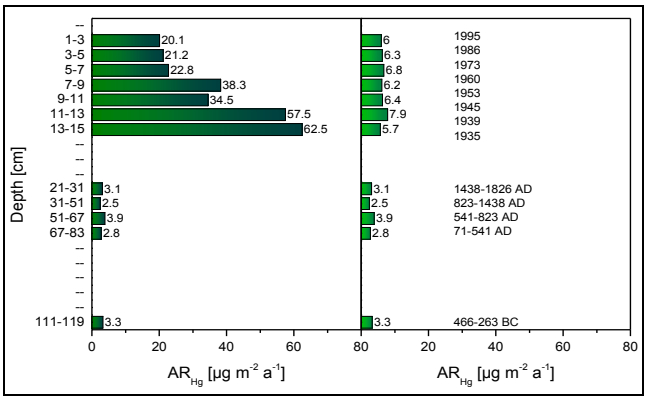

Fig. 5-3 **Uncorrected (left) and corrected (right) net accumulation rates of Hg in selected sections of core GC1. Ages of the uppermost 20 cm were calculated based on ^{210}Pb (CRS model); other ages were obtained by means of ^{14}C AMS dating. The correction is done for differences in peat accumulation rates in high and low decomposed peat sections. (Biester et al., 2002)**

One other evidence that recent Hg depositions determined with help of Hg accumulation rates in bogs probably are overestimated is the comparison with Hg accumulation rates in the lacustrine sediment LMP1. For the lake sediment LMP1, only the upper part of the sediment core was analyzed for mercury. Here, modern accumulation rates of Hg were found to be approximately 5 µg m^{-2} a^{-1} (Franzen and Biester, 2003). Even though there is no Hg enrichment factor compared to preindustrial times available, the very low modern Hg accumulation rate shows that there is no recent mercury source, which could explain the enormous enrichment factor calculated from the uncorrected Hg accumulation rates

5.3 Mercury Accumulation Rates in the Raised Bogs GC1, Sky1, and PBr2

The raised bogs Sky1 and PBr2 show more moderate industrial Hg enrichment factors. However, also for these bogs Hg accumulation rates were corrected in the same manner as for GC1 (Biester et al., 2003). After correction, the industrial Hg enrichment factors were 1.5 for both bogs.

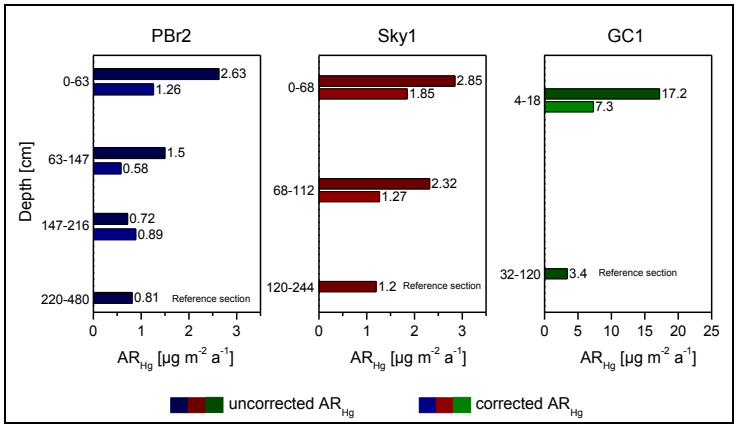

Fig. 5-4 **Mercury accumulation rates in three ombrotrophic peat cores before and after correction for mass losses occurring during peat decomposition (Biester et al., 2003).**

5.4 Atmospheric Mercury Deposition

Mercury is removed from the atmosphere through both wet and dry processes acting on Hg^0, Hg(II) and $Hg_{(p)}$ species (Schroeder and Munthe, 1998). Which one of these two processes is the most important one is site specific since the actual deposition flux depends on the individual concentrations of the different mercury species, the presence of other atmospheric constituents, the type of surface, and meteorological parameters (Schroeder and Munthe, 1998). Wet Deposition requires precipitation. The rate of dry deposition varies with mercuric species, boundary layer stability and land surface cover (Lin et al., 2006). RGM and $Hg_{(p)}$ are generally considered to be uni-directional processes, whereas air-surface exchange of Hg^0 can occur bi-directionally, with daytime emission and nighttime deposition (Schroeder and Munthe, 1998; Zhang et al., 2009)

The measurement of Hg wet deposition is an accepted standardized method, which is used by national and regional networks (e.g. NADP-MDN) and merely needs the accurate measurement of mercury concentration in precipitation and the precipitation depths. In contrast, the accurate measurement and modeling of Hg dry deposition is difficult and remains the most challenging gap in the understanding of mercury fluxes. Dry deposition occurs via two processes. One is the direct deposition of the gas-phase compounds Hg^0 and RGM and, to a lesser extent, deposition of atmospheric particles containing Hg (Hg_P) (Lindberg et al., 2007). There are three general methodologies for the estimation of Hg dry deposition rates. The “direct” methodology that includes surrogate surfaces, dew fall, litterfall, and throughfall; the “inferential” methodology that uses Hg species air concentrations and meteorological measurements to model deposition rates and the “micrometeorological” approach that includes gradient, modified Bowen ratio and relaxed eddy accumulation methods (Lindberg et al., 2007).

5.4.1 Mercury Wet Deposition at GC

Due to the extremely high precipitation rates at Gran Campo Nevado, Patagonia, it can be expected that for this region the wet deposition is the predominant one and for most of the times, dry deposition can be neglected.

Taking the VWM (volume-weighted mean) concentrations in precipitation (Tab. 4-5) for GC and the precipitation depth of the sampling period September to October (Fig. 4-3) the following wet deposition rates can be calculated for these periods in 2002 and 2003. In the two months-period September to October 2002 0.227 µg m^{-2} were deposited; in the two months-period September to October 2003 0.441 µg m^{-2}. From this relatively

short period, the projection on the annual deposition rate can only be roughly estimated. This is done in two ways. First, the two months deposition was extrapolated to twelve months by just multiplying by 6. Second, the VWM mercury concentration in precipitation measured during the study period was multiplied by the annual precipitation depths (APD), measured for 2002 and 2003. In these ways, different annual Hg wet deposition rates were obtained. For 2002 the estimations were 1.36 µg m^{-2} a^{-1} and 1.26 µg m^{-2} a^{-1}, respectively, for 2003 they were 2.65 µg m^{-2} a^{-1} and 3.52 µg m^{-2} a^{-1}, respectively.

Tab. 5-1 Mercury wet deposition rates calculated for the two months-sampling period[a)] and the projection on the annual Hg wet deposition for 2002 and 2003; calculated with the two months precipitation depth and subsequent extrapolation on 12 months[b)] and calculated with the annual precipitation depths[c)], with APD 2002: 2633 mm and APD 2003: 4513 mm.

Period	Precipitation Depth [mm]	VWM concentration [ng L^{-1}]	Hg Wet Deposition in two months[a)] [µg m^{-2}]	Annual Hg Wet Deposition[b)] [µg m^{-2} a^{-1}]	Annual Hg Wet Deposition[c)] [µg m^{-2} a^{-1}]
09/10 2002	472	0.48	0.227	1.36	1.26
09/10 2003	566	0.78	0.441	2.65	3.52

In order to ascertain whether it is possible to project the annual Hg wet deposition from the short-term measurements it is necessary to clarify the following questions. To what extent do the Hg concentrations in precipitation diversify over the year due to variation in meteorology? Do higher precipitation depths result in higher Hg wet deposition or do they result in a diluting effect concerning the Hg concentrations.

Even though several authors have shown that there is seasonality in Hg concentrations in precipitation (e.g. Guentzel et al., 1995; Hoyer et al., 1995; Burke et al., 1995; Landis et al., 2002b; Dvonch et al., 2005; Keeler et al., 2005), in all studies the higher Hg deposition rates, typically observed during the warmer months, was likely the result of a mix of meteorological, source emission, and atmospheric chemistry influences. However, for the study area Gran Camp Nevado, the variation in mean temperatures over the year (Fig. 4-2) is not as large as in other studies. Thus, these differences in temperature will probably lead only to a moderate change in Hg concentrations in precipitation over the year. Also, wind direction and wind speed do not change significantly over the year resulting in a consistent atmospheric catchment.

Dvonch et al. (2005) showed that higher precipitation depths do not necessarily lead to lower VWM Hg concentrations in precipitation and that the concentrations are independent from precipitation depths. Similar results can be found in Gratz et al. (2009). Hence, for this study it can be assumed that differences in precipitation rates do not lead to different VWM Hg concentrations but to different deposition rates. Therefore, it is most

reasonable to calculate the annual Hg wet deposition with the annual precipitation depth (Tab. 5-1, [c)]).

5.4.2 Mercury Wet Deposition at GC, Sky, and PBr

The mercury wet deposition rates are much higher at the sampling area GC (1.26 µg m^{-2} a^{-1} for 2002 and 3.52 µg m^{-2} a^{-1} for 2003) compared to the sampling areas Sky (0.24 µg m^{-2} a^{-1} and 0.56 µg m^{-2} a^{-1}) and PBr (0.39 µg m^{-2} a^{-1} for 2003) (Tab. 5-2).

Tab. 5-2 Mercury wet deposition rates calculated for the two months-sampling period and the projection on the annual Hg wet deposition for 2002 and 2003; calculated with the two months precipitation depth and subsequent extrapolation on 12 months.

	Annual Precipitation Depth [mm]	VWM Hg concentration [ng L^{-1}]	Annual Hg Wet Deposition [µg m^{-2} a^{-1}]
GC 2002	2633	0.48	1.26
GC 2003	4513	0.78	3.52
Sky 2002	608.2	0.39	0.24
Sky 2003	937.2	0.60	0.56
PBr 2002	361.4	ND	ND
PBr 2003	467.4	0.83	0.39

Since the VWM Hg concentrations in precipitation being in the same range at the three sites the differences are predominantly a result of different precipitation depths.

5.5 Conclusion

The differences in Hg wet deposition rates with highest rates at GC intermediate rates at Sky and lowest rates PBr are consistent with the west to east trend in Hg accumulation rates calculated by Biester et al. (2003) for the three raised bogs GC1, Sky1, and PBr2 (Fig. 5-4).

The calculated mercury wet deposition rates of 1.3 – 3.5 µg m^{-2} a^{-1} found for the different sampling sites in Patagonia show a much better correlation to the estimates of deposition determined from the lake sediment LMP1 and from the mass-loss-corrected peat bogs and evidence that the uncorrected accumulation rates in the upper part of peat bogs and thus the assumed contemporary atmospheric flux might be overestimated. This is evident for the mass-loss-correction method of Biester et al. (2002, 2003, 2007) being reliable.

6 MERCURY TRANSFER FROM SNOW TO ATMOSPHERE

6.1 Sampling Sites

Snow samples were taken at three different altitudes above sea level within the area of Kühtai. The lowest samples (AP1) were taken at an altitude of 2070 m a.s.l. in the vicinity of the valley station of the ski lift “Hochalterbahn”. The intermediate samples (AP2) were taken at an altitude of 2280 m a.s.l. in the vicinity of the ski hut “Zum Kaiser Maximilian”. The uppermost samples (AP3) were taken directly above Lake Gossenkölle at an altitude of 2468 m a.s.l. At all sites, samples from different depths were taken. The first sample was directly taken from the surface. One other sample was taken from a lower part of the surface stratum which was buried directly due to prolonged snowfall. A third sample was taken from an older stratum. Each sample was taken in triplicates.

Additionally, two depth profiles were taken directly at Lake Gossenkölle. One profile (DP1) was taken on the surface of the lake, in a snow pit, which was excavated a couple of days ago by a research team of the University of Innsbruck. One other profile (DP2) was taken from a freshly excavated snow pit.

The snow strata were identified by characterizing snow cover profiles based on the “International Classification for Seasonal Snow on the Ground” (Colbeck et al., 1985).

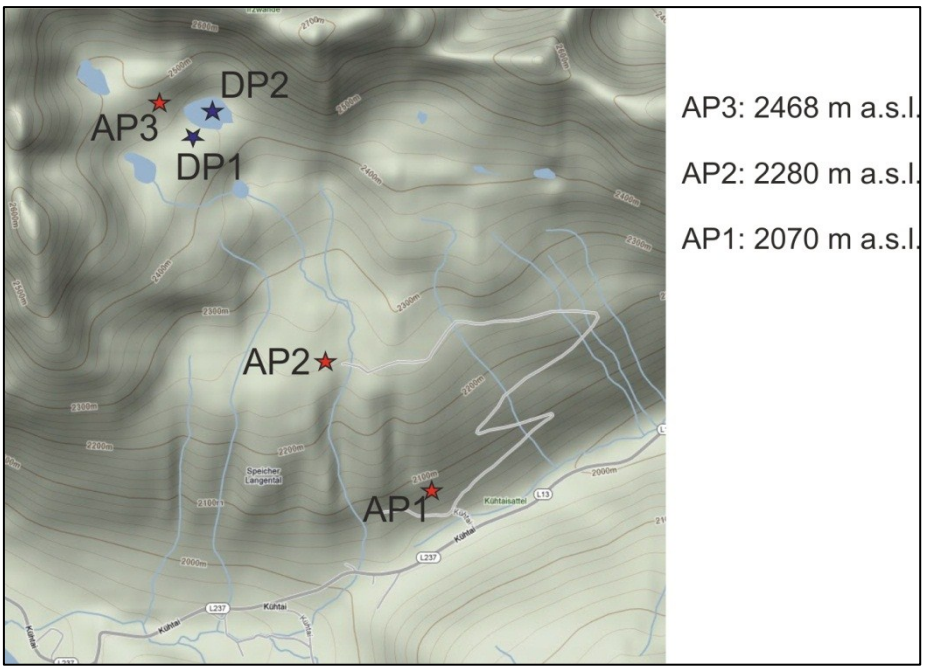

Fig. 6-1 **Sampling Sites of mercury in snow packs at, Kühtai, Austria. Elevation map taken from Google Maps.**

6.2 Results

6.2.1 Mercury in Surface Snow

The surface snow showed similar mercury concentrations at the different altitudes within the area of Kühtai with mean concentrations of the topmost samples of 0.780 ng L^{-1} for AP1, 0.771 ng L^{-1} for AP2, and 0.786 ng L^{-1} for AP3. The differences between the mercury concentrations at the lower part of the surface stratum (1.912 ng L^{-1} for AP1, 2.006 ng L^{-1} for AP2, and 1.732 ng L^{-1} for AP3) and for the 2nd stratum (1.505 ng L^{-1} for AP1, 1.339 ng L^{-1} for AP2, and 1.213 ng L^{-1} for AP3) are slightly bigger.

Within each profile, lowest mercury concentrations were found in the uppermost part with a concentration of 0.81 ng L^{-1}, averaged over all three profiles. Highest concentrations were found at the lower part of the surface stratum with 1.88 ng L^{-1}, averaged over all three profiles. In the second stratum intermediate concentrations were found with 1.35 ng L^{-1}, averaged over all three profiles. A summary of the concentrations is shown in Tab. 6-1.

Tab. 6-1 Mercury concentration in seasonal snow samples. Given are mean values of three samples for each sampling point. Concentrations are given in ng L^{-1} and in pM.

	AP1 2070 m a.s.l.		AP2 2280 m a.s.l.		AP3 2468 m a.s.l.	
	[ng L^{-1}]	[pM]	[ng L^{-1}]	[pM]	[ng L^{-1}]	[pM]
Surface Strat./ uppermost cm	0.780	3.890	0.771	3.842	0.886	4.417
Surface Strat./ lower part	1.912	9.534	2.006	10.003	1.732	8.636
2nd Stratum	1.505	7.505	1.339	6.676	1.213	6.049

6.2.2 Depth Profiles of Mercury in Seasonal Snow Pits

Mercury concentrations in the depth profiles showed different values with higher values for the freshly excavated pit DP1 (Fig. 6-2, a) with mean concentration of 1.38 ng L^{-1} and lower values for the pit DP2, which had been excavated a couple of days before (Fig. 6-2, b) with mean concentrations of 0.59 ng L^{-1}. Within each profile, the concentrations were relatively uniform with a range from 1.22 ng L^{-1} to 1.58 ng L^{-1} for DP1 and with a range from 0.45 ng L^{-1} to 0.68 ng L^{-1} for DP2. A summary of the concentrations is shown in Tab. 6-2.

Tab. 6-2 **Mercury concentration in the snow pits DP1 and DP2. Given are mean values of two samples for each depth of DP1 and of three samples for each depth of DP2. Concentrations are given in ng L−1 and in pM.**

	DP1			DP2	
cm above ground	**[ng L^{-1}]**	**[pM]**	**cm above ground**	**[ng L^{-1}]**	**[pM]**
210	1.46	7.26	**65**	0.52	2.61
160	1.40	6.98	**35**	0.58	2.87
110	1.39	6.90	**10**	0.63	3.16
60	1.36	6.76	**3**	0.65	3.22
10	1.33	6.61			

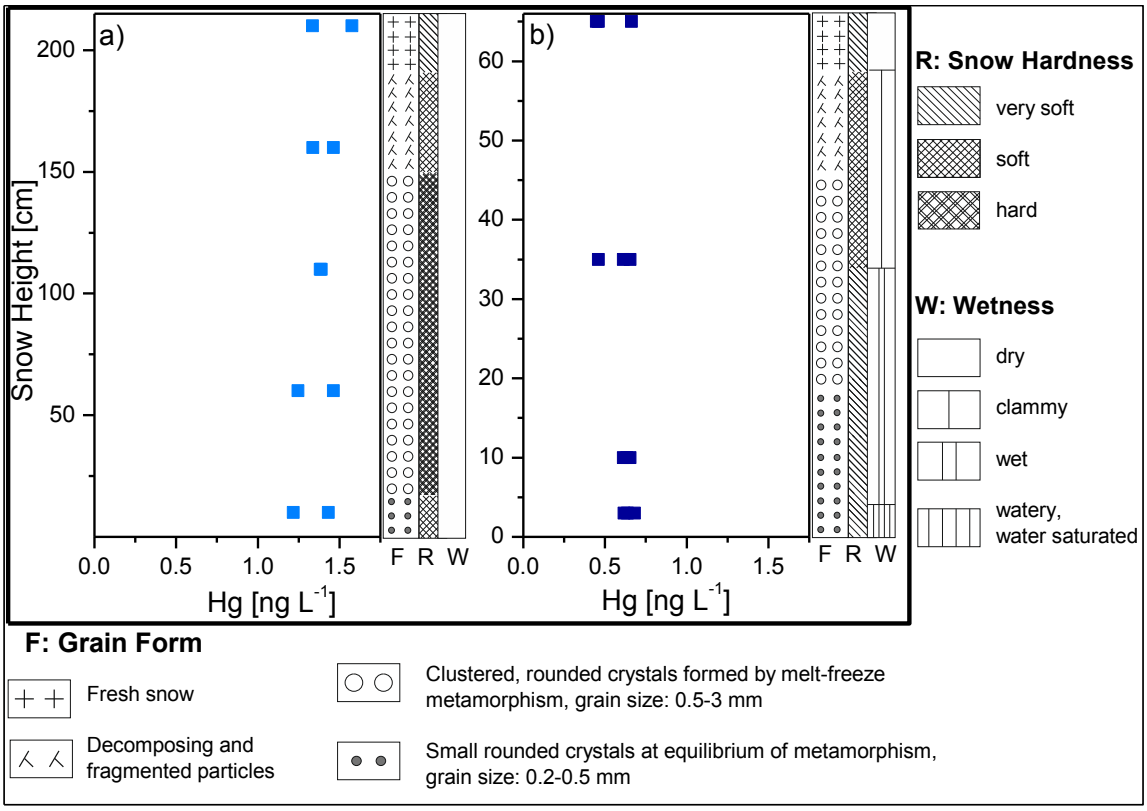

Fig. 6-2 **Mercury in snow pits DP1 (a) and DP2 (b) at Lake Gossenkölle, Kühtai, Austria. Additionally, the characterization of each snow pit is shown on the right side of each profile.**

6.3 Discussion

6.3.1 Mercury Loss from Surface Snow

An examination of the surface snow samples AP1, AP2, and AP3 yields a big distinction in Hg_T concentrations between different sections within the surface stratum. The snow of the lower part which was directly buried due to continuing snow fall contains much higher Hg_T (1.88 ng L^{-1}) than the uppermost cm which were exposed to sunlight (0.81 ng L^{-1}).
These differences are a strong evidence for photo-induced Hg(II) reduction in snow and subsequent gas transfer of Hg^0 to the atmosphere. The same inference can be drawn when the two different depth profiles are compared. The freshly excavated snow pit shows generally higher mercury concentrations (1.38 ng L^{-1}) than the snow pit, where the intire strata have been exposed to sunlight for a couple of days (0.59 ng L^{-1}).

It is known that some of the mercury deposited onto the cryosphere is rapidly emitted back to the atmosphere (Lalonde et al., 2002). It seems likely that outside of melting periods, loss of mercury from snow is due primarily to the emission of GEM back to the atmosphere (Lalonde et al., 2002, 2003). Lalonde et al. (2003) showed a decrease of Hg_T in snow within 24 hours from 7.08 pM to 4.23 pM (averaged over all snow periods) which results in a loss of Hg_T of more than 40 %. Also literature data aggregated in Durnford et al. (2012) shows 24-h-losses between 30 and 51 %.
These results are highly consistent with the mercury concentrations in the surface strata of the snow from Kühtai (Tab. 6-1). The higher concentrations in Hg_T in the lower part of the surface stratum and also in the second stratum are a result of limited sunlight penetration at depth.

Although photoreduction of Hg(II) has been reported to be forced by both visible (Poulain et al., 2004; Johnson, 2008) and UV-A radiation (Poulain et al, 2004; Faïn et al., 2008), it is primarily forced by UV-B radiation (Lalonde et al., 2003; Poulain et al, 2004; Dommergue et al., 2007; Faïn et al, 2007).
The Hg_T profiles within the surface snow of this study are a further evidence for the Hg(II) reduction mostly being mediated by UV-B-irradiation. A Hg(II) reduction induced by visible light would occur down to deeper depths than a UV mediated reduction of Hg(II) (King and Simpson, 2001). The authors reported an e-folding depth (the depth of snow that attenuates diffuse radiation to 1/e or ~37%) of ~5 cm for UV-B in a uniform Arctic snowpack. Also Durnford and Dastoor (2011) conclude that insufficient UV-B radiation is almost certainly the most important factor in limiting the reduction of mercury within snow packs. Field and laboratory studies suggest that Hg^0 is revolatilized from the top ~2 cm of

snow packs (Dommergue et al., 2007; Faïn et al., 2007; Brooks et al., 2008a; Johnson et al., 2008).

Regarding the snow pit (DP2), which was exposed to radiation for a couple of days, it becomes obvious that even in the presence of sufficient insolation not all mercury is reduced and emitted. This underlines the results of Dommergue et al. (2007) who state that not all forms of oxidized mercury are reducible by photodissociation or photoreduction (Dommergue et al., 2007, 2010). Lindqvist and Rodhe (1985) reported that some fraction of both RGM and PHg is not easily reducible. If PHg is far less reducible than RGM, as is likely (Durnford and Dastoor, 2011), the presence of PHg will affect the photo-reactivity of the snow pack's mercury content (Larose et al., 2010). Durnford and Dastoor (2011) consolidate various literature data to conclude that there is evidence that PHg in the snow pack is at most minimally reduced and emitted. If this conjecture is accurate, the wide range of mercury concentrations observed in surface snow and seasonal snow packs of different studies, aggregated in Durnford and Dastoor 2011 and Durnford et al., 2012 may reflect the fact that PHg exhibits significant spatial variability.

6.4 Conclusion

In this study, more than the half of the mercury deposited via snow is rapidly reemitted to the atmosphere. It could be shown that this reemission is mediated by insolation which only penetrates the top few centimeters of the snow. A fraction that constitutes ~43°% of mercury is not reduced and revolatilized. This fraction probably represents PHg.
The fast reemission of some of the Hg is an evident reason for the definite diurnal variation in TGM measured above snow, shown in Chapter 4.3.7.

7 SUMMARIZING CONCLUSIONS

In this study, the atmospheric mercury compounds TGM, RGM, TPM and mercury in precipitation have been measured during several campaigns at remote terrestrial sites both, in the Southern- (three sites in Patagonia, Chile) and the Northern Hemisphere (one site in Galicia, Spain and one site in Kühtai, Austria). These short-term measurements are a complementary approach to the few stationary sites established for long term observations; especially for remote southernmost South America, where no baseline measurements have been performed before. The combination of this study and long-term measurements provides basic and important information about the worldwide distribution and trend of atmospheric mercury fluxes.

In general, the atmospheric data show that there is a significant diurnal and spatial variability of the different Hg species, mainly controlled by meteorological conditions and the soil processes.
It could be shown, that TGM values were significantly lower at the sampling sites in the Southern Hemisphere than those at sampling sites in the Northern Hemisphere, reflecting the general inter-hemispherical gradient.
However, the divalent mercury species RGM and TPM were higher in Patagonia. The most probable interpretation is that higher emission rates from the Sea and more active photochemical and halogen promoted processes in the MBL result in a more rapid Hg cycling. One other evidence for MBL provoking higher RGM values is the comparison between RGM values from the coastal sampling site in Galicia, Spain and values from the inland sampling site Kühtai, Austria, with higher RGM and TPM values for the coastal site.Comparing the calculated mercury wet deposition rates of 1.3 – 3.5 $\mu g\ m^{-2}\ a^{-1}$ in Patagonia with mercury accumulation rates in peat bogs and lacustrine sediments from previous studies show much better correlation to the estimates of catchment corrected Hg accumulation rates determined from the lake sediment LMP1 and from mass-loss-corrected peat records. This evidences that the uncorrected accumulation rates in the upper part of peat bogs and thus the assumed contemporary atmospheric flux might be overestimated.

8 LITERATURE

ÅBERG B., EKMAN L., FALK R., GREITZ U., PERSSON G., SNIHS J.O. (**1969**): Metabolism of methyl mercury (203Hg) compounds in man. *Arch. Environ. Health* 19(4): 478-484.

AMAP (**1998**): Arctic Pollution Issues: A State of the Arctic Environment Report.

AMAP/UNEP (**2008**): Technical Background Report to the Global Atmospheric Mercury Assessment. Arctic Monitoring and Assessment Programme/UNEP Chemical Branch. 159 pp.

AMOUROUX, D., WASSERMAN, J.C., TESSIER, E., DONARD, O.F.X. (**1999**): Elemental mercury in the atmosphere of a tropical Amazonian forest (French Guiana): *Environ. Sci. Technol.* 33: 3044-3048.

ANDERSSON, A. (**1979**): Mercury in Soils -. In: The Biogeochemistry of Mercury in the Environment. Nriagu, J. O. (Ed.). Elsevier/North Holland Biomedical Press: Elsevier: 79-112.

ARIMOTO, R., SCHLOESSLIN, C., DAVIS, D., HOGAN, A., GRUBE, P., FITZGERALD, W., LAMBORG, C. (**2004**): Lead and mercury in aerosol particles collected over the South Pole during ISCAT-2000. *Atmos. Environ*. 38: 5485-5491.

ARIYA, P.A., KHALIZOV, A., GIDAS, A. (**2002**): Reactions of Gaseous Mercury with Atomic and Molecular Halogens: Kinetics, Product Studies, and Atmospheric Implications. *J. Phys. Chem. A.* 106: 7310-7320.

ASTON, S. R., BRUTY, D., CHESTER, R., PADGHAM, R.C. (**1973**): Mercury in lake sediments: a possible indicator of technological growth. *Nature* 241: 450-451.

BAEZA URREA, O. (**2005**): Lake and fjord sediments as late Glacial to Holocene environmental and climate archives of the southernmost Andes at 53°, Chile. Ph.D thesis, University of Freiburg, Germany.

BAHLMANN, E. (**2004**): Aufklärung der Kinetik des Boden-Luft-Transfers von Hg anhand ausgewählter Umweltparameter. Ph.D. thesis, University of Lüneburg, Germany.

BAHLMANN, E., EBINGHAUS, R., RUCK, W. (**2006**): Development and application of a laboratory flux measurement system (LFMS) for investigation of the kinetics of mercury emissions from soils. *J. Environ. Manag*. 81: 114-125.

BAKER, P.G.L., BRUNKE, E.-G., SLEMR, F., CROUCH, A.M. (**2002**): Atmospheric mercury measurements at Cape Point, South Africa. *Atmos. Environ*. 36: 2459-2465.

BALABANOV, N.B., PETERSON, K.A. (**2003**): Mercury and Reactive Halogens: The Thermochemistry of Hg + {Cl_2, Br_2, BrCl, ClO, and BrO}. *J. Phys. Chem.* A. 107: 7465-7470.

BANIC, C.M., SCHROEDER, W.H., BEAUCHAMP, S.T., TORDEN, R.J. (**1997**): Concentration of mercury in the troposphere at altitudes up to 5 km in the vicinity of Southern Nova Scotia, Canada; AUG Fall Meeting: San Francisco, CA, USA, Dec. 8-12.

BARNES, H.L., SEWARD, T.M. (**1997**): Geothermal Systems and Mercury Deposits Chapter 14. In: Barnes H.L. (Ed.), Geochemistry of Hydrothermal Ore Deposits, 3rd ed. Wiley.

BARREGÅRD L, SÄLLSTEN G, SCHÜTZ A, ATTEWELL R, SKERFVING S, JARVHOLM B. (**1992**): Kinetics of mercury in blood and urine after brief occupational exposure. *Arch. Environ. H*ealth 7(3): 176-184.

BERGAN, T.; RHODE, H. (**2001**): Oxidation of elemental mercury in the atmosphere; Constraints imposed by global scale modelling. *J. Atmos. Chem*. 40: 191-212.

BERLIN, M. (**1986**): Mercury. In: Handbook on the toxicology of Metals, 2nd Ed. L. Friberg, G.F. Nordberg, V.B. Vouk (eds.) pp. 387-445, New York, Elsevier.

BIEBER, E., ALTHOFF, S. (**1995**): Methods for sampling and analysis of total mercury in precipitation in the air pollution network of the German Federal Environment Agency (Umweltbundesamt). In: JAMP Guidelines for the sampling and analysis of mercury in air and precipitation. London, OSPAR (Technical Annex 2, 20-23).

BIESTER, H., KILIAN, R., FRANZEN, C., WODA, C., MANGINI, A., SCHÖLER, H.F. (**2002**): Elevated Mercury Accumulation in a Peat Bog of the Magellanic Moorlands Chile (53°S), - An Anthropogenic Signal from the Southern Hemisphere. *EPSL* 201: 609-620.

BIESTER, H., MARTÍNEZ-CORTIZAS, A., BIRKENSTOCK, S., KILIAN, R. (**2003**): Effect of Peat Decomposition and Mass Loss on Historic Mercury Records in Peat Bogs from Patagonia. *Environ. Sci. Technol*. 37: 32-39.

BIESTER, H., BINDLER, R., MARTÍNEZ-CORTIZAS, A., ENGSTROM, D.R. (**2007**): Modeling the Past Atmospheric Deposition on Mercury Using Natural Archives. *Environ. Sci. Technol*. 41: 4581-4859.

BINDLER, R., RENBERG, I., APPLEBY, P.G. ANDERSON, N.J., ROSE, N.L. (**2001**): Mercury accumulation rates and spatial patterns in lake sediments from west Greenland: a coast to ice margin transect. *Environ. Sci. Technol*. 35: 1736-1741.

BINDLER, R. (**2003**): Estimating the natural background atmospheric deposition rate of mercury utilizing ombrotrophic bogs in south Sweden. *Environ. Sci. Technol.* 37: 32-39.

BLOOM, N.S., FITZGERALD, W.F. (**1988**): Determination of volatile mercury species at the picogram level by low-temperature gas chromatography with cold vapor atomic fluorescence detection. *Analytica Chimica Acta* 209: 151-161.

BLOOM, N. S., WATRAS, C. J., HURLEY, J. P. (**1991**): Impact of Acidification on the Methylmercury Cycle of Remote Seepage Lakes. *Water Air Soil Pollut.* 56:477-491.

BLOOM, N.S., PRESTBO, E.M., VONDERGEEST, E. (**1996**): Abstracts of the 4th International Conference on Mercury as a Global Pollutant, Hamburg, Germany.

BLOOM, N. S. (**2000**): Analysis ans atability of mercury speciation in petroleum hydrocarbons. Seepage Lakes. *Fres. J. Anal. Chem..* 366:438-443.

BORNMANN, G., HENKE, G., ALFES, H., MÖLLMANN, H. (**1970**): Über die enterale Resorption von metallischem Quecksilber. *Arch. Toxicol.* 26: 203-209.

BOUTRON, C.F., VANDAL, V.M., FITZGERALD, W.F., FERRARI, C.P. (**1998**): A Forty Year Record of Mercury in Central Greenland Snow. *Geophys. Res. Letters* 25: 3315-3318

BRAMAN, R.S., JOHNSON, D.L. (**1974**): Selective absorption tubes and emission technique for determination of ambient forms of mercury in air. *Environ. Sci. Technol.* 8: 996-1004.

BRITISH GEOLOGICAL SURVEY (**2010**): World Mineral Production 2004-2008. Keyworth, Nottingham, British Geological Survey.

BROOKS, S., ARIMOTO, R., LINDBERG, S., SOUTHWORTH, G. (**2008a**): Antarctic polar plateau snow surface conversion of deposited oxidized mercury to gaseous elemental mercury with fractional long-term burial. *Atmos. Environ*. 42: 2877-2884.

BROOKS, S., LINDBERG, S. SOUTHWORTH, G., ARIMOTO, R. (**2008b**): Springtime atmospheric mercury speciation in the McMurdo, Antarctica coastal region. *Atmos. Environ*. 42: 2885-2893.

BROSSET, C. (**1982**): Total airborne mercury and its origin. *Water Air Soil Pollut*. 17: 37-50.

BROSSET, C. (**1987**): The behaviour of mercury in the physical environment. *Water Air Soil Pollut*. 34: 145-166.

BROSSET, C., LORD, E. (**1995**): Methylmercury in ambient air. Method of determination and some measurement results. *Water Air Soil Pollut.* 82: 739-750.

BRUNKE, E.-G., LABUSCHAGNE, C., EBINGHAUS, R., KOCK, H.H., SLEMR, F. (**2010**): Gaseous elemental mercury depletion events observed at Cape Point during 2007-2008. *Atmos. Chem. Phys*. 10: 1121-1131.

BURKE, J., HOYER, KEELER, G., SCHERBATSKOY, T. (**1995**): Wet Deposition of Mercury and Ambient Mercury Concentrations at a Site in the Lake Champlain Basin. *Water Air Soil Pollut.* 80: 353-362.

CASASSA, G. (**1985**): Clasificación del clima en la región Austral de Chile. *Trapananda* 5: 174-175.

CHAZIN, J.D., ALLEN, M.K., RODGER, B.C. (**1995**): Measurement of mercury deposition using passive samplers based on the Swedish design. *Atmos. Environ*. 29: 1201-1209.

CHERIAN, M.G., HURSH, J.B., CLARKSON, T.W., ALLEN. J. (**1978**): Radioactive mercury distribution in biological fluids and excretion in human subjects after inhalation of mercury vapor. *Arch. Environ. Health* 33(3): 109-114.

COLBECK, S., AKITAYA, E.; ARMSTRONG, R., GUBLER, H., LAFEUILLE, J., LIED, K., MCCLUNG, D., MORRIS, E. (**1985**): The International Classification for Seasonal Snow on the Ground. Issued by the International Commission on Snow and Ice of the International Association of Scientific Hydrology and the International Glaciological Society. 37pp.

COLE, A.S., STEFFEN, A. (**2010**): Trends in long-term gaseous mercury observations in the Arctic and effects of temperature and other atmospheric conditions, *Atmos. Chem. Phys*. 10, 4661–4672.

CORONATO, F., BISIGATO, A. (**1998**): A temperature pattern classification in Patagonia. *International Journal of Climatology* 18: 765-773.

COTTON, F.A., WILKINSON, G. (**1985**): Anorganische Chemie. Eine zusammenfassende Darstellung für Fortgeschrittene. VCH-Weinheim.

COX, C., CLARKSON, T.W., MARSH, D.O., AMIN-ZAKI, L., TIKRITI, S., MYERS, G.J. (**1989**). Dose-response analysis of infants prenatally exposed to methylmercury: An application of a single compartment model to single-strand hair analysis. *Environ. Res.* 49: 318-332.

COX, C., MARSH, D., MYERS, G., CLARKSON, T. (**1995**): Analysis of data on delayed development from the 1971-1972 outbreak of methylmercury poisoning in Iraq: assessment of influential points. *Neurotoxicology* 16: 727-730.

DE LA ROSA, D.A., VOLKE-SEPULVEDA, T., SOLORZANO, G., GREEN, C., TORDON, R., BEAUCHAMP, S. (**2004**): Survey of atmospheric total gaseous mercury in Mexico. *Atmos. Environ*. 38: 4839-4846.

DE MORA, S.J., PATTERSON, J.E., BIBBY, D.M. (**1993**): Baseline atmospheric mercury studies at Ross Island, Antarctica. *Antarct. Sci*. 5: 323-326.

DOMMERGUE, A., FERRARI, C.P., PLANCHON, F.A.M., BOUTRON, C.F. (**2002**): Influence of anthropogenic sources on total gaseous mercury variability in grenoble suburban air (France). *Sci. Tot. Environ*. 297: 203-213.

DOMMERGUE, A., BAHLMANN, E., EBINGHAUS, R., FERRARI, C., BOUTRON, C. (**2007**): Laboratory simulation of Hg^0 emissions from a snowpack. *Anal. Bioanal. Chem*. 388: 319-327.

DOMMERGUE, A., SPROVIERI, F., PIRRONE, N., EBINGHAUS, R., BROOKS, S., COURTEAUD, J., FERRARI, C.P. (**2010**): Overview of mercury measurements in the Antarctic troposphere. *Atmos. Chem. Phys*. 10: 3309-3319.

DRASCH, G., SCHUPP, O., HOFL, H., REINKE, R., ROIDER, G. (**1994**): Mercury burden of human fetal and infant tissues. *Eur. J. Pediatr.* 153: 607-610.

DRISCOLL, C.T., YAN, C., SCHOFIELD, C.L., MUNSON, R., HOLSAPPLE, J. (**1994**): The Mercury Cycle and Fish in the Adirondack Lakes. *Environ. Sci. Technol.* 28(3): 136A-143A.

DUMAREY, R., TEMMERMANN, E., DAMS, R., HOSTE, J. (**1985**): The accuracy of the vapour-injection calibration method for the determination of mercury by amalgamation (cold-vapour atomic absorption spectrometry. *Analytica Chimica Acta* 170: 337-340.

DURNFORD, D., DASTOOR, A. (**2011**): The behavior of mercury in the cryosphere: A review of what we know from observations. *J. Geophys. Res*. 116: D06305.

DURNFORD, D., DASTOOR, A.P., STEEN, A.O., BERG, T., RYZHKOV, R., FIGUERAS-NIETO, D., HOLE, L.R., PFAFFHUBER, K.A., HUNG, H. (**2012**): How relevant is the deposition of mercury onto snowpacks? – Part1: A statistical study on the impact of environmental factors. *Atmos. Chem. Phys*. 12: 9221-9249.

DVONCH, J.T., KEELER, G.J., MARSIK, F.J. (**2005**): The Influence of Meteorological Conditions on the Wet Depostion of Mercury in Southern Florida. *J. Appl. Meteo*. 44: 1421-1435.

EBINGHAUS, R., KOCK, H.H., JENNINGS, S.G., MCCARTIN, P.; ORREN, M.J. (**1995**): Measurements of Atmospheric Mercury Concentrations in Northwestern and Central

Europe – Comparison of Experimental Data and Model Results. *Atmos. Environ.* 29: 3333-3344.

EBINGHAUS, R., TRIPATHI, R.M., WALLSCHLÄGER, D., LINDBERG, S.E. (**1999a**): Natural and Anthropogenic Mercury Sources and their Impact on the Air-Surface Exchange of Mercury on Regional and Global Scales. In: Mercury contaminated Sites. Ebinghaus, R., Turner, R.R., de Lacerda, L.D., Vasilev, O., Salomons, W. (Eds.). Springer Verlag, Heidelberg.

EBINGHAUS, R., JENNINGS, S.G., SCHROEDER, W.H., BERG, T., DONAGHY, T., GUENTZEL, J., KENNY, C., KOCK, H.H., KVIETKUS, K., LANDING, W., MUNTHE, J., PRESTBO, E.M., SCHNEEBERGER, D., SLEMR, F., SOMMAR, J., URBA, A., WALLSCHLÄGER, D., XIAO, Z. (**1999b**): International field intercomparison measurements of atmospheric mercury species at Mace Head, Ireland. *Atmos. Environ.* 33: 3063-3073.

EBINGHAUS, R., SLEMR, F. (**2000**): Aircraft measurements of atmospheric Mercury over southern and eastern Germany. *Atmos. Environ.* 34: 895-903.

EBINGHAUS, R., KOCK, H.H., COGGINS, A.M., SPAIN, T.G., JENNINGS, S.G., TEMME, C. (**2002a**): Long-term measurements of atmospheric mercury at Mace Head, Irish west coast, between 1995 and 2001. *Atmos. Environ.* 36: 5267-5276.

EBINGHAUS, R., KOCK, H.H., TEMME, C., EINAX, J.W., LÖWE, A.G., RICHTER, A., BURROWS, J.P., SCHROEDER, W.H. (**2002b**): Antarctic Springtime Depletion of Atmospheric Mercury. *Environ. Sci. Technol*. 36: 1238-1244.

EBINGHAUS, R., BANIC, C., BEAUCHAMP, S., JAFFE, D., KOCK, H.H., PIRRONE, N., POISSANT, L., SPROVIERI, F., WEISS-PENZIAS, P.S. (**2009**): Spatial Coverage and Temporal Trends of Land-based Atmospheric Mercury Measurements in the Northern and Southern Hemisphere. In: Mercury Fate and Transport in the Global Atmosphere, Pirrone, N., Mason, R. (Eds.), 223-291, Springer, New York, USA.

EDNER, H., FARIS, G.W., SUNESSON, A., SVANBERG, S. (**1989**): Atmospheric atomic mercury monitoring using differential absorption LIDAR technique. *Applied Optics* 28: 921.

EDNER, H., FARIS, G.W., SUNESSON, A. (**1991**): Lidar search for atmospheric atomic mercury in Icelandic geothermal fields. *J. Geophys. Res.* 96D: 2977-2986.

EDWARDS, G.C., HOWARD, D.A. (**2012**): Air-surface exchange measurements of gaseous elemental mercury over naturally enriched and background terrestrial landscapes in Australia. *Atmos. Chem. Phys. Discuss*. 12: 27927-27954.

ENDLICHER, W. (**1991a**): Zur Klimageographie und Klimaökologie von Südpatagonien. 100 Jahre klimatologische Messungen in Punta Arenas. *Freiburger Geographische Hefte* 32: 181-211.

ENDLICHER, W. (**1991b**): Südpatagonien - Klima und agrarökologische Probleme an der Magellanstraße. *Geographische Rundschau* 43: 143-151.

ENDLICHER, W., SANTANA, A. (**1988**): El clima del sur de la Patagonia y sus aspectos ecológicos. Un siglo de mediciones climatológicas en Punta Arenas. *Anales del Instituto de la Patagonia, Serie Ciencias Naturales* 18: 57-86.

ENVIRONMENTAL PROTECTION AGENCY (**1998**): EPA Method 7473 – Mercury in solids and solutions by thermal decomposition, amalgamation, and atomic absorption spectrophotometry.

EU-POSITION PAPER (**2001**): Ambient Air Pollution by Mercury (Hg). ISBN 92-894-4260-3

FAÏN, X., GRANGEON, S., BAHLMANN, E., FRITSCHE, J., OBRIST, D., DOMMERGUE, A., FERRARI, C.P., CAIRNS, W, EBINGHAUS, R., BARBANTE, C., CESCON, P.,BOUTRON, C. (**2007**): Diurnal production of gaseous mercury in the alpine snowpack before snowmelt. *J. Geophys. Res*. 112: D21311.

FAÏN, X., FERRARI, C.P., DOMMERGUE, A., ALBERT, M., BATTLE, M., ARNAUD, L., BARNOLA, J.-M., CAIRNS, W., BARBANTE, C., BOUTRON, C. (**2008**): Mercury in the snow and firn at Summit Station, central Greenland, and implications for the study of past atmospheric mercury levels. *Atmos. Chem. Phys*. 8: 3441-3457.

FALBE, J., REGITZ, M. (**1995**): Römpp Chemie Lexikon, 9. Auflage; Thieme Verlag, Stuttgart, Germany.

FENG, X., SOMMAR, J., GÅRFELDT, K., LINDQVIST, O. (**2000**): Improved determination of gaseous divalent mercury in ambient air using KCl coated denuders. *Fresenius J. Anal. Chem*. 366: 423-428.

FENG, X., TANG, S., SHANG, L., YAN, H., SOMMAR, J., LINDQVIST, O. (**2003**): Total gaseous mercury in the atmosphere of Guiyang, PR China. *Sci. Tot. Environ*. 304: 61-72.

FENG, X., SHANG, L., WANG, S., TANG, S., ZHENG, W. (**2004**): Temporal variation of total gaseous mercury in the air of Guiyang, PR China. *J. Geophys. Res.* 109: D03303.

FERRARA, R., MASERTI, B.E., DE LISO A., Cioni, R., Raco, B., Taddeucci, G., Edner, H., Ragnarson, P., Svanberg, S., Wallinder E. (**1994**): Atmospheric mercury emission at Solfatara volcano (Pozzuoli, Phlegraean Fields – Italy). *Chemosphere* 29: 1421-1428.

FERRARI, C.P., GAUCHARD, P.-A., ASPMO, K., DOMMERGUE, A., MAGAND, O., BAHLMANN, E., NAGORSKI, S., TEMME, T., EBINGHAUS, R., STEFFEN, A., BANIC, C., BERG, T., PLANCHON, F., BARBANTE, C., PAOLO CESCON, P. BOUTRON, C.F. (**2005**): Snow-to-air exchanges of mercury in an Arctic seasonal snow pack in Ny-Ålesund, Svalbard. *Atmos. Environ*. 39: 7633-7645.

FERRARI, C.P., PADOVA, C., FAÏN, X., GAUCHARD, P.-A., DOMMERGUE, A., ASPMO, K., BERG, T., CAIRNS, W., BARBANTE, C., CESCON, P., KALESCHKE, L., RICHTER, A., WITTROCK, F., BOUTRON, C. (**2008**): Atmospheric mercury depletion event study in Ny-Ålesund (Svalbard) in spring 2005. Deposition and transformation of Hg in surface snow during springtime. *Sci. Tot. Environ*. 397: 167-177.

FINLAYSON-PITTS, B.J., PITTS, JR., J.N. (**1986**): Atmospheric Chemistry: Fundamentals and Experimental Techniques. Viley, New York.

FITZGERALD, W.F. (**1989**): Atmospheric and oceanic cycling of mercury. Chapter 57, Volume 10 of *Chemical Oceanography Series*. J.P. Riley and R. Chester (eds.), Academic Press, 151-186.

FITZGERALD, W.F., CLARKSON, T.W. (**1991**): Mercury and monomethylmercury: present and future concerns. *Environ. Health Perspect*. 96: 159-166.

FITZGERALD, W.F., MASON, R.P., VANDAL, G.M. (**1991**): Atmospheric cycling and air water exchange of mercury over mid continental lacustrine regions. *Water Air Soil Pollut.* 56: 745-767.

FITZGERALD, W.F. (**1995**): Is Mercury increasing in the Atmosphere? The Need for an Atmospheric Mercury Network (AMNET). *Water Air Soil Pollut*. 80: 245-254.

FITZGERALD, W.F. (**1996**): Mercury emissions from volcanoes. In: 4th Int. Conf. on Mercury as a global pollutant, Book of Abstracts. Ebinghaus, R., Petersen, G., Tümpling U.V. (Eds.) Hamburg.

FITZGERALD, W. F. MASON, R. P. (**1996**): The Global Mercury Cycle: Oceanic and anthropogenic aspects. In: Global and Regional mercury cycles: sources. fluxes and mass balances. W. Baeyens, R. Ebinghaus, O. Vasiliev (Eds.), 85-108 Kluwer Academic Publishers, Dordrecht.

FITZGERALD, W.F., ENGSTROM, D.R., MASON, R.P., NATER, E.A. (**1998**): The case of atmospheric mercury contamination in remote areas. *Environ. Sci. Tchnol.* 32: 1-7.

FOSTIER, A.H., MICHELAZZO, P.S.M. (**2006**): Gaseous and particulate atmospheric mercury concentrations in the Campinas Metropolitan Region (São Paulo State, Brazil); *J. Brazilian Chem. Soc.* 17: 886-894.

FRANZEN, C., BIESTER, H. (**2003**): Do Hg accumulation rates in peat bogs reflect atmospheric deposition rates? 6th International Symposium on Environmental Geochemistry, September 07-11 2003, Edinburgh, Scotland.

FRANZEN, C., KILIAN, R., BIESTER, H. (**2004**): Natural mercury enrichment in a minerogenic fen – evaluation of sources and processes. *J. Environ. Monit*. 6: 466-472.

FUJITA, S., HORII, H., TANIGUCHI, S. (**1973**): Pulse radiolysis of mercuric Ion in aqueous solutions. *Journal of Physical Chemistry* 77: 2868.

GARCÍA-SÁNCHEZ, A., CONTRERAS, F., ADAMS, M., SANTOS, F. (**2006**): Airborne total gaseous mercury and exposure in a Venezuelan mining area. *Int. J. Environ. Health Res.* 16: 361-373.

GIVELET, N., ROOS-BARRACLOUGH, F., GOODSITE, M.E., CHEBURKIN, A.K., SHOTYK, W. (**2004**): Atmospheric mercury accumulation rates between 5900 and 800 calibrated years BP in the high arctic of Canada recorded by peat hummocks. *Environ. Sci. Technol.* 38: 4964-4972.

GLASS, G.E., LEONARD, E.N., CHAN, W.H., ORR, D.B. (**1986**): Airborne Mercury in Precipitation in the Lake Superior Region. *J. Great Lakes Res.* 12: 37-51.

GOBEIL, C., MACDONALD, R.W., SMITH, J.N. (**1999**): Mercury Profiles in Sediments of the Arctic Ocean Basins. *Environ. Sci. Technol*. 33: 4194-4198.

GRATZ, L.E., KEELER, G.J., MILLER, E.K. (**2009**): Long-term relationships between mercury wet deposition and meteorology. *Atmos. Environ*. 43: 6218-6229.

GUENTZEL, J.L., LANDING, W.M., GILL, G.A., POLLMAN, C.D. (**1995**): Atmospheric deposition of mercury in Florida: The FAMS project (1992-1994). *Water Air Soil Pollut.* 80: 393-402.

GUSTIN, M.S., LINDBERG, S.E. (**1997**): Natural sources of mercury emissions to air. Proc. EPRI Conf. on Managing Hazardous Air Pollutants. Washington, DC.

GUSTIN, M.S., LINDBERG, S.E., MARSIK, F., CASIMIR, A., EBINGHAUS, R., EDWARDS, G., HUBBLE-FITZGERALD, C., KEMP, R., KOCK, H.H., LEONARD, T., LONDON, J., SCHAEDLICH, F., SCHNEEBERGER, D., SCHROEDER, W., SOMMAR, J., TURNER, R., VETTE, A., WALLSCHLÄGER, D., XIAO, Z, ZHANG, H. (**1999**): The Nevada SToRMS Project: Towards scaling up mercury emissions from natural enriched surfaces. *J. Geophys. Res.* 104: 21831-21844.

GUSTIN, M.S., BIESTER, H., KIM, C.S. (**2002**): Investigation of light-enhanced emission of mercury from naturally enriched substrates. *Atmos. Environ*. 36: 3241-3254.

GUSTIN, M.S. STAMENKOVIC, J. (**2005**): Effect of watering and soil moisture on mercury emissions from soils. *Biogeochem.* 76: 215-232.

HACHIYA, N., TAKIZAWA, Y., HISAMATSU, S., ABE, T., ABE, Y., MOTOHASHI, Y. (**1998**): Atmospheric mercury concentrations in the basin of the Amazon, Brazil. *Environ. Health Prev. Med.* 2: 183-187.

HÅKANSSON, L., NILSSON, Å., ANDERSSON, T. (**1988**): Mercury in fish in Swedish lakes. *Environ. Pollut*. 49: 145-162.

HALL, B. (**1995**): The gas phase oxidation of elemental Mercury by Ozone. *Water Air Soil Pollut*. 80: 301-315.

HAMDY, M.K., NOYES, O.R. (**1975**): Formation of Methyl Mercury by Bacteria. *Appl. Microbiol*. 424-432.

HARADA, M. (**1995**): Minamata Desease: Methylmercury poisoning in Japan caused by environmental pollution. *Crit. Rev. Toxicol.* 25(1): 1-24.

HARRISON, R.M., KITTO, A.-M.N. (**1990**): Field intercomparison of filter pack and denuder sampling methods for reactive gaseous and particulate pollutants *Atmos. Environ*. 24A: 2633-2640.

HEDGECOCK, I.M., PIRRONE, N. (**2001**): Mercury and photochemistry in the marine boundary layer – modelling studies suggest the in situ production of reactive gas phase mercury. *Atmos. Environ.* 35: 3055-3062.

HEDGECOCK, I.M., PIRRONE, N., SPROVIERI, F., PESENTI, E. (**2003**): Reactive Gaseous Mercury in the Marine Boundary Layer: Modeling and Experimental Evidence of its Formation in the Mediterranean Sea. *Atmos. Environ*. 37(S1): S41-S49.

HEDGECOCK, I.M., TRUNFIO, G.A., PIRRONE, N., SPROVIERI, F. (**2005**): Mercury chemistry in the MBL: Mediterranean case and sensitivity studies using the AMCOTS (Atmospheric Mercury Chemistry over the Sea) model. *Atmos. Environ*. 39: 7217-7230.

HEISBERGER, F. (**1988**) Die Böden im Einzugsgebiet des Gossenköllesees und des Mutterbergersees. In: Psenner, R., Arzet, K., Brugger, A., Franzoi, J., Heisberger, F., Honsig-Erlenburg, W., Horner, F., Mueller, W., Nickus, U., Pfister, P., Schaber, P., Zapf, F. (eds), Versauerung von Hochgebirgsseen in kristallinen Einzugsgebieten Tirols und Kärntens. Zustand, Ursachen, Auswirkungen, Entwicklungen. Bundesministerium für Land und Forstwirtschaft, Wien, 259-322.

HERMANSON, M.H. (**1998**): Anthropogenic mercury deposition to arctic lake sediments. *Water Air Soil Pollut.*101: 309-321.

HERNÁNDEZ, A., JÉBRAK, M., HIGUERAS, P., OYARZUN, R., MORATA, D., MUNHÁ, J. (**1999**): The Almadén mercury mining district, Spain. *Mineralium Deposita* 34: 539-548.

HERTEL, C. (**2001**): Natürliche Quecksilberanreicherungen in einem minerogenen Torfmoor aus Südpatagonien, Chile. Diplomarbeit, University of Heidelberg, Germany. Unpublished.

HEUSSER, C.L., HEUSSER, L.E., LOWELL, T.V., MOREIRA, M.A., MOREIRA M.S. (**2000**): Deglacial paleoclimate at Puerto del Hambre, subantarctic Patagonia, Chile. *J. Quart. Sci.* 15: 101-114.

HIGUERAS, P., OYARZUN, R., LILLO, J., OYARZUN, J., MATURANA, H. (**2005**): Atmospheric mercury data for the Coquimbo region, Chile: Influence of mineral deposits and metal recovery practices. *Atmos. Environ.* 39: 7587-7596.

HIGUERAS, P., OYARZUN, R., LILLO, J., SÁNCHEZ-HERNÁNDEZ, J.C., MOLINA, J.A., ESBRÍ. J.M., LORENZO S. (**2006**): The Almadén district (Spain): Anatomy of one of the world's largest Hg-contaminated sites. *Sci. Tot. Environ*. 356: 112-124.

HOBBS, J.E., LINDESAY, J.A., BRIDGEMAN, H.A. (**1998**): Introduction: A southern hemisphere overview. In: Climates of the Southern Continents: Present, Past and Future. Hobbs, J.E., Lindesay, J.A., Bridgeman, H.A. (Eds.). New York, NY: Wiley.

HOLLEMANN, A.F., WIBERG, E. (**1985**): Lehrbuch der Anorganischen Chemie; de Gruyter; Berlin, New York.

HORVAT, M. (**2002**): Mercury as a Global Pollutant, *Analytical and Bioanalytical Chemistry* 374/6: 981-982.

HOYER, M.E., BURKE, J.B., KEELER, G.J. (**1995**): Atmospheric sources, transport and deposition of mercury in Michigan Two years of event precipitation. *Water Air Soil Pollut.* 80: 199-208.

HUDSON, R.J.M., GHERINI, S.A., FITZGERALD, W.F., PORCELLA, D.B. (**1995**): Anthropogenic influences on the global mercury cycle: A model-based analysis. *Water Air Soil Pollut.* 80: 265-272.

HURSH, J.B., GREENWOOD, M.R., CLARKSON, T.W., ALLEN, J., DEMUTH, S. (**1980**): The effect of ethanol on the fate of mercury vapor inhaled by man. *J Pharmacol. Exp. Therapeutic*s 214: 520-527.

IVERFELDT, Å., LINDQVIST, O. (**1986**): Atmospheric oxidation of elemental mercury by ozone in the aqueous phase. *Atmos. Environ*. 20: 1567-1573.

IVERFELDT, Å. (**1991a**): Occurrence and turnover of atmospheric mercury over Nordic countries. *Water Air Soil Pollut.* 56: 251-265.

IVERFELDT, Å. (**1991b**): Mercury in canopy throughfall water and its relation to atmospheric deposition. *Water Air Soil Pollut.* 56: 533-542.

IVERFELDT, Å., SJÖBERG, K. (**1992**): Intercomparison of methods for the determination of mercury deposition to convention waters. IVL Report B 1082, Swedish Environmental Research Institute (IVL), P.O. Box 47086, S- 40258 Göteborg, Sweden.

IVERFELDT, Å., MUNTHE, J. (**1993**): In: Proceedings from the EPA/A&WMA Symposium Measurement of Toxic and Related Air Pollutants, Durham, NC.

JENSEN, A., JENSEN, A. (**1981**): Historical deposition rates of mercury in Scandinavia estimated by dating and measurement of mercury in cores of peat bogs. *Water Air Soil Pollut*. 56: 769-778.

JENSEN, A., IVERFELDT, Å. (**1994**): Atmospheric bulk deposition of mercury to the southern Baltic sea area. In: Mercury as a Global Pollutant. Huckabee, J., Watras, C. (Eds.) Cleveland, CRC Press.

JIANG, S., LIU, X., CHEN, Q. (**2011**): Distribution of total mercury and methylmercury in lake sediments in Arctic Ny-Ålesund. *Chemosphere* 83: 1108-1116.

JOHANSSON, K, AASTRUP, M., ANDERSSON, A., BRINGMARK, L., IVERFELDT, Å. (**1991**): Mercury in Swedish forest soils - Assessment of critical load. *Water Air Soil Pollut*. 56: 267-281.

JOHNSON, K.P., BLUM, J.D., KEELER, G.J., DOUGLAS, T.A. (**2008**): Investigation of the deposition and emission of mercury in arctic snow during an atmospheric mercury depletion event. *J. Geophys Res*. 113, D17304.

JUNGE, C. (**1972**): The cycle of atmospheric gases – natural and man-made. *Quarterly Journal of the Royal Meteorological Society* 98 (418): 711-729.

KAISER, G., TÖLG, G. (**1980**): Mercury. In: The Handbook of Environmental Chemistry Vol. 3 Part A. Hutzinger (Ed.) Springer, Berlin-Heidelberg.

KAMENIK, C., KOINIG, K.A., SCHMIDT, R., APPLEBY, P.G., DEARING, J.A., LAMI, A., THOMPSON, R., PSENNER R. (**2000**): Eight hundred years of environmental changes in a high Alpine lake (Gossenköllesee, Tyrol) inferred from sediment records. *J. Limnol*. 59 (Suppl. 1): 43-52.

KAMMAN, N.C., ENGSTROM, D.R. (**2002**): Historical and present fluxes of mercury to Vermont and New Hampshire lakes inferred from ^{210}Pb dated sediment cores. *Atmos. Environ.* 36: 1599-1609.

KEELER, G.J., GLINSORN, G., PIRRONE, N. (**1995**): Particulate mercury in the atmosphere: Its significance, transport, transformation and sources. *Water Air Soil Pollut.* 80: 159-168.

KEELER, G.J., GRATZ, L.E., AL-WALI, K. (**2005**): Long-term Atmospheric Mercury Wet Deposition at Underhill, Vermont. *Ecotoxicology* 14: 71-83.

KEELER, G.J., PIRRONE, N., BULLOCK, R., SILLMAN, S. (**2009**): The Need for a Coordinated Global Mercury Monitoring Network for Global and Regional Models Validations. In: Mercury Fate and Transport in the Global Atmosphere, Pirrone, N., Mason, R. (Eds.), 391-424, Springer, New York, USA.

KERNDORFF, H. SCHNITZER, M. (**1980**): Sorption of metals on humic acid. *Geochim. Cosmochim. Acta* 44: 1701-1708.

KERSHAW TG, CLARKSON TW, DHAHIR PH. (**1980**): The relationship between blood levels and dose of methylmercury in man. *Arch. Environ. Health* 35(1): 28-36.

KILIAN, R., SCHNEIDER, C., KOCH, J., FESQ-MARTIN, M., BIESTER, H., CASASSA, C., ARÉVALO, M., WENDT, G., BAEZA, O., BEHRMANN, J. (**2007**). Palaeoecological constraints on Late Glacial and Holocene ice retreat in the Southern Andes (53°S). *Global and Planetary Change* 59: 49-66.

KIM, K.H., LINDBERG, S.E. (**1995**): Design and initial tests of a dynamic enclosure chamber for measurements of vapour-phase mercury fluxes over soils. *Water Air Soil Pollut.* 80: 1059-1068.

KIM, K.H., LINDBERG, S.E., MEYERS, T.P. (**1995**): Micrometeorological measurements of mercury vapor fluxes over background forest soils in eastern Tennessee. *Atmos. Environ*. 29: 267-282.

KING, M.D., SIMPSON, W.R. (**2001**): Extinction of UV radiation in Arctic snow at Alert, Canada (82°N). *J. Geophys. Res*. 106: 12499-12507.

KOCH, J., KILIAN, R. (**2002**): Dendroecological potential of commontree species along a transect across the southernmost Andes, Chile(53°S). *Anales Instituto Patagonia, Serie Cs. Nat.* (Chile), 30:123-132.

KOCK, H.H., BIEBER, E., EBINGHAUS, R., SPAIN, T.G., THEES, B. (**2005**): Comparison of long-term trends and seasonal variations of atmospheric mercury concentrations at the

two European coastal monitoring stations Mace Head, Ireland, and Zingst, Germany. *Atmos. Environ*. 39: 7549-7556.

KRABBENHOFT, D.P., BABIARZ, C.L. (**1992**): The role of groundwater transport in aquatic mercury cycling. *Water Resour. Res.* 28: 3119-3128.

KREUTZMANN, J., HOLZ, J., JANDL, G. (**1995**): Untersuchung des atmosphärischen Schadstoffeintrages in Nord- und Ostsee – Messungen. Umweltforschungsplan des Bundesministers für Umwelt, Naturschutz und Reaktorsicherheit, Forschungsbericht 104 02 667.

KROL, M., VAN LAEUWEN, P.J., LELIEVELD, J. (**1998**): Global OH trend inferred from methylchloroform measurements. *J. Geophys. Res. – Atmospheres* 103: 10697-10711.

KRUPP, R.E. (**1988**): Physicochemical aspects of mercury metallogenesis. *Chem. Geol.* 69: 345-356.

KUDO, A., TURNER, R.R. (**1999**): Mercury Contamination in Minamata Bay. In: Mercury Contaminated Sites. Ebinghaus, R., Turner, R.R., de Lacerda, L.D., Vasilev, O., Salomon, W. (Eds.), 143-158 Springer Verlag, Heidelberg.

LALONDE, J.D., AMYOT, M., KRAEPIEL, A.M., MOREL, F.M.M. (**2001**): Photooxidation of Hg(0) in artificial and natural waters. *Environ. Sci. Technol*. 35: 1367-1372.

LALONDE, J.D., POULAIN, A.J., AMYOT, M. (**2002**): The role of mercury redox reactions in snow on snow-to-air mercury transfer. *Environ. Sci. Technol*. 36: 174-178.

LALONDE, J.D., AMYOT, M., DOYON, M.-R., AUCLAIR, J.-C. (**2003**): Photo-induced Hg(II) reduction in snow from the remote and temperate Experimental Lakes Area (Ontario, Canada). *J. Geophys. Res*. 108: D6.

LAMBORG, C.H., FITZGERALD, W.F., VANDAL, G.M., ROLFHUS, K.R. (**1995**): Atmospheric mercury in northern Wisconsin: Sources and species. *Water Air Soil Pollut.* 80: 189-198.

LAMBORG, C.H., ROLFHUS, K.R., FITZGERALD, W.F., KIM, G. (**1999**): The atmospheric cycling and air-sea exchange of mercury species in the south and equatorial Atlantic Ocean. *Deep Sea Res. II* 46: 957-977.

LANDIS, M.S., STEVENS, R.K., SCHAEDLICHER, F., PRESTBO, E.M. (**2002a**): Development and Characterization of an Annular Denuder Methodology for the Measurement of Divalent Inorganic Reactive Gaseous Mercury in Ambient Air. *Environ. Sci. Technol*. 36: 3000-3009.

LANDIS, M.S., VETTE, A.F., KEELER, G.J. (**2002b**): Atmospheric mercury in the Lake Michigan Basin: Influence of the Chicago/Gary urban area. *Environ. Sci. Technol*. 36: 4508-4517.

LANDOLT-BÖRNSTEIN (**1969**): Zahlenwerte und Funktionen aus Physik, Chemie, Astronomie, Geophysik, Technik, 6.Auflage, Band II/2a; Springer-Verlag.

LAROSE, C., DOMMERGUE, A., DE ANGELIS, M., COSSA, D., AVERTY, B., MARUSCZAK, N., SOUMIS, N., SCHNEIDER, D., FERRARI, C. (**2010**): Springtime changes in snow chemistry lead to new insights into mercury methylation in the Arctic. *Geochim. Cosmochim. Acta* 74: 6263-6275.

LATHROP, R.C., RASMUSSEN, P.W., KNAUER, D.R. (**1991**): Mercury concentrations in walleyes from Wisconsin (USA) lakes. *Water Air Soil Pollut.* 56: 295-307.

LAURIER, F., MASON, R., WHALIN, L., KATO, S. (**2003**): Reactive gaseous mercury formation in the North Pacific Ocean's marine boundary layer: a potential role of halogen chemistry. *J. Geophys. Res.*108: 4529.

LEE, Y.-H., IVERFELDT, Å, (**1991**): Measurement of methylmercury and mercury in run-off, lake and rain waters. *Water Air Soil Pollut.* 56: 309-321.

LEICESTER, H.M: (**1961**): The Historical Background of Chemistry; John Wiley Inc., New York, USA.

LIN, C.-J., PEHKONEN, S.O. (**1997**): Aqueous free radical chemistry of mercury in the presence of iron oxides and ambient aerosol. *Atmos. Environ.* 31: 4125-4137.

LIN, C.-J., PEHKONEN, S.O. (**1999**): The Chemistry of Atmospheric Mercury: A Review. *Atmos. Environ.* 33: 2067-2079.

LIN, C.-J., PONGPRUEKSA, P., LINDBERG, S.E., PEHKONEN, S.O., BYUN, D., JANG, C. (**2006**): Scientific uncertainties in atmospheric mercury models I: Model science evaluation. *Atmos. Environ*. 40: 2911-2928.

LINDBERG, S.E., JACKSON, D.R., HUCKABEE, J.W., JANZEN, S.A., LEVIN, M.J., LUND, J.R. (**1979**): Atmospheric emissions and Plant Uptake of Mercury from Agricultural Soils near the Almadén Mercury Mine. *J. Environ. Qual*. 8: 572-578.

LINDBERG, S.E. (**1986**): Mercury Vapor in the Atmosphere: Three Case Studies on Emission, Deposition, and Plant Uptake. In: Toxic Metals in the Atmosphere, Nriagu, J.O.; Davidson, C.I.,(Eds.), John Wiley & Sons: New York.

LINDBERG, S.E, MEYERS, T.P, TAYLOR, G.E., TURNER, R.R. SCHROEDER, W.H. (**1992**): Atmospheric/surface exchange of mercury in a forest: results of modelling and gradient approaches. *J. Geophys. Res.* 97: 2519-2528.

LINDBERG, S.E., STRATTON, W.J. (**1998**): Atmospheric Mercury Speciation: Concentration and Behavior of Reactive Gaseous Mercury in Ambient Air. *Environ. Sci. Technol*. 32: 49-57.

LINDBERG, S.E., ZHANG, H., GUSTIN, M.S., VETTE, A., MARSIK F., OWENS, J., CASIMIR, A., EBINGHAUS, R., EDWARDS, G., FITZGERALD, C., KEMP, J., KOCK, H.H., LONDON, J., MAJEWSKI, M., POISSANT, L., PILOTE, M., RASMUSSEN, P., SCHAEDLICH, F., SCHNEEBERGER, D., SOMMAR, J., TURNER, R., WALLSCHLÄGER, D., XIAO, Z. (**1999**): Increases in mercury emissions from desert soils in response to rainfall and irrigation. *J. Geophys. Res*. 104: 21879-21888.

LINDBERG, S.E., BROOKS, S., LIN, C.J., SCOTT, K.J., LANDIS, M.S., STEVENS, R.K., GOODSITE, M., RICHTER, A. (**2002**): Dynamic oxidation of gaseous mercury in the Arctic troposphere at polar sun-rise. *Environ. Sci. Technol*. 36: 1245–1256.

LINDBERG, S.E., BULLOCK, R., EBINGHAUS, R., ENGSTROM, D., FENG, X., FITZGERALD, W., PIRRONE, N., PRESTBO, E., SEIGNEUR, C. (**2007**): A Synthesis of Progress and Uncertainties in Attributing the Sources of Mercury in Deposition. *Ambio* 36: 19-32.

LINDQVIST, O., JERNELÖV, A., JOHANSSON, K., RODHE, H. (**1984**): Mercury in the Swedish environment, global and local sources. SNV PM 1816, Swedish Environmental Protection Agency, S-171 85 Solna, Sweden.

LINDQVIST, O., RODHE, H. (**1985**): Atmospheric Mercury-a review. *Tellus* 37B:136-159.

LINDQVIST, O. (**1991**): Mercury in the Swedish Environment. *Water Air Soil Pollut.* 55, 7-17.

LINDQVIST, O., JOHANSSON, K., AASTRUP, M., ANDERSSON, A., BRINKMARK, L., HOVSENIUS, G., HÅKANSON, L., IVERFELDT, A., MEILI, M., TIMM, B. (**1991**): Mercury in the Swedish Environment - Recent Research on Causes, Consequences, and Corrective Methods. *Water, Air, Soil Pollut.* 55: 1-261.

LÓPEZ, M.L., PALANCAR, G.G., TOSELLI, B.M. (**2009**): Effect of different types of clouds on surface UV-B and total solar irradiance at southern mid-latitudes: CMF determinations at Córdoba, Argentina. *Atmos. Environ*. 43: 3130-3136.

LU, J.Y., SCHROEDER, W.H., BERG, T., MUNTHE, J., SCHNEEBERGER, D., SCHAEDLICH, F. (**1998**): A Device for Sampling and Determination of Total Particulate Mercury in Ambient Air. *Anal. Chem.* 70: 2403-2408.

LU, J.Y., SCHROEDER, W.H. (**1999a**): Comparison of conventional filtration and a denuder-based methodology for sampling of particulate-phase mercury in ambient air. *Talanta* 49: 15-24.

LU, J.Y., SCHROEDER, W.H. (**1999b**): Sampling and Determination of Particulate Mercury in Ambient Air: A Review. *Water Air Soil Pollut.* 112: 279-295.

LUCOTTE, M., MUCCI, A., HILLAIRE-MARCEL, C., PICHET, P., GRONDIN, A. (**1995**): Anthropogenic Mercury Enrichment in Remote Lakes of Northern Quebec (Canada). *Water Air Soil Pollut.* 80: 467-476.

MAGOS, L. (**1988**): Mercury, in: H.G. Seiler, H. Siegel (eds.), Handbook on Toxicity of Inorganic Compounds, Marcel Dekker, New York, 419-436.

MARQUARDT, H. (**1994**): Lehrbuch der Toxikologie, Wissenschaftsverlag, Mannheim

MARTÍNEZ-CORTIZAS, A., PONTVEDRA-POMBAL, X., GARCÍA-RODEJA, E., NÓVOA-MUÑOZ, J.C., SHOTYK, W. (**1999**): Mercury in a Spanish Peat Bog: Archive of Climate Change and Atmospheric Metal Deposition. *Science* 284: 939-942.

MARTÍNEZ-CORTIZAS, A., GARCÍIA-RODEJA, E., PONTEVEDRA POMBAL, X., NÓVOA-MUÑOZ, J.C., WEISS, D., CHEBURKIN, A. (**2002**): Atmospheric Pb deposition in Spain during the last 4600 years recorded by two ombrotrophic peat bogs and implications for use of peat as archive. *Sci. Tot. Environ.* 292: 33-44.

MASON, R.P., VANDAL, G.M., FITZGERALD, W.F. (**1992**): The sources and composition of mercury in Pacific Ocean rain. *J. Atmos. Chem*. 14: 489-500.

MASON, R.P. FITZGERALD, W.F., MOREL, F.M. (**1994**): The biogeochemical cycling of elemental mercury: anthropogenic influences. *Geochim. Cosmochim. Acta* 58/15: 3191-3198.

MASON, R.P. (**2009**): Mercury emissions from natural processes and their importance in the global cycle. In: Mercury Fate and Transport in the Global Atmosphere. Mason, R.P., Pirrone, N. (Eds.) Springer, New York, USA, 173-191.

MCKEAGUE, J.A., WOLYNETZ, M.S. (**1980**): Background levels of minor elements in some Canadian soils. *Geoderma* 24: 299-307.

MCMURTRY, M.J., WALES, D.L., SCHEIDER, W.A., BEGGS, G.L., DIMOND, P.E. (**1989**): Relationship of mercury concentrations in lake trout (*Salvelinus namaycush*) and smallmouth bass (*Micropterus dolomieui*) to the physical and chemical characteristics of Ontario lakes. *Can. J. Fish. Aquat. Sci.* 46: 426-434.

MEILI, M. (**1991a**): Fluxes, pools and turnover of mercury in Swedish forest lakes. *Water, Air, Soil Pollut.* 56: 719-727.

MEILI, M. (**1991b**): The coupling of mercury and organic matter in the biogeochemical cycle - towards a mechanistic model for the boreal forest zone. *Water, Air, Soil Pollut.* 56: 333-348.

MILLER, A. (**1976**): The climate of Chile. In: Climates of Central and South America. World Survey of Climatology. Schwerdtfeger, W. (Ed.). Amsterdam, The Netherlands: Elsevier, 113-146.

MINISTRY OF THE ENVIRONMENT, GOVERNMENT OF JAPAN (**2002**): Minamata Disease The History and Measures. http://www.env.go.jp/en/chemi/hs/minamata2002/

MOORE, C., CARPI, A. (**2005**): Mechanisms of the emission of mercury from soil: Role of UV radiation. *J. Geophys. Res*. 110: D24302.

MUNTHE, J. (**1992**): The aqueous oxidation of elemental mercury by ozone. *Atmos. Environ.* 26A: 1461:1468.

MUNTHE, J., MCELROY, W. (**1992**): Some aqueous reactions of potential importance in the atmospheric chemistry of mercury. *Atmos. Environ.* 26A:553-557.

MUNTHE, J. (**1996**): Guidelines for the sampling and analysis of mercury in air and precipitation. Göteborg (IVL-report L 96/204).

MUNTHE, J., WÄNGBERG, I., PIRRONE, N., IVERFELDT Å, FERRARA, R., EBINGHAUS, R., FENG, X., GÅRFELDT, K., KEELER, G., LANZILOTTA, E., LINDBERG, S.E., LU, J., MAMANE, Y., PRESTO, E., SCHMOLKE, S., SCHROEDER, W.H., SOMMAR, J., SPROVIERI, F., STEVENS, R.K., STRATTON, W., TUNCEL, G., URBA, A. (**2001**): Intercomparison of methods for sampling and analysis of atmospheric mercury species. *Atmos. Environ.* 35: 3007-3017.

MUNTHE, J., WÄNGBERG, I., IVERFELDT, Å, LINDQVIST, O., STRÖMBERG, D., SOMMAR, J., GÅRFELDT, K., PETERSEN, G., EBINGHAUS, R., PRESTBO, E., LARJAVA, K., SIEMENS, V. (**2003**): Distribution of atmospheric mercury species in Northern Europe: final results from the MOE project. *Atmos. Environ*. 37 Suppl. 1: S9-S20.

NADP (2003): National Atmospheric Deposition Program 2002 Annual Summary. NADP Data Report 2003-01. Illinois State Water Survey, Champaign, IL.

NADP (2004): National Atmospheric Deposition Program 2003 Annual Summary. NADP Data Report 2004-01. Illinois State Water Survey, Champaign, IL.

NATER, E.A., GRIGAL., D.F. (**1992**): Regional trends in mercury distribution across the Great Lakes states, north central USA. *Nature* 358: 139-141.

NGDTJ – NATIONAL GEOSCIENCE DATABASE OF TAJIKISTAN: http://www.ngdtj.com.

NORRBY, L.J. (**1991**): Why is mercury liquid? Or, why do relativistic effects not get into chemistry textbooks? *J. Chem. Educ*. 68: 110-113.

NRIAGU, J.O. (**1989**): A global assessment of natural sources of atmospheric trace metals. *Nature* 338: 47-49.

NRIAGU, J.O., PACYNA J.M. (**1988**): Quantitative assessment of worldwide contamination of air, water and soils by trace metals. *Nature* 333: 134-139.

OBOLENSKY, A.A. (**1996**): Natural mercury sources in the environment: contribution of Siberia. In: Global and Regional Mercury Cycles: Sources, Fluxes and Mass Balances. Baeyens, W., Ebinghaus, R., Vasiliev, O. (Eds.). NATO-ASI-Series 2. Environment Vol. 21. Kluwer, Dodrecht, The Netherlands, 453-462.

OLID, C., GARCIA-ORELLANA, J., MARTÍNEZ-CORTIZAS, A., MASQUÉ, P., PEITEADO-VARELA, E., SANCHEZ-CABEZA, J-A. (**2010**): Multiple site study of recent atmospheric metal (Pb, Zn and Cu) deposition in the NW Iberian Peninsula using peat cores. *Sci. Tot. Environ.* 408: 5540-5549.

OSPAR (**1997**): JAMP Guidelines for the sampling and analysis of mercury in air and precipitation. London.

PACYNA, J.M., KEELER, G. (**1995**): Sources of mercury in the Arctic. *Water Air Soil Pollut.* 80: 621-632.

PACYNA, J.M. (**1996**): Emission inventories of Atmospheric mercury from Anthropogenic sources. In: Global and Regional Mercury Cycles: Sources, Fluxes, and Mass Balances. Baeyens, W. Ebinghaus, R., Vasiliev, O. (Eds). 161-178 NATO-ASI Series 2. Environment Vol.21. Kluwer, Dordrecht, Niederlande.

PACYNA J. M. AND PACYNA P.E, (**1996**): Global emissions of mercury to the atmosphere. Emission from anthropogenic sources. A report for the arctic monitoring and assessment programme (AMAP), Oslo, June 1996.

PACYNA, E.G., PACYNA, J.M, STEENHUISEN, F., WILSON, S. (**2006**): Global anthropogenic mercury emission inventory for 2000. *Atmos. Environ*. 40: 4048-4063.

PACYNA, E.G., PACYNA, J.M., SUNDSETH, K., MUNTHE, J., KINDBOM, K., WILSON, S., STEENHUISEN, F., MAXSON, P. (**2010**): Global emission of mercury to the atmosphere

from anthropogenic sources in 2005 and projections to 2020. *Atmos. Environ*. 44: 2487-2499.

PEHKONEN, S.O., LIN, C.-J. (**1998**): *Journal of AWMA* 48: 144-150.

PETERSEN, G., EPPEL, D., GRASSL, H., IVERFELDT, A., MISRA, P.K., BLOXAM, R., WONG, S., SCHROEDER, W.H., VOLDNER, E., PACYNA, J. (**1989**): Model Studies on the Atmospheric Transport and Deposition of Mercury. In: Proc. Int. Conf. on Heavy Metals in the Environment. J.P. Vernet (Ed.), CEP Publ., Edinburgh, UK. Vol. 1: 48-52.

PETERSEN, G., IVERFELDT, Å, MUNTHE, J. (**1995**): Atmospheric mercury species over Central and Northern Europe: model calculations and comparison with observations form the Nordic air and precipitation netword for 1987 and 1988. *Atmos. Environ.* 29: 47-67.

PETERSEN, G, MUNTHE, J., PLEIJEL, L., BLOXAM, R., KUMAR, V.A. (**1998**): A comprehensive eulerian modelling framework for airborne mercury species: Development and testing of the tropospheric chemistry module (TCM). *Atmos. Environ.* 32: 829-843.

PHEIFFER-MADSON, P. (**1981**): Peat bog records of atmospheric mercury deposition. *Nature* 293: 127-130.

PIRRONE, N., KEELER, G.J., ALLERGRINI, I. (**1996a**): Particle Size Distributions of Atmospheric Mercury in Urban and Rural Areas. *Journal of Aerosol Science* 27: 13-14.

PIRRONE, N., KEELER, G.J., NRIAGU, J.O. (**1996b**): Regional Differences in Worldwide Emissions of Mercury to the Atmosphere. *Atmos. Environ.* 30: 2981-2987.

PIRRONE, N., KEELER, G.J., NRIAGU, J.O., WARNER, P.O. (**1996c**): Historical Trends of Airborne Trace Metals in Detroit from 1971 to 1992. *Water Air Soil Pollut*. 88: 145-165.

PIRRONE, N., ALLEGRINI, I., KEELER, G.J., NRIAGU, J.O., ROSSMANN, R., ROBBINS, J.A. (**1998**): Historical Atmospheric Mercury Emissions and Depositions in North America Compared to Mercury Accumulations in Sedimentary Records. *Atmos. Environ.* 32: 929-940.

PIRRONE, N., HEDGECOCK, I., FORLANO, L. (**2000**): The Role of the Ambient Aerosol in the Atmospheric Processing of Semi-Volatile Contaminants: A Parameterised Numerical Model (GASPAR). *Journal of Geophysical Research* 105/D8: 9773-9790.

PIRRONE, N., FERRARA, R., HEDGECOCK, I.M., KALLOS, G., MAMANE, Y., MUNTHE, J., PACYNA, J.M., PYTHAROULIS, I., SPROVIERI, F., VOUDOURI, A., WÄNGBERG, I. (**2003**): Dynamic processes of mercury over the Mediterranean region: results from the

Mediterranean Atmsopheric Mercury Cycle System (MACMS) project. *Atmos. Environ.* 37 Suppl. 1: S21-S39.

PIRRONE, N., CINNIRELLA, S., FENG, X., FINKELMANN, R.B., FRIEDLI, H.R., LEANER, J., MASON, R., MUKHERJEE, A.B., STRACHER, G.B., STREETS, D.G., TELMER, K. (**2010**): Global mercury emissions to the atmosphere from anthropogenic and natural sources. *Atmos. Chem. Phys.* 10: 5951-5964.

PLEIJEL, K., MUNTHE, J. (**1995**): Modelling the Atmospheric Mercury Cycle – Chemistry in Fog Droblets. *Atmos. Environ.* 29: 1441-1457.

POISSANT, L., PILOTE, M., CASIMIR, A. (**1999**): Mercury flux measurements in a naturally enriched area: correlation with environmental conditions during the Nevada Study and Tests of the Release of Mercury from Soils (STORMS). *J. Geophys. Res.* 104: 21,845-21,858.

POISSANT, L., PILOTE, M., BEAUVAIS, C., CONSTANT, P., ZHANG, H.H. (**2005**): A year of continuous measurements of three atmospheric mercury species (GEM, RGM, Hg_P) in southern Québec, Canada. *Atmos. Environ*. 39: 1275-1287.

PORCELLA, D.B., CHU, P., ALLAN M.A. (**1996**) Inventory of North American mercury emissions to the atmosphere: relationship to the global mercury cycle. In: Global and regional mercury cycles: sources, fluxes and mass balances. Bayens W., Ebinghaus, R., Vasiiev, O. (Eds.). NATO-ASI Series 2. Environment Vol. 21. Kluwer, Dordrecht, The Netherlands, 179-190.

POULAIN, A.J. LALONDE, J.D., AMYOT, M., SHEAD, J.A., RAOFIE, F., ARIYA, P.A. (**2004**): Redox transformations of mercury in an Arctic snowpack at springtime. *Atmos. Environ.* 38: 6763-6774.

PRESTBO, E.M., GAY, D.A. (**2009**): Wet deposition of mercury in the U.S. and Canada, 1996-2005: Results and analysis of the NADP mercury deposition network (MDN). *Atmos. Environ.* 43: 4223-4233.

RAOFIE, F., ARIYA, P.A. (**2004**): Product Study of the Gas-Phase BrO-Initiated Oxidation of Hg^0: Evidence for Stable Hg^{1+} Compounds. *Environ. Sci. Technol.* 38: 4319-4326.

RASMUSSEN, P.E. (**1994**): Current methods of estimating atmospheric fluxes in remote areas. *Environ. Sci. Technol*. 28: 2233-2241.

RIBEIRO GUEVARA, S., MEILI, M., RIZZO, A., DAGA, R., ARRIBÉRE, M. (**2010**): Sediment records of highly vaiable mercury inputs to mountain lakes in Patagonia during the past millennium. *Atmos. Chem. Phys*. 10: 3433-3453.

ROELS H.A, BOECKX M., CEULEMANS E., LAUWERYS R.R. (**1991**): Urinary excretion of mercury after occupational exposure to mercury vapour and influence of the chelating agent meso-2,3-dimercaptosuccinic acid (DMSA). Br. J. Ind. Med. 48(4): 247-253.

ROOS-BARRACLOUGH, F., SHOTYK, W. (**2003**): Millennial-scale records of atmospheric mercury deposition obtained from ombrotrophic and minerotrophic peatland in the Swiss Jura mountains. *Environ. Sci. Technol*. 37: 235-244.

SÄLLSTEN, G., BARREGÅRD, L., SCHÜTZ, A. (**1993**): Decrease in mercury concentration in blood after long term exposure: a kinetic study of chloralkali workers. *Br. J. Ind. Med.* 50(9): 814-821.

SÄLLSTEN, G., BARREGÅRD, L., SCHÜTZ, A. (**1994**): Clearance half-life of mercury in urine after the cessation of long term occupational exposure: influence of a chelating agent (DMPS) on excretion of mercury in urine. *Occup. Environ. Med*. 51(5): 337-342.

SCHLÜTER, K. (**2000**): Review: evaporation of mercury from soils. An integration and synthesis of current knowledge. *Environ. Geol*. 39: 249-271.

SCHNEIDER, C., GLASER, M., KILIAN, R., SANTANA, A., BUTOROVIC, N., CASASSA, G. (**2003**): Weather Observations across the Southern Andes at 53°S. *Physical Geography* 24/2: 97-119.

SCHROEDER, W.H. (**1989**): Developments in the speciation of mercury in natural waters. *Trends Anal. Chem.* 8: 339-342.

SCHROEDER, W.H.; YARWOOD, G.; NIKI, H. (**1991**): Transformation Processes Involving Mercury Species in the Atmosphere - Results from a Literature Survey. *Water Air Soil Pollut.* 56: 653-666.

SCHROEDER, W.H., KEELER, G., KOCK, H., ROUSSEL, P., SCHNEEBERGER, D., SCHAEDLICH, F. (**1995a**): International field intercomparison of atmospheric mercury measurement methods. *Water Air Soil Pollut*. 80: 611-620.

SCHROEDER, W.H., LAMBORG, C., SCHNEEBERGER, D., FITZGERALD, W.F. SRIVASTAVA, B. (**1995b**): Comparison of a manual method and an automated analyser for determining total gaseous mercury in ambient air. Proceedings of 10th International Conference on Heavy Metals in the Environment, Wilden, R.D., Förster, U., Knöchel, A. (Eds.) CEP Consultants Ltd., Publisher, Edinburgh, U.K., 2, 57-60.

SCHROEDER, W.H., ANLAUF, K.G., BARRIE, L.A., LU, J.Y., STEFFEN, A., SCHNEEBERGER, D.R., BERG, T. (**1998**): Arctic springtime depletion of mercury. *Nature* 394: 331-332.

SCHROEDER, W.H., MUNTHE, J. (**1998**): Atmospheric Mercury – an overview. *Atmos. Environ.* 29, 809-822.

SCHUSTER, E. (**1991**): The behaviour of mercury in the soil with special emphasis on complexation and adsorption processes - a review of the literature. *Water Air Soil Pollut.* 56: 667-680.

SCIENCE24: http://www.ngdtj.com/Default.asp?

SEIGNEUR, C., WROBEL, J., CONSTANTINOU, E. (**1994**): A Chemical Kinetic Mechanism for Atmospheric Inorganic Mercury. *Environ. Sci. Technol.* 28: 1589-1597.

SELIN, N.E., JACOB, D.J., YANTOSCA, R.M., STRODE, S., JAEGLÉ, L., SUNDERLAND, E.M. (**2008**): Global 3-D land-ocean-atmosphere model for mercury: Present-day versus preindustrial cycles and anthropogenic enrichment factors for deposition. *Global Biogeochem. Cycl.* 22: 1-13.

SHEPPARD, D.S., PATTERSON, J.E., MCADAM, M.K. (**1991**): Mercury content of Antarctic ice and snow: Further results. *Atmos. Environ*. 25A: 1657-1660.

SHEU, G-R., MASON, R.P. (**2001**): An Examination of Methods for the Measurements of Reactive gaseous Mercury in the Atmosphere*. Environ. Sci. Technol*. 35: 1209-1216.

SHEU, G-R., MASON, R.P. (**2004**): An Examination of the Oxidation of Elemental Mercury in the Presence of Halide Surfaces. *J. Atmos. Chem*. 48: 107-130.

SHMV (**2006**): Schadstoffhöchstmengen Verordnung – Verordnung über Höchstmengen an Schadstoffen in Lebensmitteln; 05.07.2006 (BGBl. I Nr. 33 vom 19.7.2006 S. 1562) Gl.-Nr.: 2125-40-89.

SHOTYK, W., GOODSITE, M.E., ROOS-BARRACLOUGH, R., FREI, R., HEINEMEIER, J., ASMUND, G., LOHSE, C., HANSEN, T.S. (**2003**) Anthropogenic contributions to atmospheric Hg, Pb, and As accumulation recorded by peat cores from southern Greenland and Denmark dated using the 14C “bomb pulse curve”. Geochim. Cosmochim. Acta 67(21): 3991-4001.

SLEMR, F., SEILER, W., SCHUSTER, G.J. (**1981**): Latitudinal distribution of mercury over the Atlantic Ocean. *Journal Geophys. Res.* 86: 1159-1166.

SLEMR, F., SCHUSTER; G., SEILER, W. (**1985**): Distribution, speciation, and budget of atmospheric mercury. *J. Atmos. Chem*. 3: 407-434.

SLEMR, F., LANGER, E. (**1992**): Increase in global atmospheric concentrations of mercury inferred from measurements over the Atlantic Ocean. *Nature* 355: 434-437.

SLEMR, F., JUNKERMANN, W., SCHMIDT, R.W.H., SLADKOVIC, R. (**1995**): Indication of change in global and regional trends of atmospheric mercury concentrations. *Geophys. Res. Lett.* 22: 2143–2146.

SLEMR, F., BRUNKE, E.-G., EBINGHAUS, R., TEMME, CH., MUNTHE, J., WÄNGBERG, I., SCHROEDER, W., STEFFEN, A., BERG, T., (**2003**): Worldwide trends of atmospheric mercury since 1977. *Geophys. Res. Lett.* 30: 1516.

SLEMR, F., BRUNKE, E.-G., LABUSCHAGNE, C., EBINGHAUS, R. (**2008**): Total gaseous mercury concentrations at the Cape Point GAW station and their seasonality. *Geophys. Res. Lett.* 35: L11807.

SLEMR, F., BRUNKE, E.G., EBINGHAUS, R., KUSS, J. (**2011**): Worldwide trend of atmospheric mercury since 1995. *Atmos. Chem. Phys*. 11: 4779-4787.

SOMMAR, J., HALLQUIST, M., LJUNGSTRÖM, EL, LINDQVIST, O. (**1997**): On the gaseous reaction between volatile biogenic mercury species and the nitrate radical. *J. Atmos. Chem.* 27: 233-247.

SOMMAR, J., FENG, X., GÅRDFELDT, K., LINDQVIST, O. (**1999**)**:** Measurements of fractionated gaseous mercury concentrations in Northwestern and Central Europe, 1995-1999. *J. Environ. Monitor*. 1: 435-439.

SOMMAR, J., GÅRDFELDT, K., STRÖMBERG, D., FENG, X. (**2001**): A kinetic study of the gasphase reaction between hydroxyl radical and atomic mercury. *Atmos. Environ.* 35: 3049-3054.

SOERENSEN, A.L., SKOV, H., JACOB, D.J., SOERENSEN, B.T., JOHNSON, M.S. (**2010**): Global Concentrations of Gaseous Elemental Mercury and Reactive Gaseous Mercury in the Marine Boundary Layer. *Environ. Sci. Technol*. 44: 7425-7430.

SPROVIERI, F., PIRRONE, N. (**2000**): A preliminary assessment of mercury levels in the Antarctic and Arctic troposphere. *J. Aerosol Sci*. 31: 757-758.

SPROVIERI, F., PIRRONE, N., HEDGECOCK, I. M., LANDIS, M. S., STEVENS, R. K. (**2002**): Intensive atmospheric mercury measurements at Terra Nova Bay in Antarctica during November and December 2000. *J. Geophys. Res.* 107 (D23, 4722, doi:10.1029/2002JD002057).

SPROVIERI, F., PIRRONE, N., GÅRDFELDT, K., SOMMAR, J. (**2003**): Mercury speciation in the marine boundary layer along a 6000 km cruise path around the Mediterranean Sea. *Atmos. Environ*. 37, S1: S63-S71.

SPROVIERI, F., PIRRONE, N., EBINGHUAS, R., KOCK, H., DOMMERGUE, A. (**2010a**): A review of worldwide atmospheric mercury measurements. *Atmos. Chem. Phys*. 20: 8245-8265.

SPROVIERI, F., PIRRONE, N., EBINGHUAS, R., KOCK, H., DOMMERGUE, A. (**2010b**): A review of worldwide atmospheric mercury measurements. *Atmos. Chem. Phys*. *Discuss*. 10: 1261-1307.

SPROVIERI, F., HEDGECOCK, I. M., PIRRONE N. (**2010c**): An investigation of the origins of reactive gaseous mercury in the Mediterranean marine boundary layer. *Atmos. Chem. Phys.* 10: 3985-3997.

STAMENKOVIC, J., LYMAN, S., GUSTIN, M.S. (**2007**): Seasonal and diel variation of atmospheric mercury concentrations in the Reno (Nevada, USA) airshed. *Atmos. Environ.* 41: 6662-6672.

STEFFEN, A., SCHROEDER, W., BOTTENHEIM, J., NARAYAN, J., FUENTES, J.D. (**2002**): Atmospheric mercury concentrations: Measurements and profiles near snow and ice surfaces in the Canadian Arctic during Alert 2000. *Atmos. Environ*. 36: 2653-2661.

STEIN, E.D., COHEN, Y., WINER, A.M. (**1996)**: Environmental distribution and transformation of mercury compounds. *Critical reviews in Environ. Sci. Technol*. 26(1): 1-43.

STEINNES, E., ANDERSSON, E.M. (**1991**): Atmospheric deposition of mercury in Norway: temporal and spatial trends. Water, Air, Soil Pollut. 56: 391-404.

STEVENS, R.K., LANDIS, M.S., SCHAEDLICH, F.A. SCHNEEBERGER, D.R., PRESTBO, E., KEELER, G.J., DVONCH, J.T., LINDBERG, S.L., (**1999**): Automated instrumentation designed to measure elemental gaseous and reactive gaseous mercury: design and operational characteristics. Presented at the 5th International Conference on Mercury as a Global Pollutant, Rio de Janeiro.

ST.LOUIS, V.L., RUDD, J.W., KELLY, C.A., BARRIE, L.A. (**1995**): *Water, Air, Soil Pollut.* 80: 405-414.

STRATTON, W.J., LINDBERG, S.E. (**1995**): Use of a Refluxing Mist Chamber for Measurement of Gas-Phase Mercury(II) Species in the Atmosphere. *Water. Air. Soil. Pollut.* 80: 1269-1278.

STRATTON, W.J., LINDBERG, S.E., PERRY, C.J. (**2001**): Atmospheric Mercury Speciation: Laboratory and Field Evaluation of a Mist Chamber Method for Measuring Reactive Gaseous Mercury. *Environ. Sci. Technol*. 35: 170-177.

SWAIN, E.B., ENGSTROM, D.R., BRIGHAM, M.E., HENNING, T.A., BREZONIK, P.L. (**1992**): Increasing Rates of Atmospheric Mercury Deposition in Midcontinental North America. *Science* 257: 784-787.

THANABALASINGAM, P; PICKERING, W.F. (**1985**): The sorption of Mercury(II) by Humic Acids. *Environ. Pollut.* B9: 267-279.

TEMME, C. (**2003**): Reaktionen des Quecksilbers und seiner Spezies in bodennahen Luftschichten der Antarktis. Ph.D. thesis, University of Jena, Germany.

TEMME, C., EINAX, J.W., EBINGHAUS, R., SCHROEDER, W.H. (**2003a**): Measurements of atmospheric mercury species at a coastal site in the Antarctic and over the South Atlantic Ocean during polar summer. *Environ. Sci. Technol.* 37: 22-31.

TEMME, C., SLEMR, F., EBINGHAUS, R., EINAX, J.W. (**2003b**): Distribution of mercury over the Atlantic Ocean in 1996 and 1999-2001. *Atmos. Environ*. 37: 1889-1897.

TEMME, C., BLANCHARD, P., STEFFEN, A., BANIC, C., BEAUCHAMP, S., POISSANT, L., TORDON, R., WIENS, B. (**2007**): Trend, seasonal and multivariate analysis study of total gaseous mercury data from the Canadian atmospheric mercury measurement network (CAMNet). *Atmos. Environ*. 41: 5423-5441.

TOKOS, J.J., HALL, B., CALHOUN, J.A., PRESTBO, E.M. (**1998**): *Atmos. Environ.* 32: 823-827.

URBA, A., KVIETKUS, K., SAKALYS, J., XIAO, Z., LINDQVIST, O. (**1995**): A new sensitive and portable Mercury vapor analyzer Gardis-1A. *Water Air Soil Pollut.* 80: 1305-1309.

URBA, A., KVIETKUS, K., SCHMOLKE, S., MUNTHE, J. (**1998**): International Field Intercomparison and Other Measurements of Total Gaseous Mercury at Preila, Lithuania, during 1996-1997. In: Proceedings of EUROTRAC Symposium 98; 364-368.

US-EPA (**2002**): Method 1631, Revision E: Mercury in Water by Oxidation, Purge and Trap, and Cold Vapor Atomic Fluorescence Spectrometry. http://water.epa.gov/scitech/methods/cwa/metals/mercury/upload/2007_07_10_methods_method_mercury_1631.pdf.

VAREKAMP, J.C., BUSECK, P.R. (**1984**): The speciation of mercury in hydrothermal systems, with applications to ore deposition. *Geochim. Cosmochim. Acta* 48: 177-185.

VAREKAMP, J.C., BUSECK, P.R. (**1986**): Global mercury flux from volcanic and geothermal sources. *Appl. Geochem*. 1:65-73.

VERMETTE, S., LINDBERG, S., BLOMM, N. (**1995**): Field tests for a gegional mercury deposition metwork – sampling design and preliminary test results. *Atmos. Environ.* 29: 1247-1251.

VIMY, M.J., TAKAHASKI, Y., LORSCHEIDER, F.L. (**1990**): Maternal-fetal distribution of mercury (203-Hg) released from dental fillings. *Am. J. Physiol.* 258: R939-945.

WALLSCHLÄGER, D (**1996**): Speziesanalytische Untersuchungen zur Abschätzung des Remobilisationspotentials von Quecksilber aus kontaminierten Elbauen., University of Bremen, Germany and GKSS Research Centre, Geesthacht, Germany.

WÄNGBERG, I., MUNTHE, J., PIRRONE, N., IVERFELDT, Å, BAHLMANN, E., COSTA, P., EBINGHAUS, R., FENG, X., FERRARA, R., GÅRDFELDT, K., KOCK, H., LANZILOTTA, E, MAMANE, Y., MAS, F., MELAMED, E., OSNAT, Y., PRESTBO, E., SOMMAR, J., SCHMOLKE, S., SPAIN, G., SPROVIERI, F., TUNCEL, G. (**2001**): Atmospheric mercury distribution in Northern Europe and in the Mediterranean region. *Atmos. Environ.* 35: 3019-3025.

WÄNGBERG, I., MUNTHE, J., BERG, T., EBINGHAUS, R., KOCK, H.H., TEMME, C., BIEBER, E., SPAIN, T.G., STOLK, A. (**2007**): Trends in air concentration and deposition of mercury in the coastal environment of the North Sea Area. *Atmos. Environ*. 41: 2612-2619.

WÄNGBERG, I., MUNTHE, J., AMOUROUX, D., ANDERSSON, M.E., FAJON, V., FERRARA, R., GÅRDFELDT, K., HORVAT, M., MAMANE, Y., MELAMED, E., MONPERRUS, M., OGRINC, N., YOSSEF, O., PIRRONE, N., SOMMAR, J., SPROVIERI, F. (**2008**): Atmospheric mercury at Mediterranean coastal stations. *Environ. Fluid Mech*. 8: 101-116.

WEISS-PENZIAS, P., JAFFE, D.A., MCCLINTICK, A., PRESTBO, E.M., LANDIS, M.S. (**2003**): Gaseous Elemental Mercury in the Marine Boundary Layer: Evidence for Rapid Removal in Anthropogenic Pollution. *Environ. Sci. Technol*. 37: 3755-3763.

WHO (**1991**): Environmental Health criteria 118: Inorganic mercury. World Health Organisation Geneva, International Programme on Chemical Safety.

WIGFIELD, D.C., PERKINS, S.L. (**1985**): Oxidation state analysis of mercury: evidence of the formation of mercurous ion in the oxidation of mercury by peracetic acid. *J. Appl. Toxicol.* 5: 339-341.

WITT, M.L.I, MATHER, T.A., BAKER, A.R., DE HOOG, J.C.M, PYLE, D.M. (**2010**): Atmospheric trace metals over the south-west Indian Ocean: Total gaseous mercury, aerosol trace metal concentrations and lead isotope ratios. *Marine Chem*. 121: 2-16.

WREN, C.D., SCHEIDER, W.A., WALES, D.L., MUNCASTER, B.W., GRAY, I.M. (**1991**): Relation between mercury concentrations in walleye (*Stizostedion vitreum vitreum*) and northern pike (*Esox lucius*) in Ontario lakes and influence of environmental factors. *Can. J. Fish. Aquat. Sci.* 48: 132-139.

XIA, C., XIE, Z., SUN, L. (**2010**): Atmospheric mercury in the marine boundary layer along a cruise path from Shanghai, China to Prydz Bay, Antarctica. *Atmos. Environ*. 44: 1815-1821.

XIAO, Z.F., MUNTHE, J., STROMBERG, D., LINDQVIST, O. (**1994**): Photochemical behaviour of inorganic Hg compounds in aqueous solution. In: Mercury as a Global Pollutant – Integration and Synthesis; Watras, C.J., Huckabee, J.W. (Eds.). Lewis Publishers, pp. 581-592.

XIAO, Z. SOMMAR, J., WEI, S., LINDQVIST, O. (**1997**): Sampling and determination of gas phase divalent mercury in the air using a KCl coated denuder. *Fres. J. Anal. Chem*. 358: 386-391.

XU, H., ALLARD, B. (**1991**): Effects of a fulvic acid on the speciation and mobility of mercury in aqueous solutions. *Water Air Soil Pollut*. 56: 709-717.

YANG, Y., ZHANG, C., SHI, X., LIN, T., WANG, D. (**2007**): Effect of organic matter and pH on mercury release from soils. *J. Environ. Sci*. 19: 1349-1354.

ZHANG,H., LINDBERG, S.E. (**1999**): Processes influencing the emission of mercury from soils: a conceptual model. *J. Geophys. Res. 104*: 21889-21896.

ZHANG, L., WRIGHT, L.P., BLANCHARD, P. (**2009**): A review of current knowledge concernign dry deposition of atmospheric mercury. *Atmos. Environ*. 43: 5853-5864.

ZOMARA, E., SANTANA, A. (**1979**): Características climáticas de la costa occidental de la Patagonia entre las latitudes 46°40' y 56°30'. *Anales del Instituto de la Patagonia, Serie Ciencias Naturales* 10: 109-143.

Acknowledgements

I would like to express my sincere gratitude to my supervisor Prof. Dr. Harald Biester, TU Braunschweig, Germany. I appreciate his balance between hands-off approach to supervision and provision of guidance whenever needed. This gave me the opportunity to find an acceptable balance between work and family while finishing this project over the course of some years.
Grateful thanks are due to Prof. Schöler for being first reviewer of this thesis and for his straightforward help to comply with all formalities.

Funding: This PhD thesis was mainly funded due to a scholarship by the Studienstiftung des deutschen Volkes. Partial funding was done by the Deutsche Forschungs-gemeinschaft (DFG: BI 734/3 to H. Biester).

Patagonia, Chile: Rolf Kilian (University of Trier), Christian Scholz (University of Heidelberg), Harald Biester (University of Braunschweig), and Gino Cassassa (Instituto Antarctico, Punta Arenas, Chile) gave me important logistic support. Without this, the field campaigns would not have been as successful. Thanks for electrical power supply and dry sleeping accommodation at the Skyring site go to the Friedli family as owners of the Estancia Skyring.
Moreover, especially Rolf managed to spark the fascination for this awesome part of the earth. Thanks to Rolf, Christian, Harald, and Damir Selimovic and thanks to the people accompanying me during prior campaigns in Patagonia (Martinus, Arne, Markus, Christoph, Miriam, Tobias, Johannes, Michael, Heide) these periods of cold and wet feet, empty stomach, frozen fingers, sore back and shoulders, wind-tousled hair…will stay in my memory as just some of the best periods during studying geosciences.

Galicia, Spain: Antonio Martínez-Cortizas and his team at the Departamento de Edafología y Química Agrícola, Universidade de Santiago de Compostela provided me great support in the field as well as due to giving me space in their lab to perform some not deferrable measurements. Additionally, great thanks go to the workers of the wind farm at the mountainside of “Pico de Cuadramón” for providing electrical power supply and an office at their monitoring station during the field campaign in July.

Lake Gossenkölle, Innsbruck, Austria: I highly appreciate the opportunity that I had to use the limnological station of the University of Innsbruck at Lake Gossenkölle. I was not only able to use this station; I was allowed to make some reconstructions of the station in

order to mount my equipment, to operate the instruments for several months and to “live” there, whenever it was necessary. For this confidence my thanks go to Prof. Roland Psenner and Birgit Sattler from the Institute of Ecology, University of Innsbruck. I also would like to thank the Institute of Mineralogy and Petrography, namely Prof. Peter Mirwald, Peter Tropper, and Jürgen Konzett, for the possibility to use the labs and equipment of the institute for many different purposes.

Rossendorf, Dresden: I gratefully acknowledge the opportunity to finish this PhD thesis partly during my employment at the Institute of Resource Ecology at the Helmholtz-Zentrum Dresden-Rossendorf. For their great support and especially for donating valuable working time, I would like to thank Vinzenz Brendler, Harald Foerstendorf, and Norbert Jordan.

Miscellaneous: Ralf Ebinghaus, Hans H. Kock, Enno Bahlmann (all at that time at GKSS, Geesthacht), Daniel Obrist, and Johannes Fritsche (University of Basel) supported me with information on atmospheric mercury measurements and conducted together with me intercomparisons between my GARDIS-3 analyzer and their Tekran instruments. This was a great help for quality control.
I would like to send my warmest thanks to Susanne Stadler for her company throughout the studies of Geosciences in Heidelberg as well as Applied Spectroscopy and Analytics in Leipzig. She has always been a good and understanding friend and a valuable supporter of this work.

Family: And finally, I would like to thank my family. My parents have always given the necessary support for me to be more or less successful and happy throughout my still lasting period of growing up.
My lovely daughters Sina and Daphne, to whom this thesis is dedicated for their life-long affiliation with it, I thank you for your patience and understanding.
Heartfelt thanks go to my dear husband Christoph, who was partner, sustainer, motivator and proof reader, who never lost his confidence and faith in me.

Eidesstattliche Versicherung gemäß § 8 der Promotionsordnung der Naturwissenschaftlich-Mathematischen Gesamtfakultät der Universität Heidelberg

1. Bei der eingereichten Dissertation zu dem Thema „Determination of Atmospheric Mercury and its Deposition in Remote Areas of the Northern and Southern Hemisphere“ handelt es sich um meine eigenständig erbrachte Leistung.

2. Ich habe nur die angegebenen Quellen und Hilfsmittel benutzt und mich keiner unzulässigen Hilfe Dritter bedient. Insbesondere habe ich wörtlich oder sinngemäß aus anderen Werken übernommene Inhalte als solche kenntlich gemacht.

3. Die Arbeit oder Teile davon habe ich bislang nicht an einer Hochschule des In- oder Auslands als Bestandteil einer Prüfungs- oder Qualifikationsleistung vorgelegt.

4. Die Richtigkeit der vorstehenden Erklärungen bestätige ich.

5. Die Bedeutung der eidesstattlichen Versicherung und die strafrechtlichen Folgen einer unrichtigen oder unvollständigen eidesstattlichen Versicherung sind mir bekannt.
Ich versichere an Eides statt, dass ich nach bestem Wissen die reine Wahrheit erklärt und nichts verschwiegen habe.

_____ _____

Ort und Datum Unterschrift